

BOOK OF ABSTRACTS

**Helicases and Nucleic Acid-Based Machines:
Structure, Mechanism and Regulation and
Roles in Human Disease**

6TH, 7TH, 8TH & 9TH JULY 2021

ONLINE

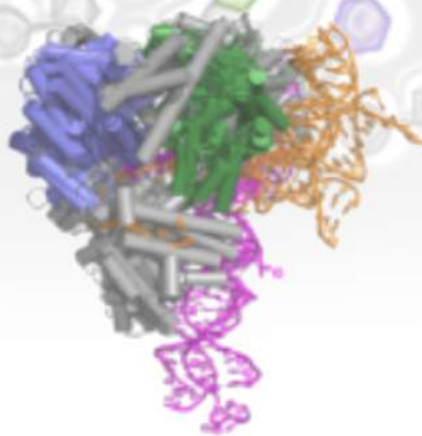


Table of Contents

The DEAD-box Helicase DDX5: From <i>S. cerevisiae</i> to Cancer	1
<u>Prof. Elizabeth Tran</u>	
The RNA helicase Dbp7 promotes domain V/VI compaction and stabilization of interdomain interactions during early 60S assembly	2
Mr. Gerald R. Aquino, Mr. Philipp Hackert, Dr. Nicolai Krogh, Dr. Kuan-Ting Pan, Prof. Henrik Nielsen, Prof. Henning Urlaub, Dr. Katherine E. Bohnsack, <u>Prof. Markus T. Bohnsack</u>	
The spatial organization of genes is associated with the control of alternative splicing and 3' end processing by RNA helicases DDX5 and DDX17	3
<u>Dr. Cyril Bourgeois</u>	
Characterization of the Escherichia coli XPD/Rad3 iron-sulfur helicase, YoaA, in complex with the DNA polymerase III clamp loader subunit, chi	4
<u>Mrs. Savannah Weeks</u> , Ms. Yasmin Ali, Mrs. Elizabeth Dudenhausen, Dr. Linda Bloom	
Searching for synthetic lethality in Escherichia coli strains lacking uup, radd, or recG	5
<u>Ms. Nina Bonde</u> , Dr. Zachary Romero, Mr. Aidan McKenzie, Prof. James Keck, Prof. Michael Cox	
SSB Increases E. coli Clamp Loader Lifetime on DNA, and is Rapidly Remodeled	6
<u>Mr. Elijah Newcomb</u> , Dr. Linda Bloom	
The Mycobacterium tuberculosis DNA-repair helicase UvrD1 is activated by redox-dependent dimerization of a 2B domain cysteine.	7
<u>Ms. Ankita Chadda</u> , Mr. Drake Jensen, Dr. Eric Tomko, Dr. Ana Ruiz Manzano, Dr. Binh Nguyen, Dr. Timothy Lohman, Dr. Eric Galburt	
Cell-cycle-regulated interaction of the Bloom syndrome helicase with Mcm6 controls DNA replication speed and the DNA-damage response	9
Dr. Vivek Shastri, <u>Mrs. Veena Subramanian</u> , Dr. Kristina Hildegard Schmidt	
Intriguing synergic and opposing activities of RecQ-like DNA helicase Hel112 in combination with enzymes involved in different DNA metabolism activities	11
<u>Dr. Mariarosaria De Falco</u> , Dr. Mariarita De Felice	
A Single Molecule Investigation of Structure and Accessibility of Long Telomeric Overhangs	12
<u>Prof. Hamza Balci</u> , Mr. Golam Mustafa, Mr. Sajad Shiekh	
DEAD box 1 (DDX1) Stabilizes Cytoplasmic mRNAs During Oxidative Stress	14
<u>Dr. Lei Li</u> , Dr. Mansi Garg, Dr. Yixiong Wang, Dr. Weiwei Wang, Dr. Roseline Godbout	
VASA helicase GLH-1 drives the phase separation of perinuclear germ granules to promote the fidelity of piRNA-mediated genome surveillance	16
Dr. Wenjun Chen, Mr. Jordan Brown, Dr. Shikui Tu, Dr. Zhiping Weng, Dr. Donglei Zhang, <u>Dr. Heng-Chi Lee</u>	
Genome-wide impact of DExH-box RNA helicases on RNA splicing and quality control	18
<u>Dr. Qing Feng</u> , Mr. Keegan Krick, Prof. Christopher Burge	

Sister chromatid exchange events and genome stability in the absence of RECQL5 helicase	20
<u>Dr. Zeid Hamadeh, Dr. Peter Lansdorp</u>	
Kinetics of Nucleotide Binding to the gp16 ATPase	21
<u>Mr. Aaron Morgan, Dr. Christopher Fischer, Dr. Paul Jardine, Dr. Allen Eastlund</u>	
Three charged amino acid residues at the extreme C-terminus of the BFK20 gp41 helicase play a role in the ATPase activity of the protein	22
<u>Dr. Nora Halgasova, Dr. Gabriela Bukovska</u>	
How to limit the speed of a motor - the intricate regulation of the XPB ATPase and translocase in TFIIH	23
<u>Ms. Jeannette Kappenberger, Dr. Wolfgang Kölmel, Dr. Elisabeth Schönwetter, Mr. Tobias Scheuer, Ms. Julia Wörner, Dr. Jochen Kuper, Prof. Caroline Kisker</u>	
A rotary-mechanism for GTP hydrolysis by the AAA+ protein McrB stimulated by the endonuclease McrC	25
<u>Prof. Saikrishnan Kayarat</u>	
Insertion of a flexible linker alters winged helix domain dynamics affecting substrate binding and unwinding activity of human RECQ1	26
<u>Ms. Tulika Das, Ms. Swagata Mukhopadhyay, Dr. Agneyo Ganguly</u>	
Molecular determinants for dsDNA translocation by the transcription-repair coupling and evolvability factor Mfd	28
<u>Prof. Alexandra Deaconescu, Dr. Christiane Brugger, Dr. Margaret Suhanovsky, Dr. Cheng Zhang, Mr. David Kim, Dr. Amy Sinclair, Dr. Dmitry Lyumkis</u>	
Light, CRISPR and DNA Repair	29
<u>Prof. Taekjip Ha</u>	
Mechanism and regulation of an RNA-guided helicase-nuclease, CRISPR-Cas3	30
<u>Prof. Ailong Ke</u>	
Vectorial folding of telomere overhang by a superhelicase, Rep-X	31
<u>Dr. Sua Myong, Dr. Tapas Paul, Prof. Taekjip Ha</u>	
Design and application of force-activated DNA substrates for helicase binding and unwinding studies	32
<u>Mr. Arnulf Taylor, Mr. Stephen Okoniewski, Mr. Lyle Uyetake, Prof. Thomas Perkins</u>	
Regulatory mechanisms of the RNA exosome helicases	33
<u>Prof. Elena Conti, Dr. Piotr Gerlach, Mr. Alexander Koegel, Mr. Felix Sandmeir, Dr. Ingmar Schaefer, Mr. Fabien Bonneau</u>	
RNA sensing mechanisms in the Mtr4 arch domain influence RNA helicase activity and conformational dynamics	34
<u>Prof. Sean Johnson</u>	
Structure of the catalytic core of the Integrator complex	35
<u>Mr. Moritz Pfeleiderer, Dr. Wojciech Galej</u>	
Structural basis for the activation of the DEAD-box RNA helicase DbpA by the nascent ribosome	36
<u>Dr. Jan Philip Wurm, Prof. remco sprangers</u>	
Activation of SF1 DNA Helicases by Protein Accessory Factors	38
<u>Dr. Timothy Lohman</u>	

Large-scale ratcheting in a bacterial DEAH/RHA-type RNA helicase that modulates antibiotics susceptibility	39
<u>Ms. Lena Grass</u> , Dr. Jan Wollenhaupt, Ms. Tatjana Barthel, Dr. Iwan Parfentev, Prof. Henning Urlaub, Dr. Bernhard Loll, Dr. Eberhard Klauck, Prof. Haike Antelmann, Prof. Markus Wahl	
Human HELB is a processive motor protein which catalyses RPA clearance from single-stranded DNA	41
Dr. Silvia Hormeno, Dr. Oliver J. Wilkinson, Dr. Clara Aicart-Ramos, Dr. Sahiti Kuppa, Prof. Edwin Antony, Prof. Mark S. Dillingham, <u>Prof. FERNANDO MORENO-HERRERO</u>	
Interactions of translocating Rep	43
<u>Ms. Olivia Yang</u> , Dr. Sonisilpa Mohapatra, Mr. Brian Soong, Prof. Taekjip Ha	
SLX4 forms SUMOylation factories via liquid phase separation.	44
<u>Mr. Emile Alghoul</u> , Dr. Jihane Basbous, Dr. Angelos Constantinou	
Motif I of the Cas3 SF2 helicase domain regulates directionality of Cas3 movement during CRISPR interference and primed adaptation	45
<u>Mr. Nikita Vaulin</u> , Dr. Anna Shiriaeva, Dr. Ekaterina Semenova, Prof. Konstantin Severinov	
A positive and a negative mechanism for directing helicase recruitment to a bacterial chromosome origin	46
<u>Dr. Charles Winterhalter</u> , Dr. Daniel Stevens, Dr. Simone Pellicciari, Dr. Stepan Fenyk, Prof. Heath Murray	
Human DNA/ RNA Topoisomerase TOP3-beta (TOP3B) is coordinated with the DEAD-box Helicases DDX5 and DDX6 to resolve R-Loops	48
<u>Dr. Sourav Saha</u> , Dr. Yves Pommier	
A 3.2 Å structure of the PriA/PriB/replication fork complex reveals mechanistic insight into bacterial DNA replication restart	49
<u>Mr. Alexander Duckworth</u> , Dr. Kenneth Satyshur, Prof. Timothy Grant, Prof. James Keck	
Functional interaction between Sgs1 and Sod2 in the suppression of oxidative-damage-induced chromosomal rearrangements and mitochondrial abnormalities in Saccharomyces cerevisiae	50
<u>Ms. Sonia Vidushi Gupta</u> , Dr. Kristina Hildegard Schmidt, Dr. Lillian Campos-Doerfler	
The evolutionary origins of Pif1 helicases from Helitron transposons	52
<u>Mr. Pedro Heringer</u> , Dr. Gustavo C. S. Kuhn	
Structural snapshots of ATPase cycle of tick-borne encephalitis virus NS3 helicase	54
<u>Dr. Paulina Duhita Anindita</u> , Dr. Pavel Grinkevich, Dr. Roman Tuma, Dr. Zdenek Franta	
New insights into the functions of SV40 T antigen helicase and beyond - The functional cooperation of SV40 T antigen monomers and hexamers is essential for viral DNA replication	55
<u>Dr. Heinz Nasheuer</u> , Dr. Nick Onwubiko, Dr. Ingrid Tessmer	
Biochemical studies of the COVID-19 Nsp13 helicase required for coronavirus replication	57
<u>Ms. Rebecca Lee</u> , Mr. Joshua Sommers, Dr. Arindam Datta, Dr. Robert Brosh	
Mechanism of RNA mediated phosphate release from the active site of the tick-borne encephalitis virus helicase.	59
<u>Mr. Marco Halbeisen</u> , Dr. Roman Tuma, Dr. Paulina Duhita Anindita, Dr. Zdenek Franta, Dr. David Reha	
Structural basis for backtracking by the SARS-CoV-2 replication-transcription complex	60
<u>Mr. Brandon Malone</u> , Dr. Elizabeth Campbell, Prof. Seth Darst	

Unwinding of duplex nucleic acids by cooperative translocation of SARS coronavirus helicase nsP13 is modulated with ATP concentration	61
<u>Prof. Dong-Eun Kim</u>	
The DEAD-box RNA helicase RhIE2 is a global regulator of Pseudomonas aeruginosa lifestyle and pathogenesis	63
Dr. Stéphane Hausmann, Dr. Diego Gonzalez, Mr. Johan Geiser, <u>Dr. Martina Valentini</u>	
The DEAD-box RNA helicase eIF4A is a promising host target for the development of potent broad-spectrum antivirals	64
<u>Prof. Arnold Grünweller</u> , Dr. Wiebke Obermann, Dr. Christin Müller, Prof. Roland K. Hartmann, Prof. John Ziebuhr	
Structural basis for resistance of Mycobacterium tuberculosis Rho to bicyclomycin	65
<u>Dr. Marc Boudvillain</u> , Dr. Emmanuel Saridakis, Dr. Rishi Vishwakarma, Mr. Kevin Martin, Mrs. Isabelle Simon, Dr. Martin Cohen-Gonsaud, Dr. Franck COSTE, Dr. Emmanuel Margeat, Dr. Patrick Bron	
EXO5-DNA Structure and BLM Interactions Direct DNA Resection Critical for ATR-dependent Replication Restart	66
<u>Dr. Chi-Lin Tsai</u> , Dr. Shashank Hambarde, Dr. Albino Bacolla, Prof. Tej Pandita, Prof. John Tainer	
Structural Basis of Mitochondria Twinkle Helicase Action and Twinkle Related Mitochondria Diseases	68
<u>Dr. Yang Gao</u>	
CryoEM structure of RadaA, a Superfamily 4 modular helicase involved in natural transformation in Streptococcus pneumoniae	69
<u>Dr. Leonardo Talachia Rosa</u> , Dr. Emeline Vernhes, Dr. Patrice Polard, Dr. Rémi Fronzes	
Structure of an MCM ring encircling bona fide melted DNA illustrates a key step of replication initiation	71
<u>Dr. Eric Enemark</u> , Dr. Sanaz Rasouli, Dr. Alexander Myasnikov	
Translocation activities of S. Cerevisiae Pif1 helicase	72
<u>Dr. Kevin Raney</u> , Dr. Jun Gao, Dr. John C. Marecki, Mr. David Proffitt, Dr. Alicia K. Byrd	
WRN helicase stabilizes deprotected replication forks in BRCA2-deficient cancer cells	73
<u>Dr. Arindam Datta</u> , Dr. Kajal Biswas, Mr. Joshua Sommers, Ms. Haley Thompson, Dr. Sanket Awate, Dr. Claudia Nicolae, Dr. George-Lucian Moldovan, Dr. Robert Shoemaker, Dr. Shyam Sharan, Dr. Robert Brosh	
Nucleosome recognition and DNA distortion by the Chd1 chromatin remodeler	75
Dr. Ilana Nodelman *, Mr. Sayan Das *, Ms. Anneliese Faustino, Prof. Stephen Fried, <u>Prof. Greg Bowman</u> , Prof. Jean-Paul Armache	
Visualizing the action of SARS-CoV-2 and eukaryotic replicative helicases	77
<u>Dr. Shixin Liu</u>	
The E. coli replisome does not require ATP to replicate DNA.	78
<u>Dr. Lisanne Spenkelink</u> , Mr. Richard Spinks, Dr. Slobodan Jergic, Dr. Jacob Lewis, Prof. Nicholas Dixon, Prof. Antoine van Oijen	
Primase – Helicase pairs from Staphylococcal mobile genetic elements	80
<u>Dr. Phoebe Rice</u> , Dr. Heewhan Shin, Dr. Aleksandra Bebel, Dr. Ignacio Mir Sanchis	

Human DNA helicase B protects stalled replication forks from degradation	81
<u>Dr. Alicia K. Byrd, Dr. Maroof Khan Zafar, Ms. Lindsey Hazeslip, Mr. Matthew Thompson</u>	
Analysis of the iron chaperone PCBP1 interactome: intersection of DNA repair and iron trafficking	82
<u>Dr. Lorena Novoa-Aponte, Dr. Sarju Patel, Dr. Olga Protchenko, Dr. James Wohlschlegel, Dr. Caroline Philpott</u>	
How XPD helicase responds to DNA damage and base composition.	83
<u>Dr. Remi Fritzen, Dr. Francesco Colizzi, Dr. Giovanni Bussi, Dr. J. Carlos Penedo, Prof. Malcolm F. White</u>	
DNA damage repair and DEAD Box 1 (DDX1) in embryonic development	84
<u>Dr. Lubna Yasmin, Dr. Yixiong Wang, Ms. Lazina Hossain, Dr. Roseline Godbout</u>	
Directed E. coli DnaB exterior surface mutations effect helicase conformation and regulate behavior to preserve genome stability in vivo	85
<u>Ms. Megan Behrmann, Prof. Michael Trakselis</u>	
The Arch domain of XPD: A regulatory multitool that is mechanistically essential for transcription and DNA repair	86
<u>Dr. Jochen Kuper, Mr. Stefan Peisert, Dr. Florian Sauer, Dr. Arnaud Poterszman, Prof. Jean-Marc Egly, Prof. Caroline Kisker</u>	
Uncovering an allosteric mode of action for a selective inhibitor of human Bloom syndrome protein	87
<u>Dr. Xiangrong(Tina) Chen</u>	
The roles of Hrq1 in ICL repair	88
<u>Mr. Robert Simmons, Ms. Alexandra Hurlock, Dr. Matthew Bochman</u>	
Structural and biochemical characterizations of DHX36 Helicase	89
<u>Prof. Xuguang Xi</u>	
Systematically mapping G-quadruplex regulatory elements on E. coli transcripts	90
<u>Ms. Rachel Cueny, Dr. Andrew Voter, Prof. James Keck</u>	
G-quadruplex processing in Bacillus subtilis	92
<u>Ms. Sarah McMillan, Prof. James Keck, Ms. Rachel Cueny</u>	
The structure of self-loading MCM-like helicases encoded by staphylococcal virus satellites reveals unique and conserved motions	93
<u>Dr. Cuncun Qiaou, Dr. Ignacio Mir Sanchis</u>	
A Mechanical Mechanism for Translocation of Hexameric and Nonstructured Helicases	94
<u>Prof. Ya-chang Chou</u>	
The E. coli RecBCD nuclease domain regulates DNA binding and helicase activity, but not ssDNA translocation	95
<u>Ms. Nicole Fazio, Dr. Linxuan Hao, Dr. Rui Zhang, Dr. Timothy Lohman</u>	
DHX36 function at G-quadruplexes and its connection to stress response	96
<u>Mr. Daniel Hilbig, Dr. Stefan Juranek, Prof. Katrin Paeschke</u>	
Revealing the dynamics of Pif1 helicase when it collides with the G4 quadruplex using single-molecule assays	97
<u>Dr. Jessica Valle Orero, Dr. Martin Rieu, Prof. Vincent Croquette, Prof. Jean-Baptiste Boule, Dr. Phong-Lan-Thao TRAN</u>	

The helicase Rrm3 is essential for replication progression through leading strand G4 rich sites in <i>Saccharomyces cerevisiae</i>	98
<u>Ms. Mor Varon</u> , Prof. Amir Aharoni	
Anyone for a PiNT? The function of the Pif1 N-Terminus	100
<u>Dr. Matthew Bochman</u> , Dr. David Nickens, Dr. Lata Balakrishnan	
Modulation of DnaB helicase conformation and contacts interrupts replisome coupling, creating genome instability	101
<u>Prof. Michael Trakselis</u> , Ms. Megan Behrmann, Ms. Himasha Perera, Ms. Malisha Welikala	
Nanopore Tweezers reveal detailed dynamics of SF1 and SF2 helicases	102
<u>Dr. Jon Craig</u> , Dr. Andrew Laszlo, Prof. Maria Mills, Dr. Momcilo Gavrilov, Mr. Dmitriy Bobrovnikov, Prof. Taekjip Ha, Dr. Keir Neuman, Prof. Jens Gundlach	
The dynamic human Origin Recognition Complex	104
<u>Dr. Matt Jaremko</u> , Dr. Ken On, Dr. Dennis Thomas, Prof. Bruce Stillman, Prof. Leemor Joshua-Tor	
Structure, Mechanism and Crystallographic fragment screening of the SARS-CoV-2 NSP13 helicase	105
<u>Dr. Joseph Newman</u>	
RIG-I's helicase domain is regulated by the intrinsically disordered CARD2-helicase linker	106
<u>Mr. Brandon Schweibenz</u> , Dr. Swapnil Devarkar, Dr. Jie Zheng, Dr. Bruce Pascal, Dr. Patrick Griffin, Dr. Smita Patel	
Successfully completing the final stretch – helicases involved in termination of DNA replication	107
Dr. Sarah Midgley-Smith, Dr. Juachi Dimude, Dr. Katie Jameson, Dr. Michelle Hawkins, <u>Dr. Christian Rudolph</u>	
Engineering photo-controlled Rep helicase	108
<u>Dr. Sonisilpa Mohapatra</u> , Dr. Tunc Kayikcioglu, Dr. Chang-Ting Lin, Prof. Taekjip Ha	
DNA replication initiation and restart: single molecule approach for the study of helicase loading.	110
<u>Dr. Simone Pellicciari</u> , Ms. Meijing Dong, Prof. Feng Gao, Prof. Heath Murray	
Transcription engine and factor protein stepping along DNA revealed from computational microscope	111
Dr. Liqiang Dai, Dr. Lin-Tai Da, Mr. Chao E, Dr. Chunhong Long, <u>Dr. Jin Yu</u>	
Human DNA Helicase B aids replication of G-quadruplexes	112
<u>Mr. Matthew Thompson</u> , Dr. Maroof Khan Zafar, Ms. Lindsey Hazeslip, Dr. Alicia K. Byrd	
Rapid single-molecule characterisation of nucleic-acid enzymes	113
<u>Mr. Stefan Mueller</u> , Dr. Lisanne Spenkelink, Prof. Antoine van Oijen	
Tradeoff between dissipation and uncertainty in helicases	115
<u>Dr. Maria Mañosas</u> , Dr. Felix Ritort, Dr. Xavier Viader, Dr. Vegard Sordal, Mr. Victor Rodriguez	
Rapid helicase-SSB assisted isothermal amplification of long DNA fragments	116
<u>Dr. Momcilo Gavrilov</u> , Dr. Chun-Ying Lee, Prof. Sua Myong, Prof. Taekjip Ha	
The human DEAD-box helicase 3 interacts with ER-alpha and regulates its activity	117
<u>Dr. Martina Schroeder</u> , Mrs. Jyotsna Pardeshi, Dr. Lili Gu, Dr. Niamh McCormack, Dr. Yvette Hoehn	

Proteomics Reveal Rocaglate Inhibitors of the eIF4A1 DEAD-box RNA Helicase Remodel the Translation Machinery and Translatome	118
<u>Dr. Jonathan Schatz</u> , Dr. David Ho, Mr. Tyler Cunningham, Ms. Paola Manara, Dr. Stephen Lee	
Translation of the eIF4B mRNA drives cell division dynamics in sea urchin embryos.	120
<u>Mr. Florian Pontheaux</u> , Dr. Julia Morales, Prof. Patrick Cormier	
G-quadruplex DNA inhibits unwinding activity but promotes liquid-liquid phase separation by the DEAD-box helicase Ded1p	121
<u>Dr. Jun Gao</u> , Mr. Zhaofeng Gao, Ms. Andrea A. Putnam, Dr. Alicia K. Byrd, Ms. Sarah Venus, Dr. John C. Marecki, Dr. Andrea D. Edwards, Ms. Haley M. Lowe, Dr. Eckhard Jankowsky, Dr. Kevin Raney	
Correlating the conformational dynamics of the DEAD-box helicase eIF4A with translation efficiencies	123
<u>Dr. Anirban Chakraborty</u> , Dr. Linda Krause, Dr. Alexandra-Zoi Andreou, Dr. Dagmar Klostermeier	
Dissecting the role of the eIF4E/5'-cap interaction for eIF4A activity with a model RNA	124
<u>Dr. Linda Krause</u> , Dr. Alexandra Zoi Andreou, Dr. Dagmar Klostermeier	
DEAD-box ATPases are regulators of RNA-containing biomolecular condensates	125
<u>Prof. Karsten Weis</u>	
DDX6 mutations responsible for intellectual disability and dysmorphic features associated with RNA mis-regulation and P-body defects	126
Mrs. Marianne Benard, Mrs. Michele Ernoult-Lange, Mrs. Ada Allam, Mr. Christopher Balak, Mrs. Amelie Piton, <u>Mrs. Dominique Weil</u>	
Translation regulation by the RNA helicase Ded1 during cell stress	128
Dr. Peyman Aryanpur, Dr. Telsa Mittelmeier, <u>Dr. Timothy Bolger</u>	
Roles of Local DNA Conformation and Conformational Dynamics on DNA Polymerase Holoenzyme Formation in the Bacteriophage T4 DNA Replication System	129
<u>Dr. Patrick Herbert</u> , Mr. Dylan Heussman, Mr. Jack Maurer, Ms. Maya Pande, Mr. Steve Weitzel, Prof. Peter von Hippel, Prof. Andrew Marcus	
SARS CoV-2 NSP13 Helicase Displaces Proteins and Rapidly Unwinds RNA and DNA	131
<u>Dr. John Marecki</u> , Mr. Harrison Russell, Mr. David Proffitt, Dr. Kevin Raney	
Force-dependent stimulation of RNA unwinding by SARS-CoV-2 nsp13 helicase	133
<u>Dr. Keith Mickolajczyk</u> , Dr. Patrick Shelton, Dr. Michael Grasso, Ms. Xiacong Cao, Ms. Sara Warrington, Dr. Amol Aher, Dr. Shixin Liu, Dr. Tarun Kapoor	

The DEAD-box Helicase DDX5: From *S. cerevisiae* to Cancer

Tuesday, 6th July - 14:30: Keynote 1 - Oral - Abstract ID: 15

Prof. Elizabeth Tran¹

1. Purdue University

Small cell lung cancer (SCLC) accounts for more than 30,000 cases per year in the United States. Although this represents a small fraction (15%) of total lung cancer cases, SCLC stands apart from the more common, non-small cell lung cancer due to its rapid metastasis, high mortality rate (9-month median survival), heterogeneous nature, and lack of effective treatments. Importantly, while SCLC is responsive to initial chemotherapies, ~90% of patients relapse within one year due to the development of chemoresistance. DDX5 is a founding member of the DEAD-box RNA helicase family that functions in multiple pre-mRNA biosynthetic steps including transcription, pre-mRNA splicing, and termination. Overexpression of DDX5 has been linked to numerous cancer types including prostate, colon, and breast cancer. However, the precise mechanism linking DDX5 overaccumulation to uncontrolled cell growth and metastasis is unclear. We now report that DDX5 is also overexpressed in SCLC and that knockdown impairs SCLC cell growth. We also find that DDX5 is necessary for cellular respiration by promoting expression of genes in the oxidative phosphorylation and TCA cycle pathways, similar to our early observations of Dbp2, its budding yeast counterpart. Because ectopic expression of *DDX5* fully complements loss of *DBP2* in *S. cerevisiae*, we are now using our previous work for over a decade on Dbp2 to inform our cancer research. Progress on the transition from a classic model system to clinically relevant discoveries will be presented.

The RNA helicase Dbp7 promotes domain V/VI compaction and stabilization of interdomain interactions during early 60S assembly

Tuesday, 6th July - 15:00: Oral Session - Oral - Abstract ID: 9

Mr. Gerald R. Aquino¹, **Mr. Philipp Hackert**¹, **Dr. Nicolai Krogh**², **Dr. Kuan-Ting Pan**³, **Prof. Henrik Nielsen**², **Prof. Henning Urlaub**³, **Dr. Katherine E. Bohnsack**¹, **Prof. Markus T. Bohnsack**¹

1. Goettingen University, 2. Copenhagen University, 3. Max-Planck-Institute for Biophysical Chemistry

RNA-protein complexes (RNPs) play key roles at all stages of gene expression and in various other cellular pathways. The production of eukaryotic ribosomal subunits is a highly dynamic process involving numerous structural rearrangements of the ribosomal RNAs (rRNAs) and the hierarchical recruitment of approximately 80 ribosomal proteins. Remodelling events not only establish the architecture present in mature complexes, but also serve as key checkpoints, ensuring the fidelity of ribosome assembly and the functionality of the ribosomal subunits. A wealth of structural information is available on late precursors of the large ribosomal subunit (pre-60S) and the small ribosomal subunit (pre-40S). While little is known about the architecture and interactions in early pre-60S intermediates, several RNA helicases have been identified as components and likely contribute to the dynamic nature and folding of these complexes.

Here, we identify the RNA helicase Dbp7 as the key player regulating a series of events that drive compaction of domain VI of early large ribosomal subunit precursors (pre-60S). Our *in vivo* RNA-protein crosslinking analyses using Crosslinking and Analysis of cDNA (CRAC) not only position Dbp7 on root helices of domain VI of the 25S rRNA involved in pre-rRNA compaction but also indicate a role for its helicase activity in triggering dissociation of the snoRNA snR190, which acts as a pre-rRNA folding chaperone. The Dbp7-dependent release of snR190 and various other assembly factors from pre-60S particles and the requirement of its remodelling activity for recruitment of the essential ribosomal protein uL3 are confirmed by proteomic and functional analyses. Binding of uL3 is critical for formation of the peptidyltransferase center and it is responsible for stabilizing interactions between the 5' and 3' ends of the 25S rRNA, an essential pre-requisite for subsequent pre-60S maturation events. Furthermore, our data suggest that remodelling by Dbp7 induces a surveillance checkpoint and that pre-60S particles lacking Dbp7 are targeted for degradation.

Therefore, by providing novel mechanistic insights in events taking place in very early pre-LSU complexes, our work illuminates a hitherto largely uncharacterized aspect of RNA helicase function during ribosomal subunit assembly.

The spatial organization of genes is associated with the control of alternative splicing and 3' end processing by RNA helicases DDX5 and DDX17

Tuesday, 6th July - 15:15: Oral Session - Oral - Abstract ID: 13

Dr. Cyril Bourgeois¹

1. Laboratory of Biology and Modelling of the Cell, ENS de Lyon, CNRS UMR 5239, Lyon, France

DEAD box helicases DDX5 and DDX17 regulate different steps of gene expression such as transcription and alternative splicing. The joint silencing of both DDX5 and DDX17 in cultured cells leads to an altered inclusion of thousands of exons, but also to an alteration of the 3' end processing of hundreds of transcripts, leading to transcriptional readthrough. We found that DDX5/DDX17-dependent internal and terminal exons are significantly closer than other exons to chromatin binding sites for the genome organizing factor CTCF, a partner of both helicases. In line with this finding, CTCF co-regulates alternative splicing and 3' end processing with DDX5/DDX17.

ChIP-qPCR experiments performed on a candidate gene showed that DDX5/DDX17 silencing impairs CTCF binding near the DDX5/DDX17-regulated alternative exon, but also at the promoter and at the end of the gene. *In silico* analyses, validated by chromosome conformation capture (3C) experiments, indicated that the promoter of DDX5/DDX17-regulated gene is spatially close to the end of the corresponding gene, and that this particular looped conformation is altered upon DDX5/DDX17 silencing. Our data support the idea that the dynamics of RNA Pol II is altered upon DDX5/DDX17 silencing, with consequences on both alternative splicing and 3' end processing.

Finally, we used a dCas9-derived approach to induce local targeted DNA looping, and we obtained the first direct evidence that modulating 3D gene structure can impact alternative splicing. Altogether our work uncovers a novel level of regulation of RNA processing by DDX5 and DDX17, and highlights the impact of local DNA folding on gene expression.

Characterization of the *Escherichia coli* XPD/Rad3 iron-sulfur helicase, YoaA, in complex with the DNA polymerase III clamp loader subunit, χ

Tuesday, 6th July - 16:00: Poster Session 1-A - Poster - Abstract ID: 29

Mrs. Savannah Weeks¹, Ms. Yasmin Ali¹, Mrs. Elizabeth Dudenhausen¹, Dr. Linda Bloom¹

1. University of Florida

Introduction: YoaA is a newly discovered *Escherichia coli* protein predicted to be a XPD/Rad3 iron-sulfur helicase. YoaA with the *E. coli* accessory clamp loader subunit of DNA polymerase III, χ , resolves DNA damage that halts DNA synthesis. Genetic studies have shown *yoaA* and *holC*(χ) are both necessary to promote azidothymidine (AZT) tolerance in cells. AZT is a thymine nucleoside analog that is a chain terminator of DNA synthesis when it is incorporated into DNA, causing single-strand (ss) DNA gaps. Recently, Sutura *et al.* revealed that YoaA interacts with χ directly rather than binding the DNA polymerase III holoenzyme via χ . Little is known about how YoaA and χ allow the replication fork to overcome damage that blocks synthesis, and biochemical activities of YoaA are unknown. Here, we characterize the novel protein, YoaA, as a helicase in complex with χ by measuring protein-protein interactions and biochemical activities.

Methods: Size exclusion chromatography and site-directed mutagenesis were used to measure YoaA- χ interactions. ATPase activity and DNA unwinding were measured for YoaA and YoaA- χ . A FRET-based helicase assay measured the substrate preferences and polarity of translocation of YoaA- χ .

Results: YoaA and χ form a 1:1 complex that can be isolated by size exclusion chromatography. YoaA's solubility is increased when YoaA binds χ . Characteristic of a XPD/Rad3 helicase, YoaA- χ contains an iron-sulfur cluster. On single and double-stranded DNA, YoaA- χ possesses DNA-dependent ATPase activity. YoaA- χ translocates in the 5' to 3' direction and unwinds double-strand DNA that contains a ss overhang or a forked overhang.

Discussion: This is the first biochemical evidence demonstrating YoaA as an *E. coli* XPD/Rad3 iron-sulfur helicase that functions in complex with χ . Future work will characterize substrates YoaA- χ can unwind. Substrates such as D-loops and DNA/RNA hybrids will be tested to understand YoaA- χ 's role in resolving AZT damage. Since single-stranded DNA-binding protein (SSB) binds to χ , we predict χ to mediate interactions with SSB that could be important for repair of AZT damage. It is possible that SSB recruits YoaA- χ to ss gaps and regulates YoaA- χ to unwind enough base pairs for a nuclease to remove the AZT lesion.

Searching for synthetic lethality in *Escherichia coli* strains lacking *uup*, *radD*, or *recG*

Tuesday, 6th July - 16:00: Poster Session 1-A - Poster - Abstract ID: 56

***Ms. Nina Bonde*¹, *Dr. Zachary Romero*¹, *Mr. Aidan McKenzie*¹, *Prof. James Keck*¹, *Prof. Michael Cox*¹**

1. University of Wisconsin-Madison

In *Escherichia coli*, the Uup, RadD, and RecG proteins have been implicated in processing branched recombination intermediates during DNA repair processes, but the exact roles, pathways, and order in which these proteins act during repair and recombination remain unresolved. Uup is an ABC family ATPase, and RadD and RecG belong to the SF2 helicase family of proteins. To gain additional insight into the genetic relationships and roles of Uup, RadD, and RecG, transposon sequencing (Tn-seq) was employed. Tn-seq libraries were created for *E. coli* MG1655 (WT) and strains lacking *uup*, *radD*, or *recG*. Synthetic genetic relationships were determined by finding genes in which insertions lead to a greater than three log-fold decrease in mapped sequencing reads between the WT and deletion strains. Genetic interactions were confirmed using a plasmid-based lethality assay. The *uup* gene has strong interactions with DNA metabolism genes (*recA*, *polA*, *dam*) and genes involved in polyamine biosynthesis, whereas *radD* has strong interactions with genes involved in DNA metabolism (*recG*, *polA*) and outer membrane structure. The *recG* gene has synthetic lethal interactions primarily with genes involved in DNA metabolism – *dam*, *uvrD*, *radA*, *rnhA*, *rep*, and *polA*. We present preliminary frameworks to describe shared and divergent *uup*, *radD*, and *recG* genetic relationships.

SSB Increases *E. coli* Clamp Loader Lifetime on DNA, and is Rapidly Remodeled

Tuesday, 6th July - 16:00: Poster Session 1-A - Poster - Abstract ID: 57

***Mr. Elijah Newcomb*¹, *Dr. Linda Bloom*¹**

1. University of Florida

Introduction: *E. coli* single-stranded DNA binding protein (SSB) binds tightly to single-stranded DNA (ssDNA) generated during many metabolic processes. Originally, it was recognized that SSB binding to ssDNA protects DNA from nuclease degradation and harmful secondary structure formation. Recently, SSB has been shown to play a central regulatory role in DNA metabolism by organizing and recruiting enzymes needed for replication and repair of DNA. These enzymes also exert an effect on SSB as they must find a way to access ssDNA coated by SSB to perform their functions. The *E. coli* processivity clamp loader was used as a model enzyme to study dynamic interactions between SSB and DNA metabolic proteins. Using fluorescence techniques, effects of SSB on the affinity of clamp loader for DNA was tested. Further, the rates of binding and dissociation of the clamp loader to SSB-bound versus naked DNA were measured. The rate by which SSB is remodeled by the clamp loader was determined.

Methods: FRET was used in equilibrium binding experiments to measure binding affinity of clamp loader to DNA with and without SSB. Stopped-flow FRET experiments measured rates of clamp loader binding to and dissociation from DNA as well as SSB remodeling on ssDNA.

Results: SSB increases affinity of the clamp loader for DNA. When SSB is present on DNA, clamp loader binding is no faster than on naked DNA, and the binding kinetics show biphasic characteristics. Clamp loader dissociation from SSB-bound DNA is slower than from naked DNA. SSB is rapidly remodeled on DNA on a similar timescale to clamp loader binding.

Discussion: Efficiency of clamp loading is increased when SSB is present on DNA because SSB enhances the lifetime of the clamp loader on DNA. The binding of clamp loader to DNA corresponds to SSB remodeling time, suggesting that the clamp loader actively remodels SSB on DNA. The biphasic binding character of clamp loader-DNA binding time courses leads us to hypothesize that the binding reaction includes an initial binding step followed by a second step in which the protein-DNA complex rearranges to form a productive clamp loading complex. This model requires further testing.

The *Mycobacterium tuberculosis* DNA-repair helicase UvrD1 is activated by redox-dependent dimerization of a 2B domain cysteine.

Tuesday, 6th July - 16:00: Poster Session 1-A - Poster - Abstract ID: 81

Ms. Ankita Chadda¹, Mr. Drake Jensen¹, Dr. Eric Tomko¹, Dr. Ana Ruiz Manzano¹, Dr. Binh Nguyen¹, Dr. Timothy Lohman², Dr. Eric Galburt¹

1. Department of Biochemistry and Molecular Biophysics, Washington University in Saint Louis, 660 South Euclid Avenue, Saint Louis, MO, 63110, USA, 2. Department of Biochemistry and Molecular Biophysics, Washington University School of Medicine, 660 S. Euclid Ave., St. Louis, MO 63110

Mycobacterium tuberculosis (*Mtb*) causes tuberculosis disease in humans. During infection, *Mtb* is exposed to reactive oxygen species (ROS) and reactive nitrogen intermediates (RNI) from the host immune response that can cause DNA damage. *Mtb* UvrD1 belongs to the SF1 family of helicases that use energy from ATP hydrolysis to catalyze DNA unwinding, a process essential for replication and DNA repair. Previous studies by Size-exclusion chromatography (SEC) and equilibrium sedimentation have suggested that UvrD1 is exclusively monomeric and is capable of unwinding dsDNA in this form. However, in one case, SEC and equilibrium sedimentation were performed in the presence of 5 mM of the reducing agent DTT and DNA unwinding assays were performed in its absence. It is well known that *E. coli* UvrD and other UvrD-family members exhibit monomer-dimer equilibria and unwind as dimers. However, the dimerization interface is unknown since the crystal structures show a monomer bound to DNA. Here using stopped-flow kinetics and analytical sedimentation methods we reconcile these incongruent studies by finding that the balance between monomer-dimer populations of *Mtb* UvrD1 is regulated by redox potential. We identify a 2B domain cysteine, conserved in many Actinobacteria, that underlies this effect. The formation of 2B-2B disulfide bond in the case of *Mtb*UvrD1 fits well in a model where 2B-2B driven dimerization results in an active helicase conformation. We also show that UvrD1 DNA unwinding activity correlates with the dimer population specifically and is thus titrated directly via increasingly positive (i.e. oxidative) redox potential. Consistent with the regulatory role of the 2B domain and the dimerization-based activation of DNA unwinding in UvrD-family helicases, these results suggest that UvrD1 is activated under oxidizing conditions when it may be needed to respond to increasing amounts of DNA damage during infection.

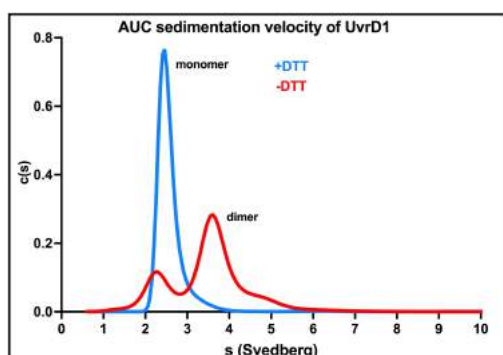


Image auc uvr1.jpg

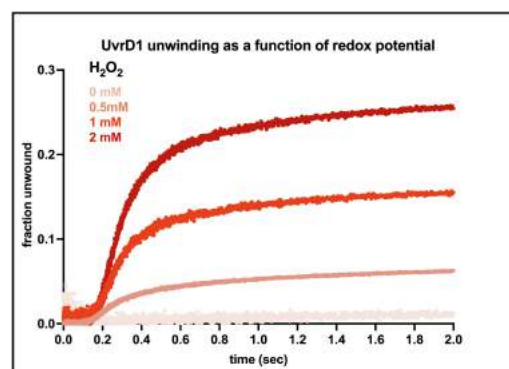


Image unwinding uvr1.jpg

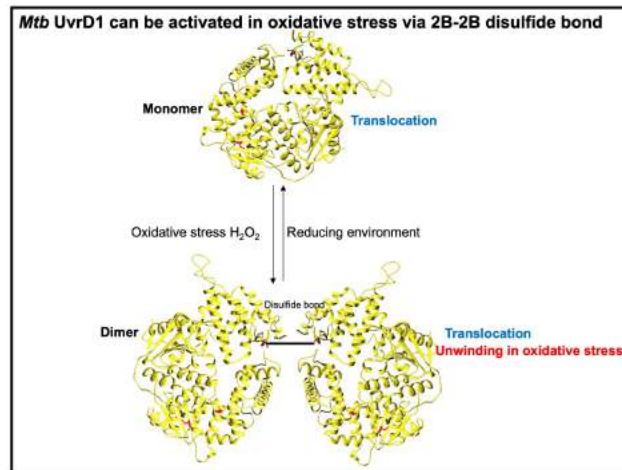


Image schematics.jpg

Cell-cycle-regulated interaction of the Bloom syndrome helicase with Mcm6 controls DNA replication speed and the DNA-damage response

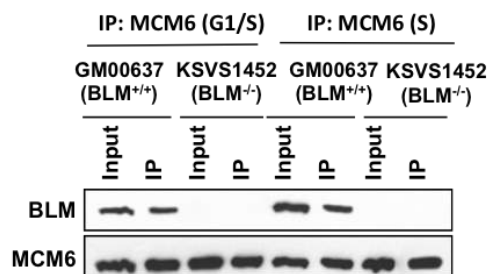
Tuesday, 6th July - 16:00: Poster Session 1-A - Poster - Abstract ID: 94

Dr. Vivek Shastri¹, Mrs. Veena Subramanian¹, Dr. Kristina Hildegard Schmidt²

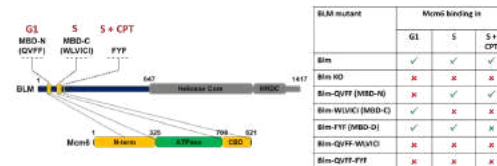
1. Department of Cell Biology, Microbiology and Molecular Biology, University of South Florida, Tampa, FL 33620, USA., 2. UNIVERSITY OF SOUTH FLORIDA

Bloom syndrome is a rare genetic disorder associated with extreme cancer predisposition – approximately 300-fold above the general population. Affected individuals have two inactive copies of the Bloom syndrome (BLM) gene, a tumor-suppressor gene that encodes a DNA helicase with major roles DNA break repair by homologous recombination. Cells lacking BLM are associated with several defects in DNA-damage response, however, whether BLM also contributes to stable genome maintenance in unperturbed cells is not understood. A proteomic screen conducted in the lab identified BLM to interact with the Mcm6 subunit of the replicative MCM helicase in unperturbed S-phase. This led us to hypothesize that BLM regulates events during DNA replication through its interaction with Mcm6, and that loss of this regulatory arrangement leads to replication defects, which might be associated with increased DNA damage and genome instability. We used a combination of mammalian two-hybrid assay, co-immunoprecipitation, fluorescence microscopy, and DNA fiber analysis to test our hypothesis.

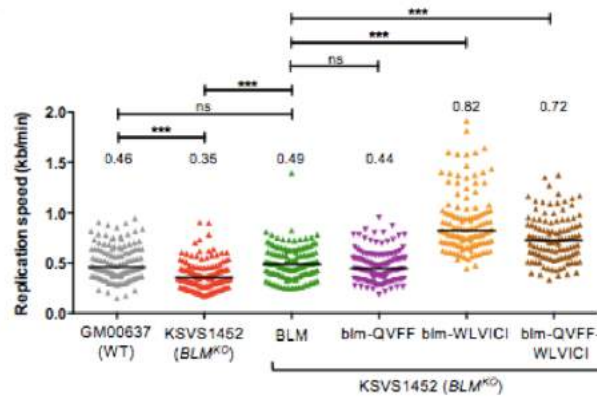
Characterization of the BLM/Mcm6 interaction revealed that BLM associates with Mcm6 in a cell cycle specific manner using distinct binding sites. Intriguingly, in G1-phase, BLM binds to the N terminal domain of Mcm6 and switches to the C-terminal domain of Mcm6 during unperturbed S phase. A third site in BLM was found to be important for its interaction with Mcm6 after DNA damage. Untethering of BLM from Mcm6 in unperturbed S-phase causes high DNA replication speed, delayed repair of replication-dependent DNA double-strand breaks and hypersensitivity to DNA damage and replication stress. Supra-normal replication speed upon uncoupling of BLM and Mcm6 was dependent on the helicase activity of BLM. Our findings reveal that BLM not only plays a role in the response to DNA damage and replication stress, but that its physical interaction with Mcm6 is needed in unperturbed cells as a negative regulator of replication speed. Elucidating the mechanism by which the BLM/Mcm6 interaction functions in DNA break repair and as a negative regulator of DNA replication speed will provide novel insights into fundamental genome maintenance mechanisms and shed light on the contribution of DNA replication defects to development of cancerogenesis.



Picture 1.png



Picture 2.png



Picture 3.png

Intriguing synergic and opposing activities of RecQ-like DNA helicase Hel112 in combination with enzymes involved in different DNA metabolism activities

Tuesday, 6th July - 16:00: Poster Session 1-A - Poster - Abstract ID: 95

***Dr. Mariarosaria De Falco*¹, *Dr. Mariarita De Felice*¹**

1. Institute of Biosciences and Bioresources

Double-stranded DNA needs to be unwound for most DNA processing such as replication, repair and transcription. DNA helicases have been purified and studied from several eukaryotic organisms.

As other replication enzymes, archaeal DNA Helicases are a simplified version of the eukaryotic counterparts. Our studies are mainly aimed at archaeal DNA Helicases, in particular we have identified a DNA helicase, known as HEL112, that possesses both helicase and annealing activities, depending on its oligomeric state. Indeed, it forms monomers and dimers in solution, the monomeric form has an ATP-dependent 3'-5' DNA-helicase activity, whereas, unexpectedly, both the monomeric and dimeric forms possess DNA strand-annealing capability. The Hel112 monomeric form is able to unwind forked and 3'-tailed DNA structures with high efficiency, whereas it is almost inactive on blunt-ended duplexes and bubble-containing molecules. This analysis reveals that *Saccharolobus solfataricus* Hel112 shares some enzymatic features with the RecQ-like DNA helicases.

Hel112 has been tested in combination with several DNA replication/repair enzymes, giving rise to very intriguing observations.

As a matter of fact, the Hel112 helicase activity on Holliday junctions is inhibited by SsTop3 (*S. solfataricus* topoisomerase 3) and, moreover, the combination of these two enzymes stimulates the formation and stabilization of such structures, suggesting that the interplay between Hel112 and SsTop3 might regulate the equilibrium between recombination and anti-recombination activities at replication forks.

Furthermore, Hel112 inhibits NurA (Nuclease of repair in Archaea) exonuclease activity, both in the presence and in the absence of HerA (Helicase of repair in Archaea). In contrast, the endonuclease activity of NurA is not affected by the presence of Hel112. These results suggest that the functional interaction between NurA/HerA and Hel112 is important for DNA end-resection in archaeal homologous recombination.

A Single Molecule Investigation of Structure and Accessibility of Long Telomeric Overhangs

Tuesday, 6th July - 16:00: Poster Session 1-B - Poster - Abstract ID: 37

***Prof. Hamza Balci*¹, *Mr. Golam Mustafa*¹, *Mr. Sajad Shiekh*¹**

1. Kent State University

Telomeric regions of almost all eukaryotic organisms contain repeating G-rich sequences, e.g. GGGTTA repeats in vertebrates, that terminate with a single-stranded overhang. This overhang is 50-300 nt long in human cells and folds into tandem G-quadruplex (GQ) structures, which stabilize these otherwise vulnerable ends and play critical roles in distinguishing them from damaged DNA. Telomeres are protected and organized by the multi-protein complexes Shelterin and CST. Due to end replication problem, telomeres gradually shorten in dividing somatic cells, which undergo senescence or apoptosis when telomeres reach a critical length. However, telomere length is maintained in most cancers by activation of telomerase, a ribonucleoprotein complex that elongates telomeres using an RNA template. Figure 1 shows an illustration of the telomeric overhang and relevant players.

A 200 nt long telomeric overhang contains 33 GGGTTA repeats (33 G-Tracts), which can form up to 8 tandem GQs. However, folding frustration likely results in some of these G-Tracts to remain open (unfolded). Depending on whether they are open, folded into GQ, or protected by Shelterin proteins, the G-Tracts have different accessibilities to nucleases, complementary nucleic acids, small molecules, water molecules and ions. Therefore, telomeres must perform their critical functions in a setting where their structure, stability, and accessibility is dynamically modulated. While commonly used single molecule and ensemble techniques (FRET, force spectroscopy, circular dichroism, NMR, gel electrophoresis, etc.) have been successfully employed to study interactions of “single” telomeric GQs with proteins and small molecules under different ionic and crowding conditions, very few such studies have been performed on long (>100 nt) telomeric sequences due to the complex structures they form.

Recently, we demonstrated the exciting potential of a new approach, based on single molecule FRET-PAINT, to uncover the folding landscape of long telomeric sequences and to quantify their accessibility. Figure 2 shows a schematic of the concept and Figure 3 shows a compilation of the data for telomeric overhangs of varying length. I will present our recent work on using this approach to answer important structural and functional questions about long telomeric overhangs and their interactions with Shelterin proteins, drug-like small molecules, and crowding agents.

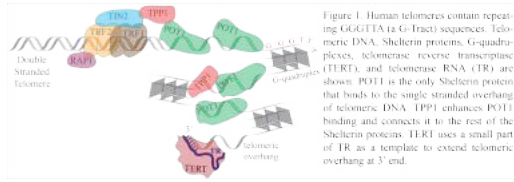


Figure 1.png

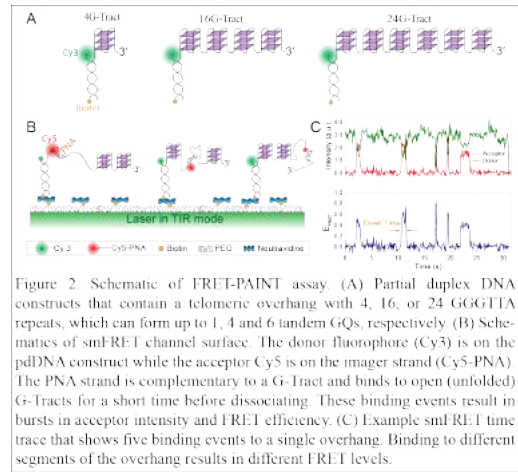


Figure 2.png

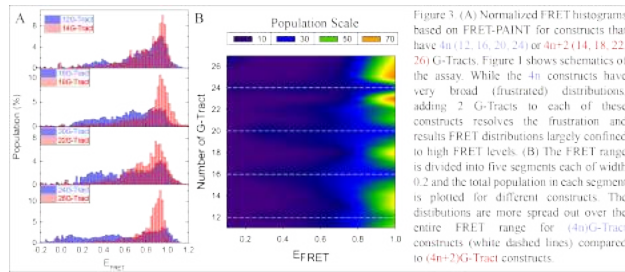


Figure 3.png

DEAD box 1 (DDX1) Stabilizes Cytoplasmic mRNAs During Oxidative Stress

Tuesday, 6th July - 16:00: Poster Session 1-B - Poster - Abstract ID: 60

Dr. Lei Li¹, Dr. Mansi Garg¹, Dr. Yixiong Wang¹, Dr. Weiwei Wang¹, Dr. Roseline Godbout¹

1. University of Alberta

Introduction: DEAD box proteins are RNA helicases that function by modifying RNA secondary structure. DEAD box 1 (*DDX1*) is overexpressed in a subset of retinoblastoma, neuroblastoma and breast cancer tumours. In breast cancer, *DDX1* overexpression is associated with a poor prognosis. We previously reported that *DDX1* protein accumulates at DNA double strand breaks (DSBs) during genotoxic stress and promotes DSB repair by homologous recombination. In the current study, we investigate the role of *DDX1* in environmental stress responses.

Methods: Fluorescence microscopy was used to study the cellular localization of *DDX1* protein during stress. RNA targets of *DDX1* were identified by RNA immunoprecipitation sequencing (RIP-Seq) and confirmed with quantitative RT-PCR. Levels of *DDX1* target RNAs were measured by quantitative RT-PCR.

Results: We show that *DDX1* is recruited to stress granules (SGs) in cells exposed to a variety of environmental stressors including arsenite, hydrogen peroxide and thapsigargin (Figure 1). We also show that *DDX1* facilitates SG resolution during stress recovery. We identify a number of mRNAs bound to endogenous *DDX1*, including RNAs transcribed from genes previously implicated in stress responses (Figure 2). The amount of target RNAs bound to *DDX1* increases when cells are exposed to both acute (arsenite-induced) and chronic (paraquat-induced) oxidative stress. *DDX1* depletion results in reduced mRNA levels of its targets in the cytoplasm during oxidative stress, whereas *DDX1* overexpression stabilizes target mRNAs (Figure 3). Although *DDX1*'s RNA-binding property is critical to increased stability of its mRNA targets, RNA binding is not required for either localization of *DDX1* to SGs or *DDX1*-mediated SG resolution during recovery.

Discussion: Regulation of mRNA stability in cells exposed to environmental stress is poorly understood. In this study, we identify a number of *DDX1* target mRNAs and demonstrate that *DDX1* stabilizes these mRNAs in the cytoplasm during stress. Our results suggest *DDX1* functions in two aspects of stress responses by: (i) stabilizing its RNA targets in the cytoplasm, (ii) interacting with its non-RNA-binding partners in SGs to facilitate cellular recovery from stress. We propose that *DDX1* is an important player in the restructuring of RNA-containing molecules that underlie a wide spectrum of stress responses.

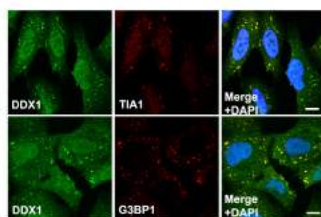


Figure 1. Localization of DDX1 in stress granules. U2OS cells were treated with 0.5 mM sodium arsenite for 45 min. Cells were fixed and immunostained with anti-DDX1 and anti-TIA1 or anti-G3BP1 (markers for SG) antibodies. Bar, 10 μ m.

Lei li figure 1.jpg

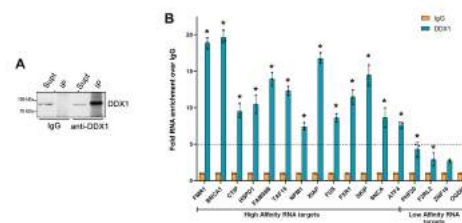


Figure 2. Identification of DDX1-bound RNAs. HeLa cells were UV-crosslinked and whole cell lysates were prepared. Lysates were immunoprecipitated with IgG or anti-DDX1 antibody. Immunoprecipitated RNAs were extracted, reverse transcribed and sequenced. (A) Western blot analysis of immunoprecipitated endogenous DDX1. Eight percent of supernatant was loaded next to 50% of IP for comparison. (B) Putative *DDX1* target mRNAs selected on the basis of 5X read count enrichment in *DDX1* RIP-Seq versus IgG RIP-Seq were confirmed by RT-qPCR. Fold enrichment of transcripts in *DDX1* RIP-Seq relative to IgG RIP-Seq which is set at 1. Error bars denote standard deviation. N = 3. * p < 0.05.

Lei li figure 2.jpg

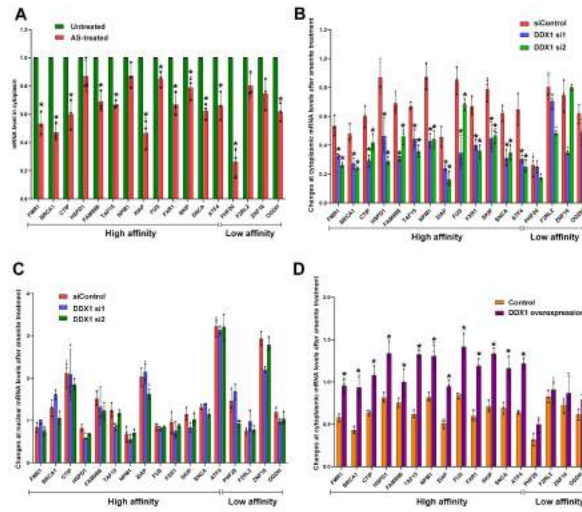


Figure 3. DDX1 protects its target RNAs in U2OS cells during stress. Control and DDX1-knockdown U2OS cells were treated with arsenite or left untreated, and cytoplasmic and nuclear fractions generated. Total RNA was isolated from each fraction, reverse transcribed, and RT-qPCR was carried out to examine the levels of DDX1 targets in each fraction. (A) Relative levels of cytoplasmic DDX1 mRNA targets in arsenite-treated cells compared to untreated cells (set at 1). (B) Relative levels of cytoplasmic DDX1 mRNA targets in DDX1-depleted vs control cells upon arsenite treatment. Values for control arsenite-treated cells are taken from (A). Values for DDX1 target mRNAs in arsenite-treated siControl, DDX1si1 and DDX1 si2 cells are relative to their respective siControl, DDX1 si1 and DDX1 si2 untreated counterparts, which were set at 1. (C) Relative levels of nuclear DDX1 mRNA targets in DDX1-depleted vs. control cells upon arsenite treatment. Changes in nuclear mRNA levels were analyzed as described in (B). (D) Cells were transfected with GFP vector or GFP-DDX1 expression constructs. Forty-eight hours after transfection, cells were treated with arsenite and fractionated. RNA isolation, reverse transcription and RT-qPCR quantification were performed as described above. Changes in cytoplasmic mRNA levels were analyzed as described in (B). Error bars represent standard deviation. N = 3. *: p < 0.05.

Lei li figure 3.jpg

VASA helicase GLH-1 drives the phase separation of perinuclear germ granules to promote the fidelity of piRNA-mediated genome surveillance

Tuesday, 6th July - 16:00: Poster Session 1-B - Poster - Abstract ID: 74

Dr. Wenjun Chen¹, **Mr. Jordan Brown**², **Dr. Shikui Tu**³, **Dr. Zhiping Weng**⁴, **Dr. Donglei Zhang**⁵,
Dr. Heng-Chi Lee²

1. University of Chicago, 2. The University of Chicago, 3. Shanghai JiaoTong University, 4. University of Massachusetts Medical School, 5. Huazhong University of Science and Technology

Introduction: piRNAs function as guardians of the genome by silencing foreign or selfish nucleic acids, such as transposons. Intriguingly, many piRNA pathway factors are enriched in perinuclear germ granules. These phase-separated granules are the major sites of mRNA export in germ cells, but whether their presence is required for piRNA biogenesis or function is not known. In addition, while VASA helicase GLH-1 has been shown to play a role in germ granule formation in *C. elegans*, how it regulates germ granule assembly is poorly understood.

Method: We analyzing various VASA *glh-1* *C. elegans* mutants (including gene-edited strains) with confocal microscopy, small RNA sequencing and mRNA sequencing.

Results: Here we show that VASA helicase GLH-1 couples distinct steps of its ATP hydrolysis cycle to regulate the formation and disassembly of germ granules. In addition, the FG repeats of GLH-1 promote the anchoring of germ granules at nuclear periphery, likely through interacting with the hydrogel formed by the FG-containing nucleoporin. Together, we found several of these VASA mutants are defective in the formation of perinuclear germ granules, resulting in the mislocalization of PIWI and other small RNA cofactors in *C. elegans*. These mutants were used to investigate the role of VASA and perinuclear germ granule in piRNA silencing. Interestingly, we found that these VASA mutant animals produce normal levels of piRNAs but are defective in triggering gene silencing by piRNAs. Furthermore, while piRNA-mediated transposon silencing is compromised without VASA, hundreds of endogenous genes become aberrantly silenced by piRNAs. These data suggest that VASA and perinuclear P granules are critical for piRNAs to identify foreign RNAs for gene silencing and to avoid the silencing of self RNAs. Finally, we found that VASA mutants exhibit a progressive sterility phenotype that correlates with accumulating piRNA-mediated gene misregulation over generations.

Discussion: Our data provide fundamental insights as to how an RNA helicase controls both the dynamics and location of germ granules. Furthermore, our study of VASA mutants provides an exciting example of how concentrating the small RNA machinery at the site of mRNA export to promote the fidelity of genome surveillance by small RNAs.

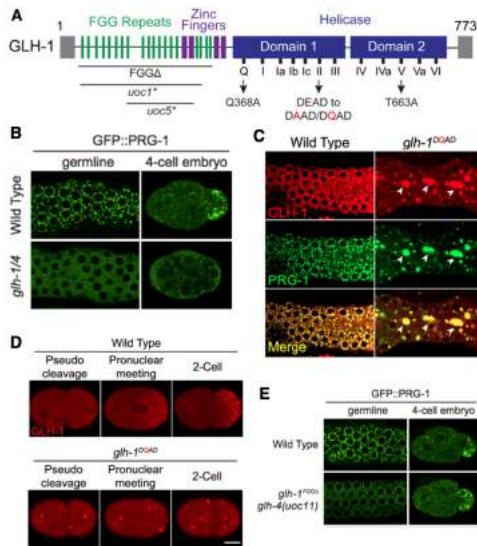


Figure 1. Various VASA helicase domains (A) of GLH-1 control the (B) formation, (C) granule dynamics, (D) sorting, and (E) nuclear anchoring of phase-separated germ (P) granules in *C. elegans*.

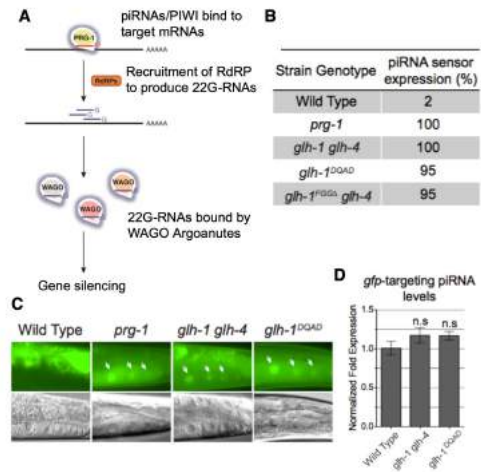


Figure 2. VASA mutants are defective in piRNA silencing but produce normal level of piRNAs.

(A) The piRNA silencing pathway (B&C) The expression of a GFP piRNA reporter in the indicated strains (D) qPCR showing the expression of the anti-*gfp* piRNA in the indicated strains.

Figure 1. vasa roles in germ granule formation .jpg

Figure 2 vasa in piRNA silencing.jpg

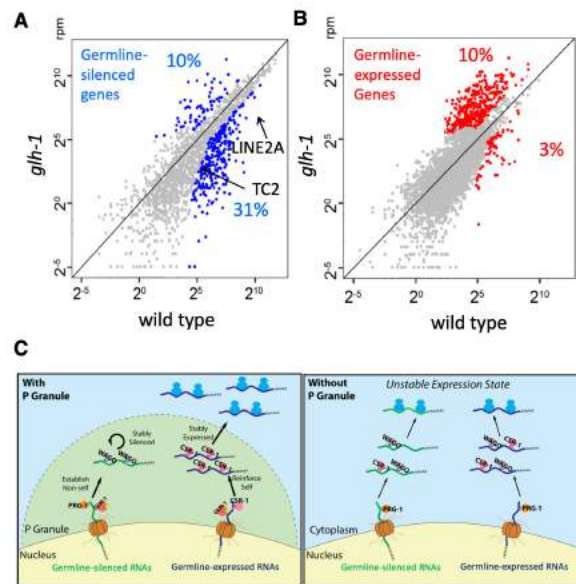


Figure 3. VASA promote the fidelity of genome surveillance by small RNAs. (A&B) The scatter blot showing (A) the overall reduction of secondary small RNAs, the WAGO 22G-RNAs, targeting germline-silenced genes, with two transposons highlighted, and (B) the overall increase of WAGO 22G-RNAs targeting functional germline-expressed genes in the VASA *glh-1* mutant (C) A model for the roles of VASA helicase GLH-1 in germ granule formation and genome surveillance

Figure 3 vasa in genome surveillance.jpg

Genome-wide impact of DEXH-box RNA helicases on RNA splicing and quality control

Tuesday, 6th July - 16:00: Poster Session 1-B - Poster - Abstract ID: 120

Dr. Qing Feng¹, Mr. Keegan Krick¹, Prof. Christopher Burge¹

1. MIT

Splicing is a multistage process mediated by the spliceosome. The transition between the sequential stages of splicing is controlled by spliceosome modulators that include four spliceosomal ATPase/DEXH-box RNA helicases (DHXs), DHX16, DHX38, DHX8, and DHX15, which are unique to the branching, exon-exon joining, mRNA releasing, and lariat releasing steps of splicing, respectively. In addition to their constitutive roles in spliceosome remodeling, various studies in cell-free systems have suggested that these spliceosomal DHXs also contribute to splicing quality control (QC)¹. During splicing QC, DHX16, DHX38, and DHX8 reject aberrant or suboptimal splicing intermediates at each corresponding step, while DHX15 disassembles rejected intermediates, to facilitate RNA extraction and recycling of spliceosomal components. Meanwhile, in mammalian cells, the scope and consequences of these splicing modulatory steps remain largely unknown.

To investigate the splicing regulatory and QC roles of spliceosomal DHXs, I have endogenously tagged each spliceosomal DHX with FKBP12^{F36V} degron via CRISPR/Cas9 gene-editing in cultured mammalian cells. To infer primary effects on splicing, I performed RNA sequencing experiments with both total and chromatin-associated nascent RNAs, upon dTAG13-mediated rapid depletion of each DHX (Fig1).

Differential gene expression and alternative splicing analysis revealed that acute depletion of certain DHXs leads to substantial changes in splicing, with only modest effects on global gene expression. Intron-centric analysis suggests a shared RNA QC mechanism between DHX38 and DHX15, resulting in changes in the abundance of hundreds or thousands of intron-containing transcripts that persist after separation from chromatin (Fig2). Splice site strength appears to be a key contributor to the direction of the observed splicing alterations, suggesting that these helicases modulate the competition between optimal and suboptimal splice sites in cells (Fig3).

References:

1. Semlow, D. R., & Staley, J. P. (2012). Staying on message: ensuring fidelity in pre-mRNA splicing. *Trends in biochemical sciences*, 37(7), 263-273.

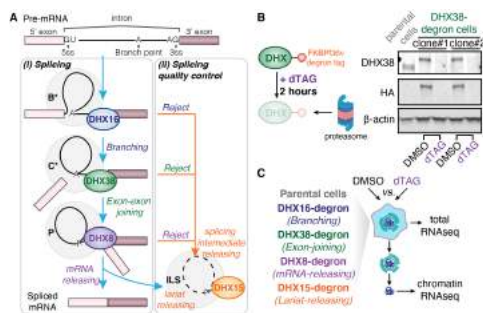


Figure 1. Stage-specific perturbation of splicing and splicing quality control. (A). (i) Stage-specific spliceosomal ATPase/DEXH-box RNA helicases DHX16 (navy), DHX38 (green), DHX8 (purple), and DHX15 (orange) drive the transition between different splicing steps. (ii) DHX16, DHX38, and DHX8 reject splicing quality control substrates to DHX15 for disassembly and degradation. (B). Left, diagram of rapid and targeted depletion of spliceosomal DEXH-box helicases (DHX) via dTAG-FKBP12^{F36V} degron system. Right, degron-tagged endogenous DHX38 undergo rapid depletion upon dTAG treatment, assayed via western blotting. (C). Total and chromatin-associated RNAs from parental control cells and four DHX-degron cell lines were collected upon dTAG treatment for RNAseq experiments.

Fig1.png

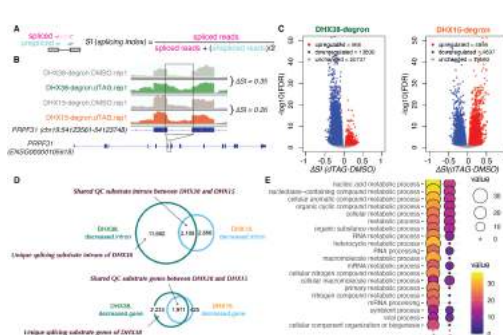


Figure 2. A shared QC mechanism between DHX38 and DHX15 suggested by shared introns containing splicing intermediate substrates. (A) Intron excision efficiency measured by splicing index (SI). (B) Heatmap coverage plot of shared intron excision of the indicated introns in PFPF31 in both DHX38- and DHX15-degron cells measured by dTAG. (C) Altered intron excision efficiency in DHX38-degron (left) and DHX15-degron (right) cells, comparing dTAG- vs. DMSO control treatments. (dRNAseq). Number of up- (red), down- (blue), and un- (grey) regulated introns are shown. (D) Venn diagram of shared QC substrates between DHX38 and DHX15. (E) Venn diagram of unique QC substrates between DHX38 and DHX15. (E) Gene Ontology enrichment analysis of genes that are shared QC substrates between DHX38 and DHX15 (Shared) or unique splicing substrate genes of DHX38 (Unique).

Fig2.png

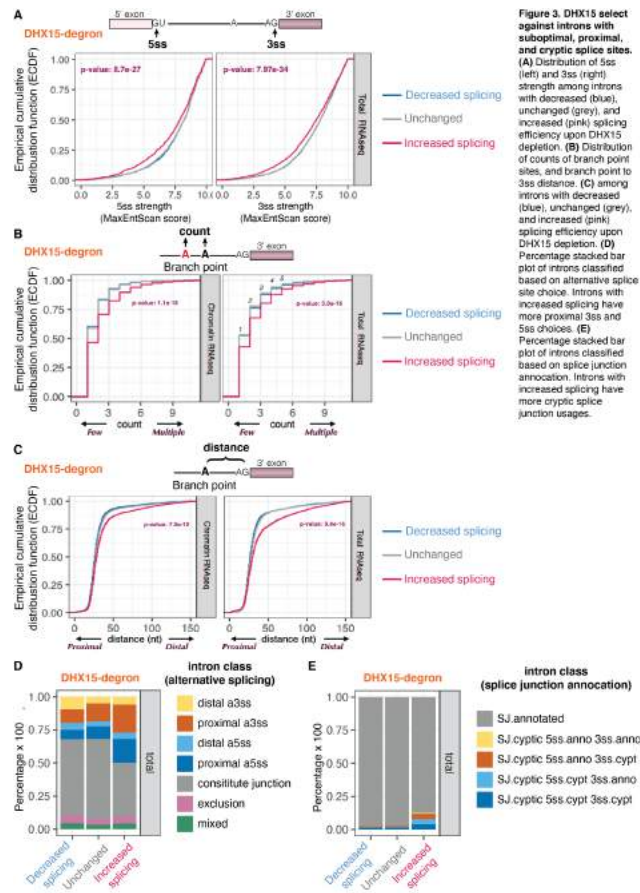


Figure 3. DHX15 select against introns with suboptimal, proximal, and cryptic splice sites. (A) Distribution of 5ss (left) and 3ss (right) strength among introns with decreased (blue), unchanged (grey), and increased (pink) splicing efficiency upon DHX15 depletion. (B) Distribution of counts of branch point sites, and branch point to 3ss distance. (C) among introns with decreased (blue), unchanged (grey), and increased (pink) splicing efficiency upon DHX15 depletion. (D) Percentage stacked bar plot of introns classified based on alternative splice site choice. Introns with increased splicing have more proximal 3ss and 5ss choices. (E) Percentage stacked bar plot of introns classified based on splice junction annotation. Introns with increased splicing have more cryptic splice junction usages.

Fig3.png

Sister chromatid exchange events and genome stability in the absence of RECQL5 helicase

Tuesday, 6th July - 16:00: Poster Session 1-B - Poster - Abstract ID: 149

Dr. Zeid Hamadeh¹, Dr. Peter Lansdorp¹

1. University of British Columbia

Introduction

Helicases are a highly conserved motor protein responsible for interacting with and unwinding canonical and non-canonical DNA structures. The RecQ class of helicases, known to suppress illegitimate recombination, are implicated in aging and cancer with three of the five human RecQ helicases directly linked to premature aging syndromes characterized by strong cancer predisposition (Figure 1). While no human disease has been associated with the RECQL5 helicase, loss of this gene in cells is known to result in elevated double strand breaks and sister chromatid exchange events (SCEs), a phenotype of genome instability similar to what is observed in RecQ helicase-linked diseases of strong cancer predisposition. Until recently, studying SCEs has been limited to cytogenetic assays that map SCE as changes in chromosome staining patterns at megabase resolution.

Methods

We generated single and double knockout models for RECQL5 and BLM using CRISPR/Cas9 in the human haploid cell line, KBM7. We also used single cell template strand sequencing (Strand-seq) to generate directional whole genome sequencing libraries. These sequencing libraries allowed us to map SCEs to the genome using custom bioinformatic approaches to improve resolution and accuracy of SCE detection.

Results

We were able to map SCEs as changes in template strand orientation before and after loss of RECQL5 at kilobase resolution. This is several orders of magnitude higher resolution than what was previously characterized. We show that SCEs in cells lacking BLM and RECQL5 occur near guanine quadruplex motifs and common fragile sites.

Discussion

These findings further supporting the role of these genes in suppressing inappropriate recombination at specific genomic elements. Uncovering the role of DNA helicases in DNA repair and replication pathways is critical for understanding their significance in cancer and aging. Strand-seq offers a unique method to study helicases by mapping the location of SCEs arising in their absence.

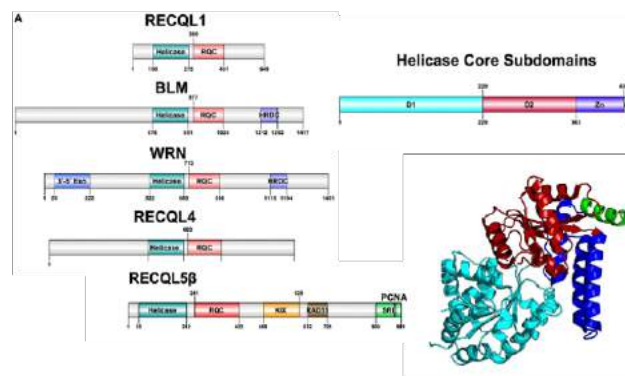


Figure1 recq helicases.png

Kinetics of Nucleotide Binding to the gp16 ATPase

Tuesday, 6th July - 16:00: Poster Session 1-C - Poster - Abstract ID: 103

Mr. Aaron Morgan¹, Dr. Christopher Fischer¹, Dr. Paul Jardine², Dr. Allen Eastlund²

1. University of Kansas, 2. University of Minnesota

The gp16 ATPase is the constituent subunit of the pentameric dsDNA (Double-stranded Deoxyribonucleic Acid) translocation motor of the *B. subtilis* Φ 29 bacteriophage. Although recent single-molecule studies have provided tantalizing clues about the activity of this motor, the mechanism by which the gp16 subunits couple the energy obtained from the binding and hydrolysis of ATP to the mechanical work of dsDNA translocation remains unknown. To address this need, we have characterized the binding of fluorophore labeled ATP and ADP to monomeric gp16 using a stopped-flow fluorescence assay. These experiments show that the binding of these nucleotides occurs through a single-step mechanism with corresponding affinities of (523.8 ± 247.3) nM for ATP and a lower limit of $30\mu\text{M}$ for ADP. When analyzed through the lens of changes in free energy of the system, this difference in binding affinities is reasonable for a cyclical process of binding, hydrolysis, and product release. In addition to answering questions about the activity of monomeric gp16, these results are also a necessary step in constructing a model for inter-subunit communication within the pentameric gp16 motor.

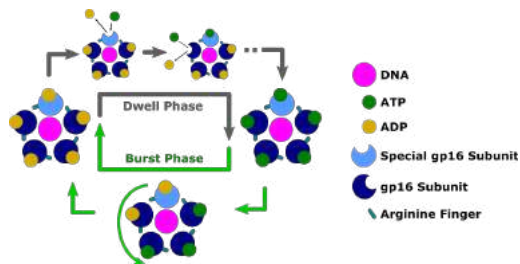


Figure 3.png

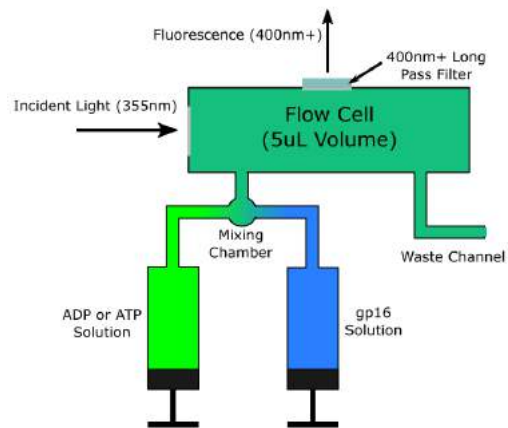


Figure 4.png

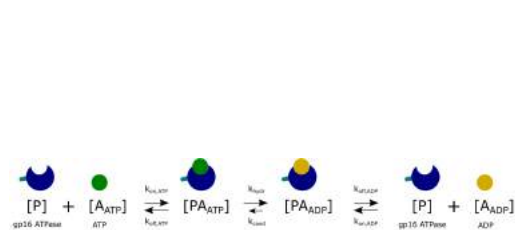


Figure 5.png

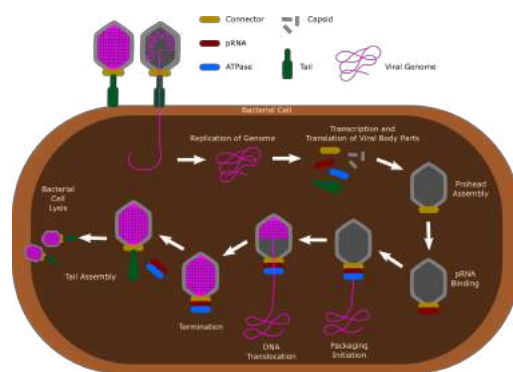


Figure 1.png

Three charged amino acid residues at the extreme C-terminus of the BFK20 gp41 helicase play a role in the ATPase activity of the protein

Tuesday, 6th July - 16:00: Poster Session 1-C - Poster - Abstract ID: 121

Dr. Nora Halgasova¹, Dr. Gabriela Bukovska¹

1. Department of Genomics and Biotechnology, Institute of Molecular Biology, Slovak Academy of Sciences, Dubravská cesta 21, 845 51 Bratislava

INTRODUCTION: BFK20 is a lytic phage of *Brevibacterium flavum*. Two helicases are encoded in the BFK20 genome. Gp43 is a multifunctional protein with a primase-polymerase and a helicase domain with conserved motifs of SF4 family helicases. Gp41 has a helicase core with conserved motifs of SF2 family helicases, and an accessory C-terminal region without defined specificity (Figure 1). Deletion of this region caused a significant decrease in the ATPase activity (Halgasova et al., 2018). A deletion mutant without last 56 C-terminal amino acids also showed only low ATPase activity (Halgasova, unpublished results). We performed site directed mutagenesis of five amino acids in the largest helix located at the extreme C-terminus of gp41 to verify their function.

METHODS: PCR based overlap extension approach was used to perform site-directed mutagenesis. Mutation primers were designed for amino acids K516, R518, D520, D521, E522. Mutated forms of *orf41* were cloned into pET28a+ vector. This strategy resulted in synthesis of five mutants each with one amino acid replaced by an alanine. Point mutants were isolated by IMAC and their ATPase activities were tested by colorimetric plate assay in the presence or absence of DNA. The results were compared to those obtained for wild type-like protein gp41HN with strong DNA dependent ATPase activity.

RESULTS: ATPase activity rates of individual mutant proteins in comparison with gp41HN are in Figure 2. The ATPase activities of mutant proteins gp41K516A, gp41R518A and gp41D521A were significantly impaired, indicating that charged residues at the extreme C-terminus of the gp41 helicase are important for its ATPase activity.

DISCUSSION: For proper function of many helicases not only residues in the helicase core, but also those in accessory regions are important. Amino acid residues in the extreme C-terminal region of gp41 play a role in the ATPase activity and probably are necessary for the function of this phage helicase. This work emphasizes the role of accessory domains in helicases function.

This study was supported by VEGA Grant 2/0139/18.

References:

Halgasova, N., Matuskova, R., Kraus, D., Tkacova, A., Balusikova, L., Bukovska, G., 2018. Gp41, a superfamily SF2 helicase from bacteriophage BFK20. *Virus Res.* 245, 7-16.

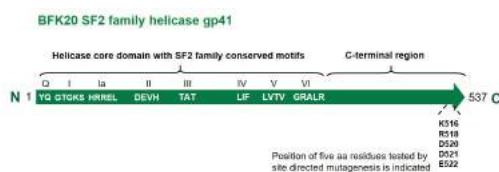


Figure 1.jpg

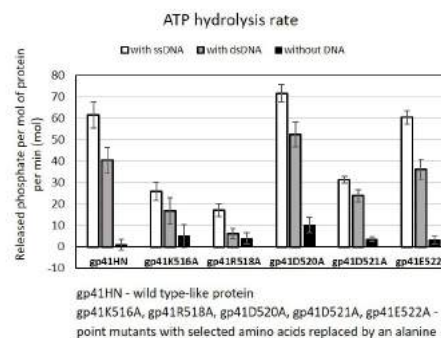


Figure 2.jpg

How to limit the speed of a motor - the intricate regulation of the XPB ATPase and translocase in TFIIH

Tuesday, 6th July - 16:00: Poster Session 1-C - Poster - Abstract ID: 123

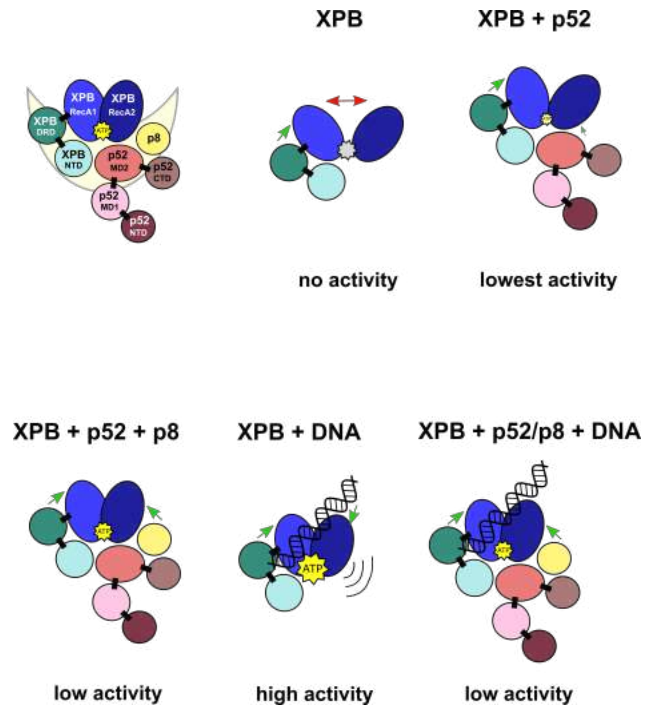
***Ms. Jeannette Kappenberger*¹, *Dr. Wolfgang Kölmel*¹, *Dr. Elisabeth Schönwetter*¹, *Mr. Tobias Scheuer*¹, *Ms. Julia Wörner*¹, *Dr. Jochen Kuper*¹, *Prof. Caroline Kisker*¹**

1. Rudolf Virchow Center for Integrative and Translational Bioimaging

The multi-subunit complex TFIIH plays a central role in the two cellular processes nucleotide excision repair (NER) and transcription initiation. Both processes crucially rely on the ATPase activity of the SF2 helicase XPB, which is an integral subunit of the general transcription factor TFIIH. Although XPB possesses all seven helicase motifs, it does not exhibit the typical helicase activity but rather acts as a double stranded DNA translocase. Defects of XPB are associated with the autosomal recessive disorders Xeroderma Pigmentosum and trichothiodystrophy and rarely with combined features of Xeroderma Pigmentosum and Cockayne syndrome.

We investigated the regulatory network that controls XPB within TFIIH and show that both, DNA and the TFIIH subunits p52 and p8 stimulate XPB's ATPase activity. Intriguingly, the lower p52/p8-mediated activation is the dominating factor when both activators are present simultaneously, rendering p52/p8 to be an internal activator and speed limiter at the same time. We therefore redefine p52/p8 as XPB's master regulator. We extended our studies towards XPB's DNA translocase activity and show that XPB only exhibits translocase activity, when it is incorporated into core TFIIH. The NER factor XPA further stimulates the translocase activity without affecting XPB's ATPase activity. Additionally, we pursued a correlative mutagenesis study of the p52-XPB interface, which led to the identification of critical p52 residues for the activation of XPB.

We set our analysis into the context of the recently published TFIIH structures, which allowed us to generate a model for the intricate activation and activity control mechanism of XPB's enzymatic function. Combined, our data reveal that XPB is tightly controlled within the scaffold of TFIIH and this regulation is embedded on different levels thereby being ideally suited to function in the underlying cellular processes XPB is involved in.



How to limit the speed of a motor.png

A rotary-mechanism for GTP hydrolysis by the AAA+ protein McrB stimulated by the endonuclease McrC

Tuesday, 6th July - 16:00: Poster Session 1-C - Poster - Abstract ID: 135

Prof. Saikrishnan Kayarat¹

1. Indian Institute of Science Education and Research Pune

Amongst AAA+ proteins McrB is unique in binding and hydrolysing GTP. McrB together with McrC forms the McrBC complex. McrBC is a modification-dependent restriction enzyme that cleaves methylated foreign DNA entering *Escherichia coli* and thus preventing bacteriophage infection or regulating horizontal gene transfer. The GTPase activity of McrB is stimulated upon complexation of McrB with the endonuclease McrC. Activation of the endonuclease for DNA cleavage is powered by the GTPase McrB. The architecture of McrBC and the mode of regulation of its GTPase activity by the endonuclease subunit had remained unknown. Using electron cryo-microscopy, we determined a 3.6 Angstrom structure of a construct of McrB, which is deficient in DNA binding but is GTPase active, in complex with McrC. McrBC has a dumbbell-like architecture in which two hexameric rings of McrB are bridged by a McrC dimer. McrC interacts asymmetrically with McrB protomers and inserts a stalk into the pore of the ring - an architecture reminiscent of the γ subunit interacting with the $\alpha_3\beta_3$ hexamer of F₁-ATPase. Complexation of McrB with McrC altering the interactions made by critical residues at and near the GTPase active site. The six nucleotide-binding sites, of which three consecutive sites are occupied by the GTP analogue GMPPNP and the remaining three by GDP, provide snapshots of a sequential mode of GTP hydrolysis.

Insertion of a flexible linker alters winged helix domain dynamics affecting substrate binding and unwinding activity of human RECQ1

Tuesday, 6th July - 16:00: Poster Session 1-C - Poster - Abstract ID: 151

***Ms. Tulika Das*¹, *Ms. Swagata Mukhopadhyay*¹, *Dr. Agneyo Ganguly*¹**

1. Department of Biotechnology, Indian Institute of Technology Kharagpur, India

RecQ helicases are SF2 helicases that can recognize and unwind wide spectrum of DNA substrates including duplex, triplex, quadruplex and Holliday junctions. Comparison of structures of human BLM, RECQ1 and *E.coli* RecQ helicases reveal considerable structural similarities in the helicase core domains with difference in orientation of the winged helix domain (WH). Structural alignment reveals that the winged helix domain (WH) of human RECQ1 and *E. coli* RecQ are differently oriented with respect to the rest of the protein domains. The WH in *E.coli* RecQ is positioned perpendicular to the D1-D2 domain imparting an open conformation; whereas in human RECQ1 it is positioned laterally to the helicase domains and directly beneath the helical hairpin (HH) of the zinc binding domain thereby assuming a closed conformation. In an attempt to understand the contribution of WH domain conformation in substrate recognition and functional diversity, we have inserted a glycine-serine rich linker (GGGGSGGGGS) between the Zn domain and WH domains of near full length human RECQ1 (RECQ1^{T1}) so as to impart more flexibility to the WH and examined the effects on enzyme functioning. We tested the ability of the mutant RECQ1^{T1Lk} to unwind a 20 mer fully complementary blunt duplex DNA which is not a preferred substrate for RECQ1. The mutant RECQ1^{T1Lk} could unwind a 20 mer duplex substrate more efficiently as compared to the wild type RECQ1^{T1}. FRET based unwinding experiments confirmed that

RECQ1^{T1Lk}

exhibited a faster rate of unwinding as compared to the RECQ1^{T1}. DNA binding experiments using fluorescence anisotropy demonstrate that the linker construct exhibited 2 fold higher affinity for blunt duplex and 3 fold higher affinity for 3'tailed duplex in presence of ADPNP as compared to the wild type enzyme. To gain an insight into the structural flexibility and alterations in C-terminal domain conformation molecular dynamics simulation was performed followed by Principal Component Analysis (PCA). Molecular dynamics simulation study suggests altered domain dynamics in RECQ1^{T1Lk} as compared to RECQ1^{T1}. Overall these data indicates that insertion of a flexible linker affects conformational dynamics of the WH domain in nucleotide bound form of RECQ1 exhibiting altered substrate binding and unwinding activity.

Molecular determinants for dsDNA translocation by the transcription-repair coupling and evolvability factor Mfd

Tuesday, 6th July - 16:00: Poster Session 1-C - Poster - Abstract ID: 154

***Prof. Alexandra Deaconescu*¹, *Dr. Christiane Brugger*¹, *Dr. Margaret Suhanovsky*¹, *Dr. Cheng Zhang*², *Mr. David Kim*¹, *Dr. Amy Sinclair*¹, *Dr. Dmitry Lyumkis*²**

1. Brown University, 2. Salk Research Institute

Mfd couples transcription to nucleotide excision repair, and acts on RNA polymerases when elongation is impeded. Depending on impediment severity, this action results in either transcription termination or elongation rescue, which rely on ATP-dependent Mfd translocation on DNA. Due to its role in antibiotic resistance, Mfd is also emerging as a prime target for developing anti-evolution drugs. Here we report the structure of DNA-bound Mfd, which reveals large DNA-induced structural changes that are linked to the active site via ATPase motif VI. These changes relieve autoinhibitory contacts between the N- and C-termini and unmask UvrA recognition determinants. We also demonstrate that translocation relies on a threonine in motif Ic, widely conserved in translocases, and a family-specific histidine near motif IVa, reminiscent of the “arginine clamp” of RNA helicases. Thus, Mfd employs a mode of DNA recognition that at its core is common to ss/ds translocases that act on DNA or RNA.

Mechanism and regulation of an RNA-guided helicase-nuclease, CRISPR-Cas3

Tuesday, 6th July - 17:00: Oral Session - Oral - Abstract ID: 4

Prof. Ailong Ke¹

1. Cornell University

CRISPR-Cas systems regulate their nuclease activity in an RNA-guided fashion – only the complementary DNA/RNA targets are degraded. Interestingly, the signature nuclease in Type I CRISPR-Cas is a nuclease and superfamily II helicase fusion enzyme. This enzyme, Cas3, is highly processive. Once activated, it is capable of deleting 3-30 kb of dsDNA through concerted DNA translocation and cleavage actions. Not surprisingly, its recruitment and activation is tightly regulated in the CRISPR system to prevent misfiring at the off-target sites. I will present a comprehensive mechanistic analysis of the CRISPR-Cas3 machinery, which is based on the series of structural analysis from my group, and on the collaborative work with Drs. Ilya Finkelstein and Yan Zhang from single molecule and genome editing efforts.

Vectorial folding of telomere overhang by a superhelicase, Rep-X

Tuesday, 6th July - 17:15: Oral Session - Oral - Abstract ID: 67

Dr. Sua Myong¹, Dr. Tapas Paul¹, Prof. Taekjip Ha¹

1. Johns Hopkins University

Telomere overhang which bears tandem repeats of TTAGGG folds into G-quadruplex (G4). Unlike in an experimental setting in which the full sequence is allowed to fold at once, the overhang is synthesized directionally (5' to 3') and released segmentally by a specialized enzyme, telomerase in cells. To depict such vectorial G4 folding process, we employed a superhelicase, Rep-X which can unwind DNA to release the TTAGGG repeats in 5' to 3' direction. We demonstrate that the folded conformation achieved by the pre-folding of full sequence is significantly different from that of the vectorial folding for two to eight TTAGGG repeats. Strikingly, the vectorially folded state leads to a remarkably higher access to complementary C-rich strand and a telomere binding protein POT1, reflecting a less stably folded state resulting from the vectorial folding. Importantly, our study points to an inherent difference between the co-polymerizing and post-polymerized folding of telomere overhang that can impact telomere architecture and downstream processes.

Design and application of force-activated DNA substrates for helicase binding and unwinding studies

Tuesday, 6th July - 17:30: Oral Session - Oral - Abstract ID: 58

*Mr. Arnulf Taylor*¹, *Mr. Stephen Okoniewski*¹, *Mr. Lyle Uyetake*¹, *Prof. Thomas Perkins*¹

1. JILA

Nucleic-acid processing enzymes are now routinely studied with single-molecule force spectroscopy using optical traps and magnetic tweezers. Substrates containing a combination of single-stranded DNA (ssDNA) and double-stranded DNA (dsDNA) are particularly useful for studies of helicases, as exemplified by the hairpin-unwinding assay (Fig. 1A). Importantly, this assay provides a 3-fold mechanical enhancement in the measured signal. Typically, DNA structures containing both ssDNA and dsDNA are assembled using a laborious, low-yield three-way hybridization (Fig. 1B, left). Here, we developed a more efficient method based on force-activation. An ssDNA segment within a larger dsDNA construct is delineated by site-specific nicks of the DNA duplex (Fig. 1B, right). The ssDNA segment is induced to dissociate from the μm -scale dsDNA construct by briefly pulling it into the threshold of DNA's overstretching transition (Fig. 1C). Using this scheme, we have designed and successfully force activated ssDNA segments of up to 1000 base pairs by engineering a 50%-GC segment to have no adjacent GC base pairs. We have developed the complex structure used in the hairpin-unwinding assay, where a hairpin is positioned adjacent to a short segment of ssDNA used to load a helicase. We have varied the length and GC content of these hairpins and successfully force-activated 20-, 40-, and 120-bp hairpins and up to 75% GC for the 20-bp hairpin. We also force-activated a 120-bp hairpin construct which alternates between 50% GC and 0% GC within the same hairpin. This construct allows us to study GC dependence of helicase unwinding for the same individual molecule. Two major benefits of our force-activated substrates are the ability to collect many data traces without exchanging buffer and each hairpin has a precisely defined user-controlled activation time. This well-defined start time allows for study of enzyme binding at a single-molecule level. For example, we measured the on-rate of *E. coli* RecQ, a 3'-to-5' DNA helicase (Fig. 2). The force activation process takes ~ 0.1 s for the hairpin construct and ~ 0.3 s for the 1000-bp construct. Finally, we are working on merging the improved throughput of force-activated substrates with resolving 1-bp steps of helicase stepping at sub-s time scales.

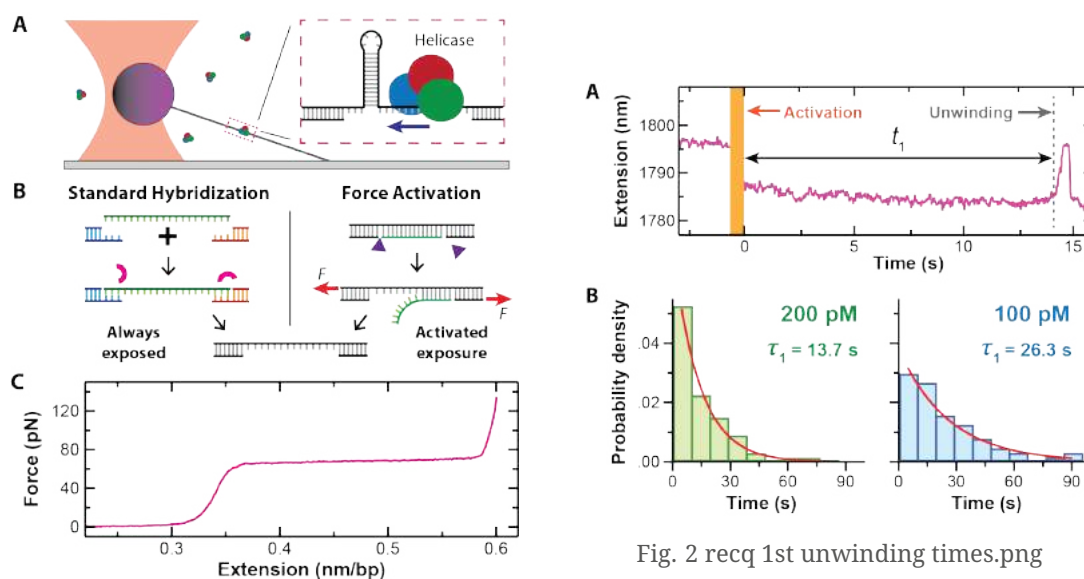


Fig. 1 force-activated substrates.png

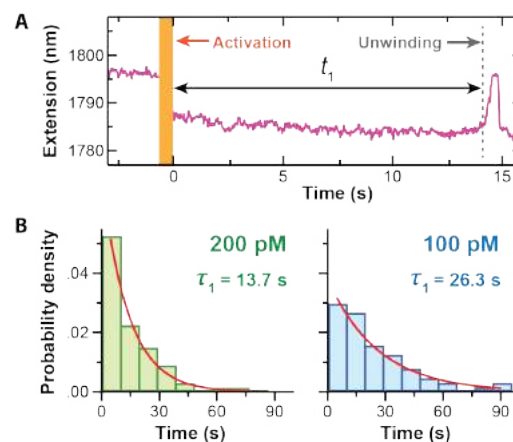


Fig. 2 recq 1st unwinding times.png

Regulatory mechanisms of the RNA exosome helicases

Tuesday, 6th July - 18:30: Keynote 3 - Oral - Abstract ID: 91

***Prof. Elena Conti*¹, *Dr. Piotr Gerlach*¹, *Mr. Alexander Koegel*¹, *Mr. Felix Sandmeir*¹, *Dr. Ingmar Schaefer*¹, *Mr. Fabien Bonneau*¹**

1. Max Planck Institute of Biochemistry

The exosome complex is a conserved RNA-degradation machinery present in both the nucleus and the cytoplasm of all eukaryotes studied to date. In the nucleus, the RNA exosome functions in the decay and processing of a large variety of non-coding transcripts as well as pre-mRNAs. In the cytoplasm, it primarily targets mRNAs. The exosome core complex has an irreversible action on any accessible RNA, yet it lacks substrate specificity. Access to substrates is controlled by compartment-specific exosome cofactors and adaptors that revolve around the recruitment and regulation of two RNA helicases, nuclear Mtr4 and cytoplasmic Ski2. Ski2 and Mtr4 harbour similar biochemical and structural properties. However, the two helicases differ in aspects that go beyond the mere presence (in Mtr4) or absence (in Ski2) of a nuclear localization signal and that may belie each helicase's ability to support their compartment-specific roles. In particular, Mtr4/hMTR4 interacts with a variety of adaptor proteins, forming mutually exclusive complexes that target the different types of RNA substrates in the nucleus. In contrast, Ski2/hSKI2 helicase is part of a single assembly, the Ski complex, which targets mainly ribosome-bound mRNAs. Recent work suggests that these helicases are regulated by gatekeeping mechanisms and architectural remodeling that in turn control RNA channeling to the RNA-degrading exosome, with unexpected conservation amongst the cytoplasmic and nuclear helicase-exosome complexes.

RNA sensing mechanisms in the Mtr4 arch domain influence RNA helicase activity and conformational dynamics

Tuesday, 6th July - 19:00: Oral Session - Oral - Abstract ID: 116

Prof. Sean Johnson¹

1. Utah State Univeristy

Mtr4 is an essential eukaryotic RNA helicase that is required for activation of the nuclear RNA exosome. One of the unique structural features of Mtr4 is a large arch domain that spans one face of the helicase core. Previous work in our lab demonstrated that the arch domain plays an important role in helicase activity, but structures are lacking that clearly define how the arch engages RNA substrates. To better define the Mtr4-RNA interface, we have now completed a detailed biochemical and hydrogen-deuterium exchange (HDX) analysis of Mtr4 in the presence of multiple RNA substrates. Our study demonstrates that the arch domain recognizes RNA substrates, interacting directly with the fist/KOW region of the arch. Importantly, differences in binding affinity are observed depending on the size and secondary structure of the RNA. Furthermore, arch-RNA interactions affect RNA unwinding activity; when those interactions are removed, unwinding activity is altered. The HDX analysis reveals RNA interactions throughout the helicase core that are consistent with existing structures, and additionally reveals interactions along the fist and surface of the core. Surprisingly, distinct deuterium uptake kinetics are observed in the arms of the arch, indicating that RNA binding induces a large conformational change in the arch. A continuous pattern of protection along the surface of the fist and core upon RNA binding further suggests that the arch adopts a closed conformation that places the fist adjacent to the RecA2 and HB domains. This conformational change is completely lost when the fist is removed, demonstrating that fist-RNA interactions drive the observed arch dynamics.

Structure of the catalytic core of the Integrator complex

Tuesday, 6th July - 19:15: Oral Session - Oral - Abstract ID: 35

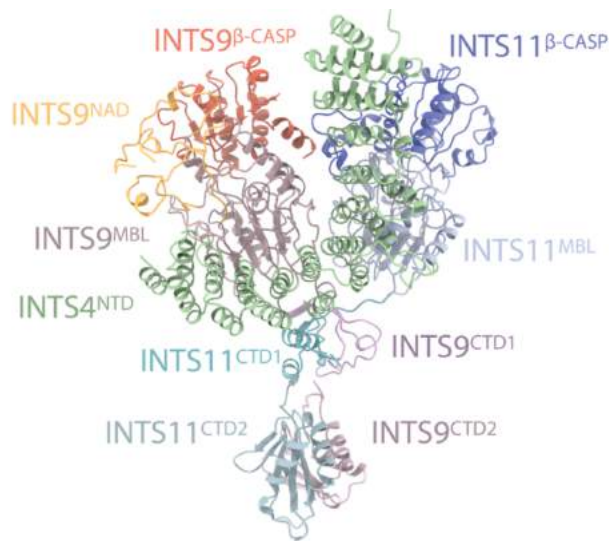
Mr. Moritz Pfeleiderer¹, Dr. Wojciech Galej¹

1. EMBL

The Integrator is a specialized 3' end-processing complex involved in cleavage and transcription termination of a subset of nascent RNA polymerase II transcripts, including small nuclear RNAs (snRNAs)[1]. We provide evidence of the modular nature of the Integrator complex by biochemically characterizing its two subcomplexes, INTS5/8 and INTS10/13/14. Using cryoelectron microscopy (cryo-EM), we determined a 3.5-Å-resolution structure of the INTS4/9/11 ternary complex, which constitutes Integrator's catalytic core [2]. Our structure reveals the spatial organization of the catalytic nuclease INTS11, bound to its catalytically impaired homolog INTS9 via several interdependent interfaces. INTS4, a helical repeat protein, plays a key role in stabilizing nuclease domains and other components. In this assembly, all three proteins form a composite electropositive groove, suggesting a putative RNA binding path within the complex. Comparison with other 3' end-processing machineries points to distinct features and a unique architecture of the Integrator's catalytic module.

[1] D Baillat, EJ Wagner (2015). Integrator: surprisingly diverse functions in gene expression. Trends Biochem Sci 40(5):257-64

[2] MM Pfeleiderer, WP Galej (2021). Structure of the catalytic core of the Integrator complex. Molecular cell 81 (6), 1246-1259.



Ints93-casp.png

Structural basis for the activation of the DEAD-box RNA helicase DbpA by the nascent ribosome

Tuesday, 6th July - 19:30: Oral Session - Oral - Abstract ID: 39

*Dr. Jan Philip Wurm*¹, *Prof. remco sprangers*¹

¹. University of Regensburg

The ATP-dependent DEAD-box RNA helicase DbpA from *E. coli* functions in ribosome biogenesis. DbpA is targeted to the nascent 50S subunit by an ancillary, C-terminal RNA recognition motif (RRM) that specifically binds to hairpin 92 (HP92) of the 23S rRNA (Fig. 1). The interaction between HP92 and the RRM is required for the helicase activity of the RecA-like core domains of DbpA. Here, we elucidate the structural basis by which DbpA activity is endorsed when the enzyme interacts with the maturing ribosome. We used NMR spectroscopy to show that the RRM and the C-terminal RecA-like domain tightly interact (Fig. 2). This orients HP92 such that this RNA hairpin can form electrostatic interactions with a positively charged patch in the N-terminal RecA-like domain. Consequently, the enzyme can stably adopt the catalytically important, closed conformation. The substrate binding mode in this complex reveals that a region 5' to helix 90 in the maturing ribosome is specifically targeted by DbpA (Fig. 3). Finally, our results indicate that the ribosome maturation defects induced by a dominant negative DbpA mutation are caused by a delayed dissociation of DbpA from the nascent ribosome. Taken together, our findings provide unique insights into the important regulatory mechanism that modulates the activity of DbpA.

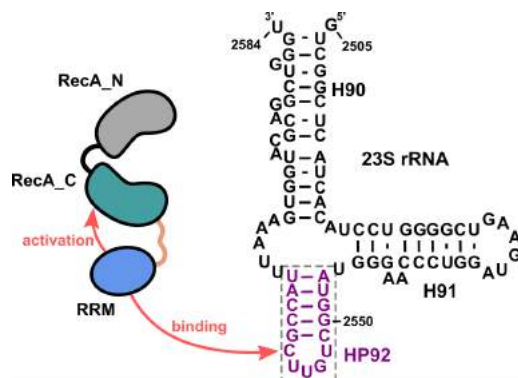


Fig1.png

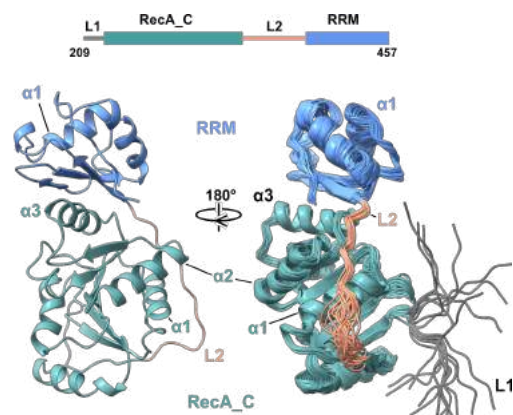


Fig2.png

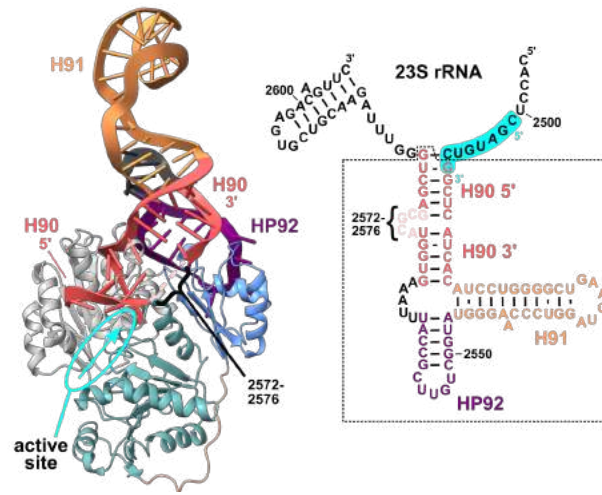


Fig3.png

Activation of SF1 DNA Helicases by Protein Accessory Factors

Wednesday, 7th July - 14:00: Keynote 4 - Oral - Abstract ID: 69

Dr. Timothy Lohman¹

1. Department of Biochemistry and Molecular Biophysics, Washington University School of Medicine, 660 S. Euclid Ave., St. Louis, MO 63110

DNA helicases have two activities: DNA unwinding and single stranded (ss) DNA translocation, both coupled to ATP hydrolysis. In fact, ssDNA translocation, rather than DNA unwinding, is often the activity required for enzyme function, for example in the removal of proteins from ssDNA. Hence, it makes sense that these two activities can be uncoupled and that the two functions need to be regulated. When the ss DNA translocase activity is required, helicase activity needs to be suppressed. When DNA unwinding activity is required, the helicase activity needs to be activated. One way to accomplish this is to have different forms of the enzyme involved in the two activities. The monomeric forms of *E. coli* SF1 helicases, UvrD and Rep, are rapid and processive ssDNA translocases, but show no helicase activity in the absence of force applied to the DNA junction. We will discuss recent studies of the mechanisms by which the helicase activities of the monomeric UvrD and Rep ssDNA translocases are activated by the protein accessory factors, *E. coli* MutL and *E. coli* PriC, respectively (supported by NIH R35GM136632).

Large-scale ratcheting in a bacterial DEAH/RHA-type RNA helicase that modulates antibiotics susceptibility

Wednesday, 7th July - 14:30: Oral Session - Oral - Abstract ID: 124

Ms. Lena Grass¹, **Dr. Jan Wollenhaupt**², **Ms. Tatjana Barthel**², **Dr. Iwan Parfentev**³, **Prof. Henning Urlaub**³, **Dr. Bernhard Loll**¹, **Dr. Eberhard Klauck**¹, **Prof. Haike Antelmann**¹, **Prof. Markus Wahl**¹

1. Freie Universität Berlin, 2. Helmholtz-Zentrum Berlin, 3. Max-Planck-Institute for Biophysical Chemistry

Introduction

Bacteria are unicellular organisms and therefore constantly exposed to unpredictable and rapidly changing environmental factors. In order to cope with, e.g., temperature changes, oxidative stress or antibiotic substances, bacteria rely on RNA-binding and RNA-remodeling proteins to regulate gene expression post-transcriptionally. RNA-dependent nucleoside-triphosphatases of the DEAH/RHA family constitute important post-transcriptional gene regulatory proteins in bacteria, but their molecular mechanisms are presently poorly understood. HrpA represents a particularly interesting member of this family as previous studies showed its impact on infectivity (*Borrelia burgdorferi*) or flagella production (*Escherichia coli*). However, no 3D structure and little mechanistic detail are presently available for HrpA proteins.

Methods

X-ray crystallography, cross-linking/mass spectrometry, survival assays, fluorescence polarization, fluorescence/stopped-flow analysis.

Results and Discussion

Here, we show that the DEAH/RHA protein, HrpA, from *Escherichia coli* is a 3'-to-5' RNA helicase that is required to modulate bacterial survival under diverse antibiotics treatments. *Via* knock-out and rescue experiments, we demonstrate that an *E. coli hrpA* mutant is impaired in survival compared to a wild type (WT) strain after exposure to certain antibiotics (Figure 1A). Near-WT levels of survival can be restored in the *hrpA* mutant only by complementation with helicase-active *ecHrpA* variants, suggesting a key role of *ecHrpA* in environmental adaptation mechanisms based on its helicase activity (Figure 1B). Limited proteolysis, crystal structure analysis and functional assays showed that HrpA contains an N-terminal DEAH/RHA helicase cassette preceded by a unique N-terminal domain and followed by a large C-terminal region that modulates the helicase activity. Structures of an expanded HrpA helicase cassette in the apo and RNA-bound states in combination with cross-linking/mass spectrometry revealed ratchet-like domain movements upon RNA engagement, much more pronounced than hitherto observed in related eukaryotic DEAH/RHA enzymes (Figure 2). Structure-based functional analyses delineated transient inter-domain contact sites that support substrate loading and unwinding, suggesting that similar conformational changes support RNA translocation (Figure 3). HrpA's RNA-bound conformation further revealed an unwinding-relevant stacking triad within an OB-fold domain that seems to act as a strand-separator element (Figure 3). Our results indicate that HrpA is an interesting target to interfere with bacterial tolerance toward certain antibiotics and suggest possible interfering strategies.

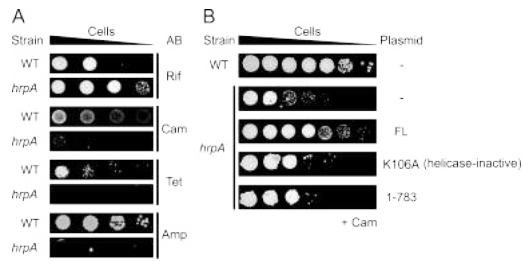


Fig 1 survival assays under antibiotic stress conditions.png

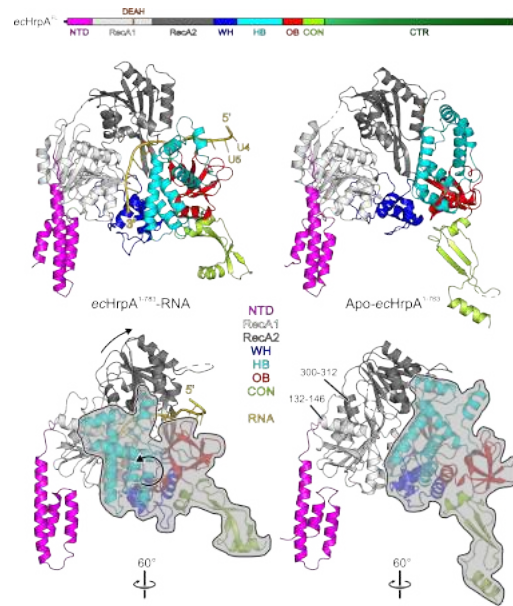


Fig 2 crystal structures of hrpa-rna and apo-hrpa.png

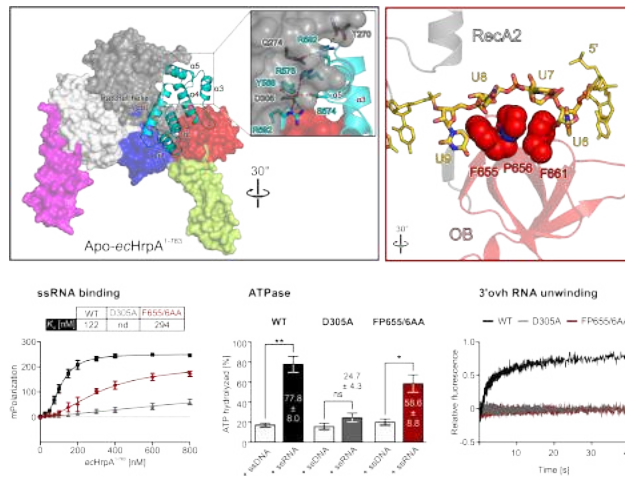


Fig 3 structure-function relationship.png

Human HELB is a processive motor protein which catalyses RPA clearance from single-stranded DNA

Wednesday, 7th July - 14:45: Oral Session - Oral - Abstract ID: 45

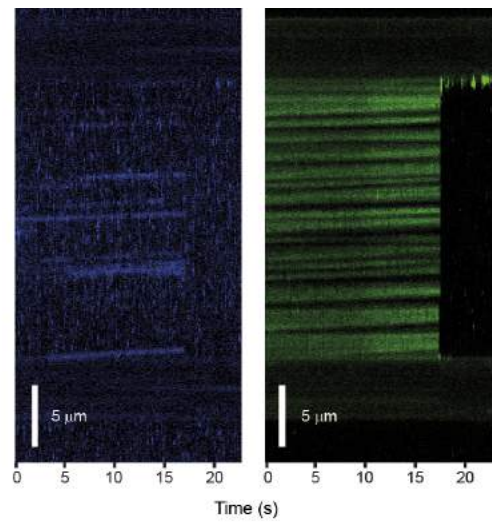
Dr. Silvia Hormeno¹, Dr. Oliver J. Wilkinson², Dr. Clara Aicart-Ramos¹, Dr. Sahiti Kuppa³, Prof. Edwin Antony³, Prof. Mark S. Dillingham², Prof. FERNANDO MORENO-HERRERO¹

1. CENTRO NACIONAL DE BIOTECNOLOGÍA CSIC, 2. University of Bristol, 3. Saint Louis University

Human DNA helicase B (HELB) is a poorly-characterised helicase suggested to play several functions in DNA metabolism including the stimulation of RAD51-mediated 5'-3' heteroduplex extension to promote homologous recombination (HR). Most recently, and in apparent contradiction to the role in the stimulation of HR, HELB was proposed to inhibit HR by antagonising the processive resection nucleases EXO1 and DNA2/BLM.

In this work, we used bulk and single molecule approaches to characterise the biochemical activities of HELB protein with a particular focus on its interactions with RPA and RPA-ssDNA filaments. We found that HELB is a monomeric protein which binds tightly to ssDNA with a site size of ~20 nucleotides. It couples ATP hydrolysis to translocation along ssDNA in the 5'-to-3' direction accompanied by the formation of DNA loops and with an efficiency of 1 ATP/base. HELB also displays classical helicase activity but this is very weak in the absence of an assisting force. HELB binds specifically to human RPA which enhances its ATPase and ssDNA translocase activities but inhibits DNA unwinding. Direct observation of HELB on RPA nucleoprotein filaments shows that translocating HELB concomitantly clears RPA from ssDNA.

Our study showed that human HELB is an efficient 5'—3' monomeric translocase but a surprisingly poor DNA helicase. Given that the protein is monomeric and that ssDNA translocation is accompanied by the formation of DNA loops, these imply the presence of an additional static DNA binding domain beyond the translocating ssDNA binding site. All ssDNA-dependent activities of HELB were stimulated only by the presence of cognate RPA and therefore we presume a sustained physical interaction. However, although it is both recruited and activated by its cognate RPA protein, HELB translocation activity then acts to remove RPA leaving naked ssDNA in its wake, and duplex unwinding is in fact inhibited by RPA. We propose that the physiological target of HELB is an RPA-ssDNA nucleoprotein filament, and that HELB is not a classical helicase, but rather an RPA displacement motor. These findings have important implications for better understanding the biochemical basis for the roles which HELB might play in DNA repair and replication.



C-trap kymographs showing HELB-QDs unidirectional movement (blue signal, left) on hRPA^{MB534}-covered ssDNA (green signal, right) under ATP conditions. Translocation of HELB results in removal of hRPA proteins.

Figure-for-abstract.png

Interactions of translocating Rep

Wednesday, 7th July - 15:00: Oral Session - Oral - Abstract ID: 106

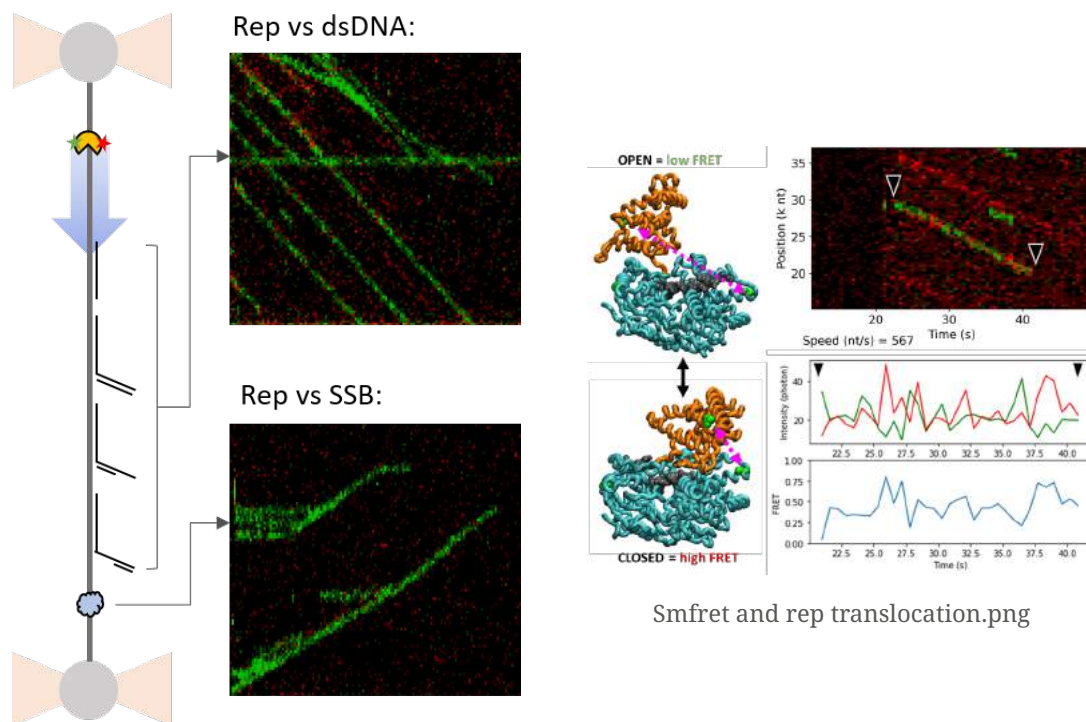
Ms. Olivia Yang¹, Dr. Sonisilpa Mohapatra¹, Mr. Brian Soong¹, Prof. Taekjip Ha¹

1. Johns Hopkins University

Rep is a helicase with tightly controlled unwinding behavior, with limited *in vitro* unwinding activity as a monomer. However, Rep has been observed to translocate directionally on single-stranded DNA (ssDNA) in an ATP dependent manner, which can serve to assist in other nucleic acid metabolism functions. As Rep translocates along ssDNA, it can encounter various roadblocks, such as stalled replication forks, Okazaki fragments, and DNA binding proteins. Using a commercial combined dual optical trap and multicolor fluorescence imaging system, and a FRET pair labeled Rep helicase, we can get some mechanistic information on how Rep translocates along long ssDNA and interacts with various roadblocks.

First, on stretched (10-30pN) ssDNA Rep is fast ($V_{max} \sim 900$ nt/s) and highly processive (at least 48knt). Second, we observed Rep can either bypass, dissociate, or unwind as it encounters dsDNA while translocating, only rarely slowing down or pausing at dsDNA. Interestingly, the most common behavior for Rep monomers is a bypass event, somehow crossing over or ignoring the dsDNA segment, while unwinding and dissociation are less likely. As the length of the dsDNA duplex encountered increases, the probability of bypass is largely unaffected, but the probability of unwinding decreases and dissociation increases. Having a 3' overhang on the dsDNA duplex, whether double-stranded or single-stranded, doesn't appear to have much effect on Rep's interaction with the duplex. In contrast, Rep can easily displace or push *E. coli* single strand DNA binding protein (SSB) without slowing down.

The ability of Rep to cross over short dsDNA without unwinding may be a useful feature for SSB and other DNA binding protein reorganization and clearance without needing to dissociate and rebind along the same stretch of DNA. Whether this feature is common across other helicases is yet to be determined.



Smfret and rep translocation.png

Translocation roadblocks.png

SLX4 forms SUMOylation factories via liquid phase separation.

Wednesday, 7th July - 16:00: Poster Session 2-A - Poster - Abstract ID: 27

***Mr. Emile Alghoul*¹, *Dr. Jihane Basbous*¹, *Dr. Angelos Constantinou*¹**

1. Institut de Génétique Humaine, CNRS, Université de Montpellier, Montpellier, France

SLX4 (FANCP) scaffolds the assembly of multiple enzymatic activities required for the maintenance of genome integrity, including structure-specific nucleases, helicases, and a yet to be defined E3 SUMO ligase activity. We will present evidence that SLX4 forms non-membrane bound compartments called biomolecular condensates. We find that multiple cooperative interactions mediated by SLX4 BTB dimerization domain, SUMO interaction motifs and the intrinsically disordered C terminal region drive the condensation of SLX4. In a purified form and in physiological salt conditions, the carboxyl terminal portion of SLX4 phase separates and forms liquid droplets that have the capacity to fuse.

We identified the E3 SUMO ligases PIAS4, RanBP2 and TRIM28 within SLX4 biomolecular condensates. Using an optogenetic platform to control the condensation of SLX4 by light in live cells, within minutes, and in the absence of DNA damage, we found that the assembly of SLX4 condensates promotes the conjugation of SLX4 and XPF to SUMO. SLX4 SUMO-SIM interactions contribute to SLX4 condensation, yet SLX4 condensates recruit the SUMO isopeptidase SENP6 and the SUMO-Targeted Ubiquitin Ligase RNF4 that precipitate their dissolution. In sum, SLX4 liquid phase separation yields locally-induced SUMOylation factories that are regulated by a balancing feedback mechanism executed by SENP6 and RNF4.

The functional consequences of client proteins SUMOylation within SLX4 condensates is under investigation. Our working hypothesis is that SLX4 condensates mark damage sites and compartmentalize mechanisms required for the rescue of stalled replication forks.

Motif I of the Cas3 SF2 helicase domain regulates directionality of Cas3 movement during CRISPR interference and primed adaptation

Wednesday, 7th July - 16:00: Poster Session 2-A - Poster - Abstract ID: 46

Mr. Nikita Vaulin¹, **Dr. Anna Shiriaeva**², **Dr. Ekaterina Semenova**³, **Prof. Konstantin Severinov**³

1. Peter the Great St.Petersburg Polytechnic University, Saint-Petersburg, Russia, 2. Skolkovo Institute of Science and Technology, Moscow, Russia, 3. Waksman Institute of Microbiology; The State University of New Jersey; Piscataway, NJ USA

CRISPR-Cas systems protect prokaryotes against mobile genetic elements (MGEs). During the first step of CRISPR-Cas immunity, called adaptation, a complex of Cas1 and Cas2 proteins integrates short fragments of invader DNA into CRISPR arrays as spacers separated by repeats. CRISPR arrays are transcribed yielding short crRNAs, each containing a single spacer. Such crRNAs bound by Cas proteins search for protospacers - sequences complementary to spacers - and degrade protospacer-containing DNA during a process called CRISPR interference.

In the type I-E CRISPR-Cas system of *Escherichia coli*, a complex of Cas proteins called Cascade bound to a crRNA locates the complementary protospacer and forms an R-loop. Protospacer-bound Cascade recruits Cas3, a superfamily 2 (SF2) helicase fused to an HD nuclease domain. Early *in vitro* experiments showed that Cas3 nicks the single-stranded DNA within the R-loop, loads onto the generated 3' end, translocates in 3' → 5' direction using ATP-hydrolysis, and feeds the unwound DNA into the HD nuclease domain. The region degraded by Cas3 serves as a source of new spacers during a process known as primed adaptation. Primed adaptation enhances the ability of cells to withstand infection by enriching CRISPR arrays with MGE-derived spacers. Recent studies demonstrate that Cas3 forms a complex with Cas1, Cas2, and Cascade that moves along the target selecting spacer precursors.

Though *in vitro* data show that Cas3 can move only in one direction - upstream of the targeted protospacer, our *in vivo* experiments demonstrate that during primed adaptation spacers are selected both upstream and downstream of Cascade-bound protospacers. This suggests that Cas3 can somehow switch to the DNA strand complementary to crRNA and start moving in the 3' → 5' direction downstream of the protospacer. Here, we demonstrate that the K320N substitution in the ATP-binding motif I of the helicase RecA1 domain of Cas3 abolishes spacer acquisition downstream of the targeted protospacer. This result suggests a key role of the K320 residue in switching strands by Cas3 by a mechanism that remains to be determined.

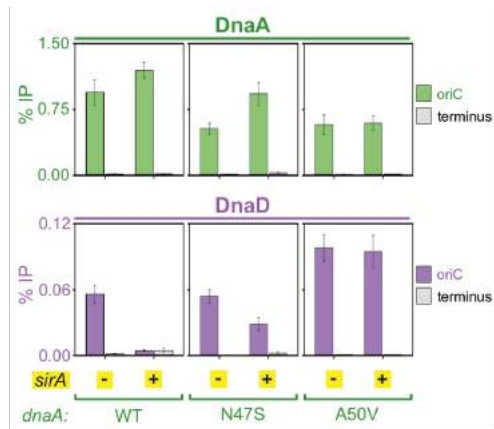
A positive and a negative mechanism for directing helicase recruitment to a bacterial chromosome origin

Wednesday, 7th July - 16:00: Poster Session 2-A - Poster - Abstract ID: 48

***Dr. Charles Winterhalter*¹, *Dr. Daniel Stevens*¹, *Dr. Simone Pellicciari*¹, *Dr. Stepan Fenyk*¹, *Prof. Heath Murray*¹**

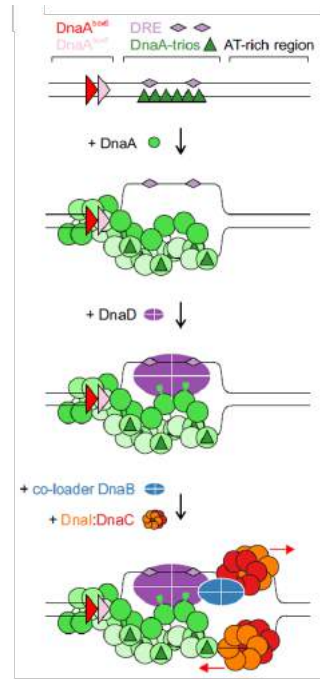
1. Newcastle university

DNA replication is universally essential for cellular life. Initiation of DNA replication occurs at a chromosome origin, where two replication forks are assembled for bidirectional DNA synthesis, each being driven by a replicative helicase at their leading edge. While the initiation pathway in both bacteria and eukaryotes culminates in helicase loading on a single DNA strand, the molecular mechanisms used to achieve this outcome appear to be distinct. Although this process is known to be tightly regulated in eukaryotes, bacteria are rather thought to modulate the ability of the ubiquitous master initiator DnaA to unwind the origin of the chromosome, and it is unclear how a second helicase may be loaded thus allowing bidirectional replication. To investigate bacterial helicase recruitment in the model organism *Bacillus subtilis*, we performed a systematic alanine scan to identify critical amino acids of the essential DNA replication initiation protein DnaD. We identified mutants disrupting the protein function *in vivo* and characterised key variants involved in protein:protein and protein:DNA interactions. We found that DnaD preferentially binds single-stranded DNA and the results suggest it is recruited to a specific strand of the open complex formed by DnaA at the chromosome origin to positively regulate loading of the helicase. Excitingly, we go on to show that this recruitment is downregulated by the developmentally expressed DNA replication inhibitor SirA by competition for the same binding site on DnaA. We propose a model providing a potential route for bidirectional helicase loading and shed light onto the specific regulation of this process throughout the bacterial cell cycle.



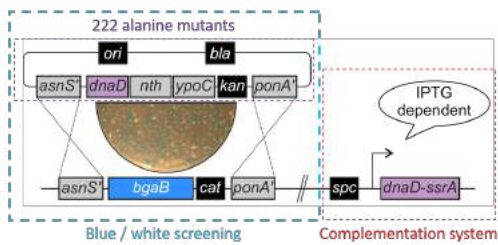
Chromatin immunoprecipitation shows that overexpression of SirA inhibits DnaD recruitment at the origin of the chromosome *oriC*. DnaA remains recruited at this site and suppressor alleles of the DnaA-SirA interaction restore DnaD recruitment.

Figure3.png



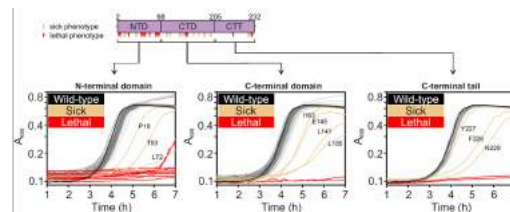
Molecular model of DNA replication initiation at the origin required for helicase loading in *B. subtilis*. DnaA binds DnaA boxes in the *incC* region, leading to downstream filament formation on DnaA-trios and dsDNA partial unwinding. DnaD is then loaded on the exposed top strand and provides a mean for bidirectional loading of the helicase following DnaB recruitment.

Figure4.png



Schematics of the DnaD blue / white screening assay in *B. subtilis*. A master plasmid carrying individual DnaD substitutions is integrated by double recombination at the *dnaD* locus, where the native operon is replaced by a *bgaB* cassette allowing blue/white screening in the presence of X-Gal. Mutant strains harbour the inducible *dnaD-ssrA* cassette required for viability during transformation and mutant propagation.

Figure1.png



DnaD structure schematics with residues marked as red for lethal and beige for sick phenotypes (population-size or slow growth). Plate reader growth analysis of DnaD variants within the N-terminal domain, C-terminal domain or C-terminal tail in the absence of DnaD-ssrA.

Figure2.png

Human DNA/ RNA Topoisomerase TOP3-beta (TOP3B) is coordinated with the DEAD-box Helicases DDX5 and DDX6 to resolve R-Loops

Wednesday, 7th July - 16:00: Poster Session 2-A - Poster - Abstract ID: 54

***Dr. Sourav Saha*¹, *Dr. Yves Pommier*¹**

1. Center for Cancer Research, National Cancer Institute, NIH

Introduction: R-loops consist of RNA–DNA hybrids and displaced single-stranded DNA segments. Excessive R-loops cause DNA breaks, replication stress and genome instability, and loss of TOP3B has been linked with increased cellular R-loops, genome instability and cancer. Present study investigated the underlying mechanism by which TOP3B regulates cellular R-loops.

Methods and Results: To understand the mechanistic role of TOP3B in R-loop resolution, we generated TOP3B-KO HCT116 cells by CRISPR-Cas9. Slot blot and immunofluorescence studies using S9.6 antibody (specific for DNA-RNA hybrids) show that, compared to wild-type cells, HCT116 TOP3B-KO have higher R-loop levels both at baseline and after treatments with the R-loop-inducing agents: camptothecin (TOP1 inhibitor) and pladienolide B (splicing inhibitor). Conversely, ectopic expression of TOP3B reduced R-loops in TOP3BKO cells. We also observed that R-loop induction concurrently induces cellular TOP3B cleavage complexes indicating that TOP3B works catalytically in the presence of R-loop structures. Furthermore, RNA/DNA Hybrid IP-Western blotting with S9.6 antibody showed that TOP3B is directly recruited to R-loops. To understand the molecular mechanisms by which TOP3B acts at R-loops, we performed *in vitro* biochemical assays using recombinant human TOP3B and oligonucleotide substrates mimicking R-loop structures. They show that TOP3B cleaves the DNA single-strand displaced by the R-loops. Because TOP3B-mediated nicking of the displaced DNA strand in R-loop structures is likely to be coupled with an RNA-DNA helicase to unwind the RNA-DNA hybrid prior to TOP3B-mediated strand passage, we searched for helicases associated with TOP3B. IP-Mass Spec and IP-Western blotting experiments revealed that TOP3B interacts with the R-loop associated helicases DDX5 and DDX6. Consistently, cellular depletion of DDX5, DDX6 or of the known R-loop resolving helicase Senataxin by siRNA produced R-loops. Notably, combined depletion of DDX5/ DDX6 and TOP3B caused no further increase in R-loops compared to siDDX5/ siDDX6 or TOP3BKO alone suggesting that DDX5/ DDX6 and TOP3B work in an epistatic manner to resolve R-loops. In contrast, combined depletion of TOP3B and Senataxin produced additive effects suggesting that TOP3B resolves R-loops independently of Senataxin.

Discussion: Our study demonstrates how DNA/RNA topoisomerase TOP3B resolves R-loop in coordination with DEAD-box helicases DDX5 and DDX6 and protects cells from genome instability.

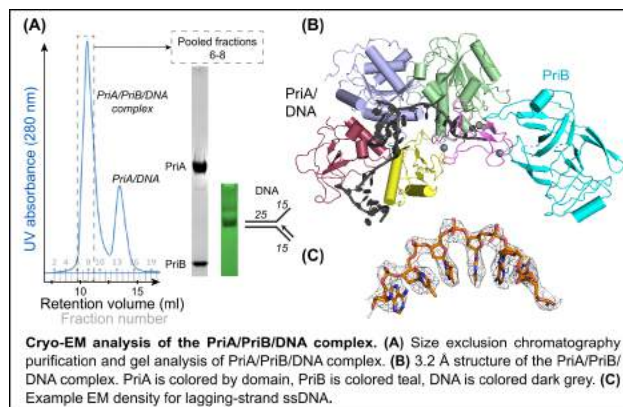
A 3.2 Å structure of the PriA/PriB/replication fork complex reveals mechanistic insight into bacterial DNA replication restart

Wednesday, 7th July - 16:00: Poster Session 2-A - Poster - Abstract ID: 59

***Mr. Alexander Duckworth*¹, *Dr. Kenneth Satyshur*¹, *Prof. Timothy Grant*¹, *Prof. James Keck*¹**

1. University of Wisconsin-Madison

The DNA replication machinery (replisome) frequently encounters blockages that causes it to dissociate from the genome, halting DNA replication and leaving abandoned DNA replication forks. To avoid the lethality of incomplete DNA replication, bacteria have evolved mechanisms to reload the replisome onto abandoned DNA forks distant from the origin of replication. This “replication restart” process is facilitated by protein complexes that recognize and remodel the DNA forks in order to load the replicative helicase onto lagging strand DNA. In *E. coli*, the PriA, PriB, and DnaT proteins form the major reloading complex. While it is known that PriA is a structure-specific helicase capable of recognizing and unwinding the nascent lagging strand, the roles of PriB and DnaT are less clear. Using Cryo-EM, we have determined a 3.2 Å structure of PriA simultaneously bound to PriB and a synthetic replication fork. The structure details the PriA-PriB interaction, involving an unexpected and large conformational change in PriA’s cysteine-rich region (CRR). Portions of the parental, leading, and lagging strand DNA are resolved bound to PriA. The single-stranded DNA lagging strand is encircled by PriA’s CRR and helicase domains in a manner that contrasts with previous hypotheses. Overall, the PriA/PriB/DNA fork structure elucidates the mechanisms of DNA fork recognition by PriA and suggests roles for PriB in the complex.



Pria-prib-dna structure figure.png

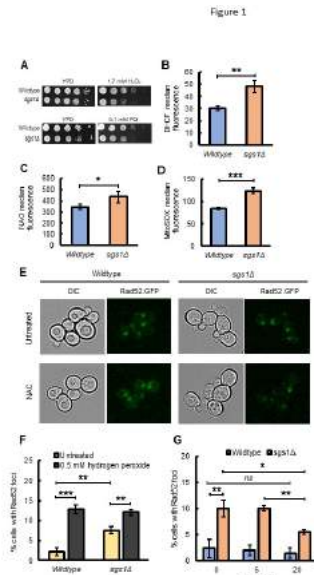
Functional interaction between Sgs1 and Sod2 in the suppression of oxidative-damage-induced chromosomal rearrangements and mitochondrial abnormalities in *Saccharomyces cerevisiae*

Wednesday, 7th July - 16:00: Poster Session 2-A - Poster - Abstract ID: 77

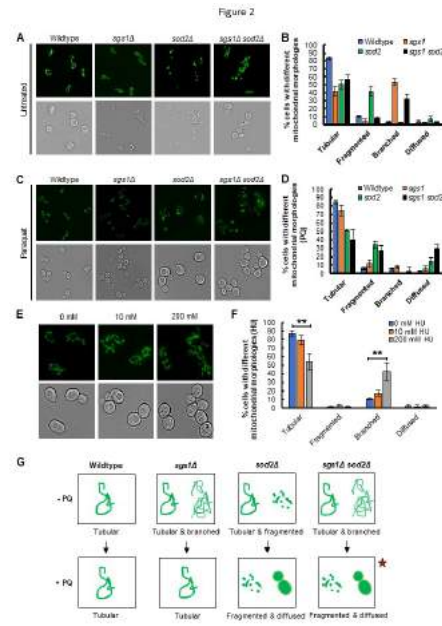
Ms. Sonia Vidushi Gupta¹, Dr. Kristina Hildegard Schmidt¹, Dr. Lillian Campos-Doerfler¹

1. UNIVERSITY OF SOUTH FLORIDA

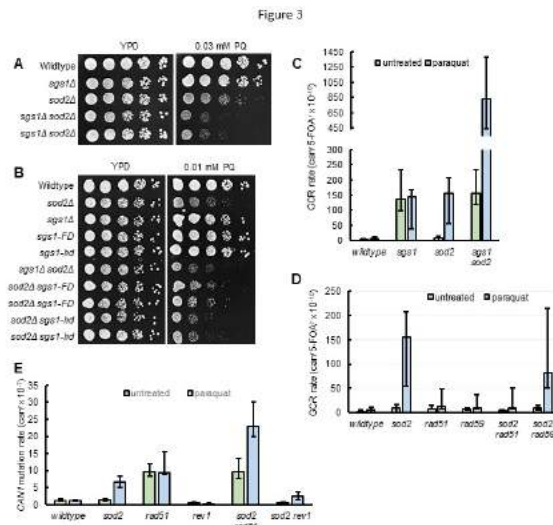
Sgs1 belongs to the RecQ-like family helicases and is important for homologous recombination in *Saccharomyces cerevisiae*. *SGS1* mutations cause hypersensitivity to DNA damaging agents, reduced replicative lifespan, and increased genome instability. Our proteomics analysis of cells lacking Sgs1 revealed upregulation of major antioxidant enzymes, such as the mitochondrial superoxide dismutase Sod2 and thioredoxin peroxidase Tsa1. *sgs1Δ* mutants have been known to exhibit elevated reactive oxygen species, but the significance of Sgs1 with respect to oxidative stress is poorly understood. Using flow cytometry, we show that loss of Sgs1 results in elevated mitochondrial superoxide and increased mitochondrial mass. Fluorescence microscopy of Rad52 foci also shows that loss of Sgs1 results in ROS-dependent DNA damage. Sgs1 mutants also display increased branched mitochondrial morphology, potentially resulting from the need of more ATP for DNA repair. This trend toward mitochondrial branching in the absence of Sgs1 is abolished by deletion of *SOD2*, which renders mitochondria more fragmented and diffused. In the absence of Sod2, oxidative stress induces gross chromosomal rearrangements that are Rad51-dependent and mutations at the *CAN1* locus that are translesion-synthesis-dependent. Sod2 and Sgs1 functionally interact to suppress hypersensitivity to oxidative stress and chromosomal rearrangements. Our study establishes the importance of Sod2 in maintaining genome integrity under oxidative stress and identifies the causes and consequences of oxidative stress in cells lacking Sgs1.



Cells lacking *sgs1* have high *ros* high mitochondrial mass and exhibit a significant amount of *ros*-dependent dsbs.jpg



Changes in mitochondrial morphology upon deletion of *sgs1* and *sod2*.jpg



Effect of *sgs1* *rad51* and *rev1* mutations on the dna damage sensitivity and genome stability of *sod2* mutants.jpg

The evolutionary origins of Pif1 helicases from Helitron transposons

Wednesday, 7th July - 16:00: Poster Session 2-A - Poster - Abstract ID: 133

Mr. Pedro Heringer¹, Dr. Gustavo C. S. Kuhn¹

1. Universidade Federal de Minas Gerais

Introduction: *Helitrons* are rolling-circle transposable elements found in genomes from all major groups of eukaryotes. They encode a transposase (RepHel) containing two major domains: the endonuclease (Rep) and helicase (Hel) domains, the latter which belongs to the Pif1 family of helicases. Pif1 helicases are also present in essentially all eukaryotes analyzed to date and are involved in functions related to nucleic acid metabolism. Because *Helitrons* constitute the only group of rolling-circle transposons that encodes a helicase, it has been suggested that Hel domains probably originated after a host eukaryotic Pif1 gene was captured by a *Helitron* ancestor. However, the few analyses exploring the evolution of *Helitron* transposases have focused on its Rep domain, which is also present in a wide variety of mobile genetic elements, including some viruses and plasmids.

Methods: We used phylogenetic and non-metric multidimensional scaling analyses to investigate the relationship between Hel domains from *Helitrons* and Pif1-like helicases from a variety of organisms.

Results: Our results show that Hel domains are only distantly related to genomic helicases from both prokaryotes and eukaryotes (Fig. 1 and Fig. 2). Thus, the proposed scenario in which this domain could have derived from a captured eukaryotic Pif1 gene is unlikely. In contrast, we suggest that *Helitrons* are descendants of a prokaryotic plasmid element that encoded a RepHel, and that invaded its first eukaryotic host before the major radiations within this domain of life (Fig. 3).

Discussion: The evolutionary relationships between Pif1 helicases from *Helitrons* and a wide variety of organisms that we present here point to a prokaryotic origin of eukaryotic rolling-circle transposons. Recent analyses restricted to the Rep domain have indicated that *Helitrons* are more closely related to prokaryotic viruses and plasmids. Our findings corroborate this hypothesis and provide a more consistent theoretical framework to explain how both domains from the RepHel might have functioned as a single enzyme in the plasmid-like elements that gave rise to *Helitrons*. The presence of a Pif1-like Hel domain might have also favored the colonization of eukaryotic genomes by *Helitrons*.

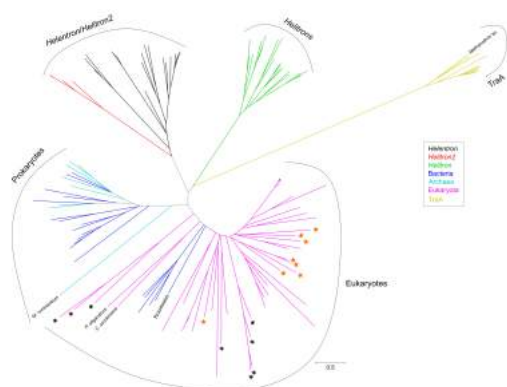


Figure 1.jpg

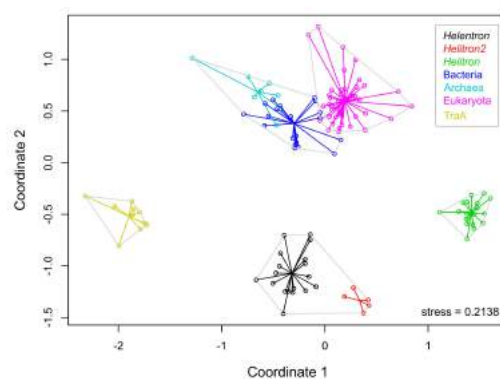


Figure 2.jpg

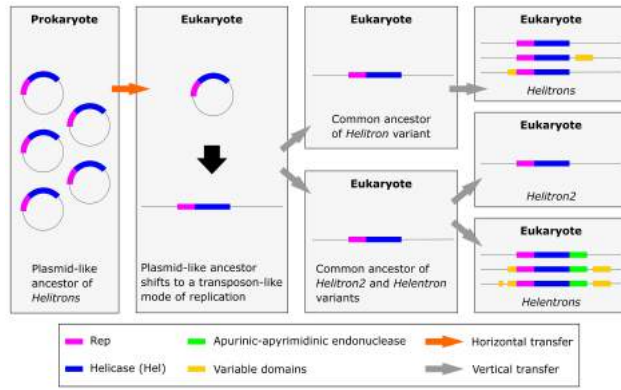


Figure 3.jpg

Structural snapshots of ATPase cycle of tick-borne encephalitis virus NS3 helicase

Wednesday, 7th July - 16:00: Poster Session 2-B - Poster - Abstract ID: 6

***Dr. Paulina Duhita Anindita*¹, *Dr. Pavel Grinkevich*¹, *Dr. Roman Tuma*¹, *Dr. Zdenek Franta*¹**

1. University of South Bohemia in Ceske Budejovice

Tick-borne encephalitis virus (TBEV) causes tick-borne encephalitis, an important arboviral disease affecting population within European and north-eastern Asian countries. Due to low vaccination coverage and expansion of ticks into new areas the TBE incidence is raising thus creating a need for new antiviral treatment. NS3 helicase (NS3H) domain plays an essential role in viral genome replication and constitutes interesting drug target. NS3H carries out three enzymatic activities: RNA 5'-triphosphatase, RNA helicase and ATP hydrolysis. The latter activity is coupled to and provides energy for the RNA helicase activity during unwinding of the double-stranded RNA replication intermediate.

Here we captured and investigated several crystal structures of NS3H, including the apo form, NS3H in complex with non-hydrolyzable ATP-analogue (AMPPNP), ADP or ADP-Pi resembling the pre- and post-hydrolysis states, respectively. The overall structure of individual complex is similar to the apo NS3H with several conformational changes observed among domains. Our structures represent conformational snapshots of the key ATP hydrolysis and nucleotide exchange stages, suggesting inorganic phosphate release is the rate limiting step in the absence of RNA. Next, we demonstrated that the ATP hydrolysis cycle is stimulated by the presence of ssRNA but not ssDNA. Our result shows that NS3H shares a common RNA-dependent ATPase activity as previously described for DENV and HCV helicases, even though HCV helicase also translocates DNA substrates. In addition to ssRNA TBEV NS3H binds ssDNA; however, the latter acts as an inhibitor by occupying the nucleic binding site. This suggests that RNA selectivity is not solely due to specific RNA recognition but rather encoded in the allosteric coupling between ATPase and RNA unwinding activities. Structural transitions associated with the coupling can be further exploited for rational drug design.

New insights into the functions of SV40 T antigen helicase and beyond - The functional cooperation of SV40 T antigen monomers and hexamers is essential for viral DNA replication

Wednesday, 7th July - 16:00: Poster Session 2-B - Poster - Abstract ID: 78

*Dr. Heinz Nasheuer*¹, *Dr. Nick Onwubiko*¹, *Dr. Ingrid Tessmer*²

1. NUI Galway, 2. Universität Würzburg

In all living organisms DNA replication is a central process to maintain genome stability. Replication of polyomavirus DNA has served as a model system to study eukaryotic DNA replication at the molecular level. The molecular details of most processes of eukaryotic DNA replication are still unclear, including those regarding lagging strand synthesis.

Using biochemical and spectroscopic analyses in combination with atomic force microscopy (AFM) as described by Onwubiko et al. (2020) we determined that monomeric and oligomeric T antigen (Tag) forms independently bind to single-stranded DNA (ssDNA) with high affinities (K_D values of 10–30 nM), which are in the same order of magnitude as hexameric Tag binding to the origin of SV40 DNA replication and human replication protein A (RPA) to ssDNA. Furthermore, we observe the formation of RPA-Tag-ssDNA complexes containing monomeric Tag. Importantly, our data indicate that monomeric but not hexameric Tag stimulates primase function in lagging strand Okazaki fragment synthesis in a model system. In contrast to Tag monomers, hexameric Tag inhibits the reaction, redefining DNA replication initiation on the lagging strand. Additionally, we determined that residues, which are required for Tag oligomerisation and which are unrelated to residues of Tag involved in Tag-Pol α -primase/p70 subunit interactions, are also necessary for primase stimulation defining new physical and functional interactions during the initiation of Okazaki fragment synthesis. These activities of SV40 Tag will be summarised in a model opening new insights into the regulation of multiple independent functions of DNA and RNA helicases in cellular and viral nucleic acid metabolism.

Onwubiko NO et al.(2020) SV40 T antigen interactions with ssDNA and replication protein A: a regulatory role of T antigen monomers in lagging strand DNA replication. *Nucleic Acids Res* 48:3657-3677. doi:10.1093/nar/gkaa138.

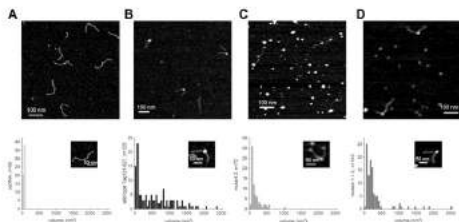


Figure 1. The SV40 T antigen proteins M1 and M2 together bind to ssDNA as dimers. Atomic force microscopy (AFM) was used to study the protein complexes bound to ssDNA in the presence of both monomeric SV40 Tag variants M1 and M2 to determine whether M1-M2 dimers bind to ssDNA. The substrate for the ssDNA binding experiment contains a ssDNA sequence in the center at 50% of the DNA length flanked by 2 dsDNA regions as previously described (Heck's paper or 1 of Ingrid's). The top panels in A to D show representative AFM pictures of ssDNA in the absence of proteins, which serves as a negative control (A), wt Tag₁₅₁₋₂₂₇ (B), M2 (C), and M1 plus M2 (D). The bar in each panel represents 100 nm. The data of a representative experiment are quantified in the panels below the AFM pictures and also contain an inset with an enlarged representation of a representative substrate molecule of the experiment (the bar marks 50 nm). **A**, The volume size of the DNA in the middle of the substrate was measured and quantified. The data suggest that the ssDNA volume without protein under AFM conditions is 50 to 100 nm³. **B**, The volume of protein-ssDNA complexes were measured in the presence of 500 nM of wt Tag₁₅₁₋₂₂₇. The majority of the protein-DNA complexes represented a size which is equivalent of being in a oligomeric state (hexamers, double hexamers and some even larger complexes). **C**, The analysis of the AFM data revealed that the M2 protein at concentrations of 500 nM binds to ssDNA part of the substrate as monomer. This finding is consistent with the data the protein only forms monomers and binds as such to ssDNA as previously described (Chang et al. (2013); Onuzko et al. (2020)). **D**, At a concentration of 500 nM of M1-M2 proteins preferentially form low molecular weight complexes with the DNA substrate and barely any high molecular weight complexes were detected. An enlargement of the small volumes reveals that M1-M2 bind as dimer to compare the numbers one has to take into account that the dimer peak volumes contain 2 molecules of Tag whereas the monomer peak has only one molecule of M1 or M2. **C**, The analysis of the AFM data reveal that the M1-M2 protein mainly bind to the central ssDNA part of the substrate with a specificity $S = 1014$ suggesting that the Tag variants preferentially bind to ssDNA. The central ssDNA region of substrate is highlighted by the bar above the diagram in panel C.

Figure 1.jpg

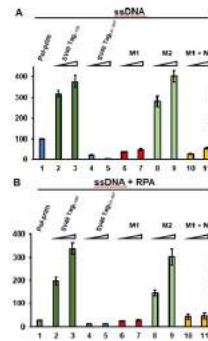


Figure 2. The SV40 T antigen helicase domain regulates Tag oligomerisation and functional interactions during Okazaki fragment synthesis. DNA synthesis on ssDNA by Pol-prim was measured in absence (A) and presence of RPA (B), to determine the stimulatory activity of SV40 Tag-derived proteins in these biochemical test systems. In panel A, the Pol-prim-dependent DNA synthesis on ssDNA in the presence of increasing amounts of Tag-derived proteins (0, 0.3 μ g and 0.6 μ g) is shown. DNA synthesis on ssDNA by 0.1 unit of Pol-prim alone and was arbitrarily set to 100% (panel A, dark blue column 1). Columns 2 and 3 (dark green) present the stimulation of Pol-prim by 0.3 μ g and 0.6 μ g of full-length Tag (Tag₁₅₁₋₂₂₇), respectively, whereas columns 4 and 5 (light blue) show the Pol-prim activity in the presence of the Tag variant Tag₁₅₁₋₂₂₇ (0.3 μ g and 0.6 μ g, respectively) consisting of origin-binding domain and the helicase domain. Mutations in this Tag variant were introduced, which suppress the oligomerisation function of Tag, and these proteins M1 and M2 can only form monomers whereas, after mixing these two proteins, they form dimers in solution and on DNA. DNA synthesis on ssDNA by Pol-prim in the presence of increasing amounts of M1 (columns 6 and 7, 0.3 μ g and 0.6 μ g, respectively, red colour) and M2 protein (columns 8 and 9, 0.3 μ g and 0.6 μ g, light green) plus M1-M2 dimer (columns 10 and 11, 0.3 μ g and 0.6 μ g, light orange) is presented. Full length Tag containing monomers and oligomers, and monomer M2 stimulated Pol-prim whereas Tag (151-227), the monomeric mutant M1 and the M1-M2 dimer inhibited Pol-prim. **B**, Similarly adding 0.5 μ g of RPA to the assay significantly reduced dNMP incorporation on ssDNA by Pol-prim to 29.2% compared to Pol-prim alone (compare panel A, column 1 with panel B, grey column 1). Then DNA synthesis by Pol-prim on RPA-bound ssDNA, 0.5 μ g of RPA, was determined in the presence of increasing amounts of the indicated Tag variants (0.3 μ g and 0.6 μ g). The Pol-prim DNA synthesis in the presence of full-length Tag (columns 2 and 3, dark green), variant Tag₁₅₁₋₂₂₇ (columns 4 and 5, light blue), mutant M1 (columns 6 and 7, red colour) and (columns 8 and 9, light green) plus M1-M2 dimer (columns 10 and 11, light orange) are shown in panel B. Full length Tag and monomeric Tag variant M2 stimulate the DNA synthesis whereas Tag₁₅₁₋₂₂₇ inhibited the DNA synthesis further in comparison to column 1, monomeric Tag M1 neither stimulated nor inhibited the reaction under the condition tested, and the dimer M1+M2 slightly stimulated the DNA synthesis on RPA-ssDNA by Pol-prim to ~45% (compare column 1 in panel B with columns 10 and 11). All experiments were performed in triplicates, and the average and standard deviation of dNMP incorporation relative to the incorporation of DNA synthesis by Pol-prim alone is presented.

Figure 2.jpg

Biochemical studies of the COVID-19 Nsp13 helicase required for coronavirus replication

Wednesday, 7th July - 16:00: Poster Session 2-B - Poster - Abstract ID: 92

Ms. Rebecca Lee¹, Mr. Joshua Sommers¹, Dr. Arindam Datta¹, Dr. Robert Brosh¹

1. Translational Gerontology Branch, National Institute on Aging, NIH

Introduction: Nsp13 helicase is a crucial component of the multi-protein SARS-CoV-2 complex responsible for coronavirus replication. However, the molecular mechanism of Nsp13 and its precise activities in the SARS-CoV-2 lifecycle are poorly understood. This study's focus was to gain molecular insight into Nsp13 by characterizing its biochemical activity and substrate specificity.

Methods: Affinity recombinant protein purification and in vitro strand displacement helicase assays

Results: A dual affinity tagged recombinant Nsp13 protein was overexpressed and purified to apparent homogeneity from insect cells (Fig. 1) and characterized by strand displacement radiometric helicase assays. Nsp13 demonstrated optimal nucleoside triphosphate duplex dependent unwinding activity in the presence of all nucleotides except dGTP. Under multi-turnover conditions (Fig. 2), Nsp13-catalyzed unwinding of double-stranded RNA was strongly protein concentration dependent even in a narrow range of 13 – 22 base pairs (bp). From single-turnover kinetic analysis (Fig. 2B), an increase in RNA duplex length from 13 to 16 bp dramatically decreased the rate of Nsp13 unwinding which was further depressed for the 19 and 22 bp substrates, suggesting poor processivity. Assessment of Nsp13 unwinding using modified forked duplex substrates demonstrated strand-specific interactions. Nsp13 preferentially unwound forked duplex DNA compared to the analogous RNA substrate; moreover, a hybrid RNA-DNA forked duplex substrate with a DNA translocating strand for the 5' to 3' Nsp13 was preferred to an RNA translocating strand substrate. Nsp13 helicase was greatly inhibited by a polyglycol linker in the translocating single-strand adjacent to the duplex, whereas little to no effect was observed by the non-translocating strand linker (Fig. 3). Based on these results, we conclude that Nsp13 requires backbone continuity in the helicase translocating strand, but surprisingly prefers DNA as its loading strand.

Discussion: Our findings demonstrate that Nsp13 unwinds RNA duplex substrates in a nucleoside triphosphate dependent manner characterized by a unidirectional translocation mechanism for initiation and low processivity during elongation, suggesting a defined substrate preference and constrained strand separation in the absence of accessory proteins. Molecular characterization of Nsp13 reaction mechanism and its protein interactions will facilitate the development of novel anti-viral therapeutics to aid those infected with SARS-CoV-2 and possibly future coronaviruses.

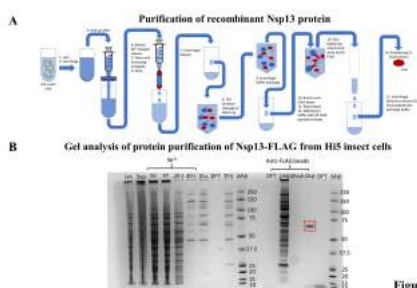


Figure 1

Abstract figure 1.jpg

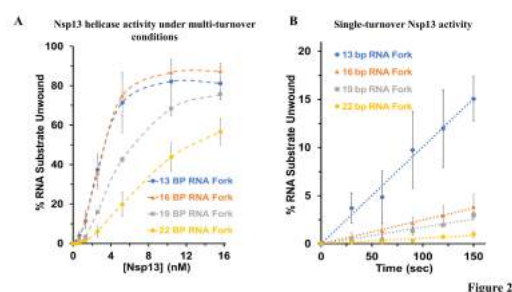
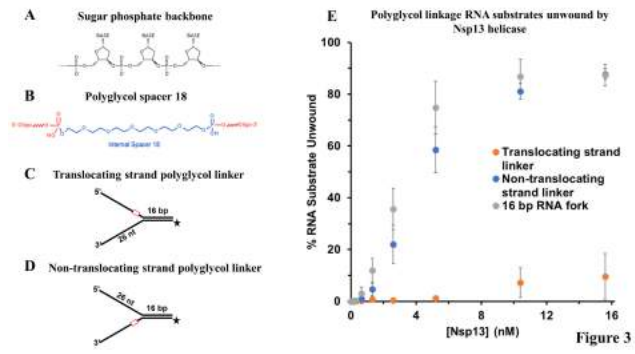


Figure 2

Abstract figure 2.jpg



Abstract figure 3.jpg

Mechanism of RNA mediated phosphate release from the active site of the tick-borne encephalitis virus helicase.

Wednesday, 7th July - 16:00: Poster Session 2-B - Poster - Abstract ID: 96

***Mr. Marco Halbeisen*¹, *Dr. Roman Tuma*¹, *Dr. Paulina Duhita Anindita*¹, *Dr. Zdenek Franta*¹, *Dr. David Reha*²**

1. University of South Bohemia in Ceske Budejovice, 2. Institute of Microbiology

Tick-borne encephalitis virus (TBEV) gained increasing attention in recent years as the main cause of tick-borne diseases in Europe. While vaccines against TBEV are available only low vaccination coverage has been achieved. Global warming is causing tick populations expansion, resulting in more cases and need for a drug targeting one of the viral enzymes.

NS3 helicase domain (NS3H) is part of the protease-helicase non-structural protein which plays an essential role in replication. NS3H belongs to helicase super-family 2 and its ATPase activity is tightly coupled to RNA binding. Based on recent biochemical and structural evidence inorganic phosphate release likely constitutes the rate limiting step which depends on RNA binding. We used recently determined high-resolution structures of NS3H complexes and all atom, explicit solvent molecular dynamics simulations to visualize intermediates on the phosphate release pathway.

A short ssRNA molecule (AGACUA) was placed into RNA binding site of NS3H apoprotein and equilibrated using amber99sb-ildn force field in Gromacs. This led to P-loop repositioning. Further conformational changes were triggered by placing ATP into the ATPase active site using ATP configuration from crystal structure of NS3H:AMP-PNP complex. Control simulations were done with ADP and/or without RNA. The presence of ssRNA and ATP led to repositioning of helices $\alpha 2$ and $\alpha 7$. Furthermore, RNA fluctuated between two states, corresponding to a slight movement along the binding groove. Frames corresponding to each RNA state were selected, ATP was replaced by ADP + P_i and simulated for up to 2 μ sec and several repeats. Only the state with the re-positioned RNA led to P_i release (release time ranging from 300 to 1500 ns, Figure 1). The release required further transient opening of the $\alpha 2$ and $\alpha 7$ helical gate. No phosphate release was observed during control simulations (2 μ s) that were based on NS3H:ADP: P_i crystal structure. In summary, RNA movement allosterically promotes opening of active site gate ($\alpha 2$ and $\alpha 7$ helices) which in turn is necessary for inorganic phosphate release.

Structural basis for backtracking by the SARS-CoV-2 replication-transcription complex

Wednesday, 7th July - 16:00: Poster Session 2-B - Poster - Abstract ID: 117

Mr. Brandon Malone¹, Dr. Elizabeth Campbell¹, Prof. Seth Darst¹

1. The Rockefeller University

Introduction

The COVID-19 pandemic has claimed millions of lives and devastated the world economy. Gaining insights into the replication cycle of the causative agent, SARS-CoV-2, will aid the development of therapeutics. SARS-CoV-2 possesses one of the largest viral RNA genomes which is approx 30 kb. To successfully replicate this genome, the virus requires the holo-RdRp that is composed of the RNA dependent RNA polymerase, nsp12, and its co-factors nsp7 and nsp8. The holo-RdRp associates with several replicative proteins which form the replication-transcription Complex (RTC). Herein, we demonstrate the basis for the coupling of the helicase, nsp13, with the holo-RdRp. The structure illuminates the basis for the helicase interaction with the polymerase and led us to propose that the helicase may promote backtracking of the RdRp. Backtracking is a regulatory feature of transcription that describes the reverse motion of the transcriptase on the nucleic acid template. We show that the helicase can promote RdRp backtracking and captured a backtracked structure.

Methods

We resolved cryo-EM structures of the nsp13 bound holo-RdRp in an elongation competent (nsp13-RTC) and backtracked state (nsp13-BTC). We identified that nsp13 triggers the formation of a backtracked ssRNA using photo-crosslinking. Unbiased molecular dynamics simulations revealed that misincorporated nucleotides spontaneously orientate into the backtracking channel.

Results & Discussion

The structure of the predominant class of the nsp13-RTC complex features two copies of nsp13. One copy (nsp13.1) is engaged with the 5'-single-stranded template strand RNA (tRNA) downstream of the RdRp active site. Nsp13 translocates in the 5'-3' direction whereas the RdRp moves in the 3'-5' direction relative to the tRNA. We hypothesized that the translocation of the helicase against a stalled RdRp would drive the RdRp backwards. This generates a 3'-single-stranded fragment of the pRNA. Analysis of the nsp13 bound holo-RdRp complex on a backtracked RNA scaffold indicates that the 3'-single-stranded pRNA is extruded out the RdRp NTP entry channel. Our results indicate that nucleotide misincorporation triggers fraying of the 3' end of the pRNA, serving to initiate backtracking. Nsp13 engagement on the tRNA enhances backtracking, which we postulate may stimulate recognition of the erroneous pRNA by the SARS-CoV-2 proofreading complex.

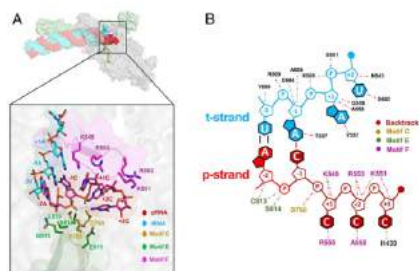


Figure 2. A) Surface rendered model of the holo-RdRp and close-up of the secondary channel/NTP entry channel from the backtracked nsp13-RTC complex. B) 2D schematic depicting amino acids involved in the recognition of the backtracked p-RNA.

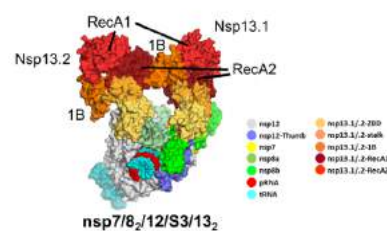


Figure 1. Structural model of nsp13-RTC bound to an RNA substrate (S3). Domains are surface rendered and colored according to the key.

Nsp13-btc structure 2d interaction schematic.png

Nsp13-rtc structure.png

Unwinding of duplex nucleic acids by cooperative translocation of SARS coronavirus helicase nsP13 is modulated with ATP concentration

Wednesday, 7th July - 16:00: Poster Session 2-B - Poster - Abstract ID: 125

Prof. Dong-Eun Kim¹

1. Konkuk University

Severe acute respiratory syndrome coronavirus nonstructural protein 13 (SCV nsP13), a superfamily 1 helicase, plays a central role in viral RNA replication through the unwinding of duplex RNA and DNA with a 5' single-stranded tail in a 5' to 3' direction. Despite its putative role in viral RNA replication, nsP13 readily unwinds duplex DNA by cooperative translocation.

Unwinding of duplex nucleic acid substrates (dsDNA or dsRNA) that had different duplex lengths and 5'-overhangs was examined under single-turnover reaction conditions in the presence of excess enzyme and varying concentrations of ATP. Unwound duplex nucleic acid substrates were assessed by electrophoretic mobility shift assay in the native PAGE and their unwinding kinetics were analyzed by fitting exponential function to the time courses of product accumulation.

We previously observed that SCV nsP13 requires the presence of a long 5'-overhang to unwind longer DNA duplexes. Unwinding of DNA substrates revealed that the amount of DNA unwound decreased significantly as the length of the duplex increased, indicating a poor in vitro processivity. Together with the propensity of oligomer formation of nsP13 molecules, we proposed that duplex DNA is unwound through cooperative translocation by the functionally interacting oligomers of the helicase molecules loaded onto the 5'-overhang (Fig. 1). Recently, we examined characteristics in duplex RNA unwinding by SCV nsP13 helicase and observed that nsP13 showed very poor processivity on duplex RNA compared with that on duplex DNA. Moreover, nsP13 inefficiently unwinds duplex RNA by increasing the 5'-overhang length. As the concentration of nsP13 increased, the amount of unwound duplex DNA increased and that of unwound duplex RNA decreased. The accumulation of duplex RNA/nsP13 complexes increased as the concentration of nsP13 increased. An increased ATP concentration in the unwinding of duplex RNA relieved the decrease in duplex RNA unwinding. Thus, nsP13 has a strong affinity for duplex RNA as a substrate for the unwinding reaction, which requires increased ATPs for processive unwinding of duplex RNA. Our results suggest that SARS coronavirus nsP13 may require more ATPs to promote stable helicase translocation necessary for delicate RNA replication (Fig. 2).

Figure 1. Proposed mechanism of DNA unwinding by the nsP13 helicase with different processivity. Cooperative translocation enhances the unwinding of duplex DNA by SARS coronavirus helicase nsP13.

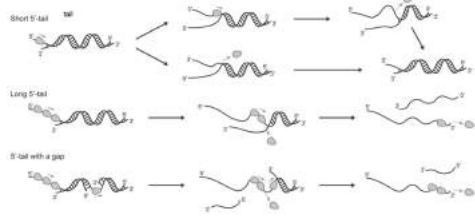


Figure 2. Proposed models of duplex RNA and DNA unwinding by nsP13 using various parameters. (A) Representative unwinding process by SCV helicase nsP13. (B) Unwinding characteristics of helicase nsP13 using various parameters (L1: length of 5'-as tail; L2: length of duplex).

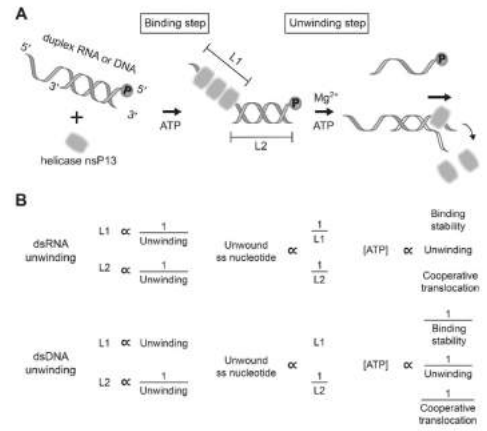


Figure 2.jpg

Figure 1.jpg

The DEAD-box RNA helicase RhIE2 is a global regulator of *Pseudomonas aeruginosa* lifestyle and pathogenesis

Wednesday, 7th July - 16:00: Poster Session 2-C - Poster - Abstract ID: 63

Dr. Stéphane Hausmann¹, **Dr. Diego Gonzalez**², **Mr. Johan Geiser**¹, **Dr. Martina Valentini**¹

1. University of Geneva, 2. University of Neuchatel

Post-transcriptional regulators are efficient regulatory resources that optimize bacterial fitness and competitiveness, both in nature and during an infection. In our laboratory, we use *Pseudomonas aeruginosa* as model organism to investigate post-transcriptional regulation in bacteria.

Pseudomonas aeruginosa is an environmental bacterium thriving in multiple ecological niches and in several hosts. It is also an important opportunistic pathogen, being one of the leading causes of nosocomial infection worldwide. Only a handful post-transcriptional regulators have been investigated in *P. aeruginosa*, and, among those, our knowledge on RNA helicases is scarce at best.

Based on a genetic screen, we have identified the DEAD-box RNA helicase RhIE2 as a new post-transcriptional regulator that is essential for the expression of many *P. aeruginosa* pathogenicity traits. Via the characterization of RhIE2 biochemical properties *in vitro* and the determination of its impact on cellular transcripts *in vivo*, we could show that RhIE2 uses the energy derived from the hydrolysis of adenosine triphosphate to alter RNA structures and modulate the stability of numerous RNA targets. The global impact of RhIE2 is mediated by its unique C-terminal extension, which supports the RNA unwinding activity of the N-terminal domain as well as an RNA-dependent interaction with the RNase E endonuclease, the major component of the RNA degradation machinery in many bacteria.

Phylogenetic analysis of the RhIE group of proteobacterial RNA helicases indicate that their C-terminal extension are very diverse and evolve quickly. In agreement, our experimental work suggest that this part of the enzyme could be involved in significant mechanistic variations and sub-functionalization events.

Given the structural similarities shared by RNA helicases, determining protein-specific enzymatic properties and interaction particularities, like the ones observed for RhIE2, could be used as a basis for the development of compounds targeting a given pathogen or cellular function with a high selectivity.

The DEAD-box RNA helicase eIF4A is a promising host target for the development of potent broad-spectrum antivirals

Wednesday, 7th July - 16:00: Poster Session 2-C - Poster - Abstract ID: 90

Prof. Arnold Grünweller¹, **Dr. Wiebke Obermann**², **Dr. Christin Müller**³, **Prof. Roland K. Hartmann**¹,
Prof. John Ziebuhr³

1. Philipps-University Marburg, Institute of Pharmaceutical Chemistry, 2. Phillips-University Marburg, Institute of Pharmaceutical Chemistry, 3. Justus-Liebig-University Giessen, Institute of Medical Virology

The pandemic potential associated with RNA viruses is once again illustrated by the ongoing worldwide outbreak of SARS-CoV-2, highlighting the urgent need for the development of potent broad-spectrum antivirals that can be deployed as first-line therapeutic interventions against (re)emerging RNA viruses. As viruses depend on the host translation machinery to synthesize their viral proteins, inhibition of the RNA helicase eIF4A, a key component of the eukaryotic translation initiation complex eIF4F, has emerged as a very promising broad-spectrum antiviral strategy [1-7]. This helicase is essential for replication of a wide range of highly pathogenic RNA viruses since the presence of complex RNA structures in the 5'-untranslated mRNA or genome regions of many of these viruses requires the unwinding activity of eIF4A to allow binding of the 43S preinitiation complex during translation initiation.

Inhibition of eIF4A with the rocaglate Silvestrol, a natural compound isolated from plants of the genus *Aglaia*, was shown to inhibit genetically diverse RNA viruses (e.g. EBOV, LASV, ZIKV, HEV and coronaviruses (CoVs)) at low nanomolar concentrations. Silvestrol clamps structured cellular and viral mRNAs onto the surface of eIF4A, thereby preventing downstream translation initiation events. The synthesis of Silvestrol is sophisticated and time-consuming, providing a major obstacle to further antiviral drug development. As potential alternatives, numerous synthetic rocaglates with very similar eIF4A-targeting characteristics (e.g. CR-31-B (-), Zotatfin) have been generated.

Here, we report on the potent and non-toxic broad-spectrum antiviral activities of rocaglates against human Coronaviruses like SARS-CoV-2 and MERS-CoV in an *ex vivo* lung epithelial cell model and we present some mechanistical aspects of the RNA clamping mechanism in the context of viral 5'-UTRs.

In summary, our data show that eIF4A is an excellent target for the development of broad-spectrum antiviral drugs. This host-targeting strategy might have significant potential to help treat newly emerging RNA viruses more effectively in future outbreak situations.

[1] Biedenkopf et al., (2017), Antiviral Res. [2] Müller et al., (2018), Antiviral Res. [3] Elgner et al., (2018), Viruses. [4] Glitscher et al., (2018), Viruses. [5] Henß et al., (2018), Viruses. [6] Müller et al., (2020), Antiviral Res. [7] Müller et al., (2021), Antiviral Res.

Structural basis for resistance of *Mycobacterium tuberculosis* Rho to bicyclomycin

Wednesday, 7th July - 16:00: Poster Session 2-C - Poster - Abstract ID: 93

Dr. Marc Boudvillain¹, **Dr. Emmanuel Saridakis**², **Dr. Rishi Vishwakarma**³, **Mr. Kevin Martin**⁴, **Mrs. Isabelle Simon**¹, **Dr. Martin Cohen-Gonsaud**³, **Dr. Franck COSTE**¹, **Dr. Emmanuel Margeat**³, **Dr. Patrick Bron**³

1. Centre de Biophysique Moléculaire, CNRS Orléans, 2. NCSR “Demokritos”, Athens, 3. Centre de Biologie Structurale, INSERM, CNRS, Université de Montpellier, France, 4. Centre de Biologie Structurale, INSERM, CNRS, Université de Montpellier

The bacterial Rho factor is a ring-shaped hexameric RNA helicase that mediates genome-wide events of transcription termination and disruption of deleterious transcriptional R-loops. Rho is widespread in the bacterial kingdom¹. It is essential in many Gram-negative species and in high G+C Gram-positive Actinobacteria such as *M. tuberculosis*² or *Micrococcus luteus*³. Since Rho has no structural homologs in eukaryotes, it is an attractive target candidate for the development of new antibiotics¹.

Some Actinobacteria of the *Streptomyces* genus produce a natural Rho inhibitor called Bicyclomycin [BCM]. BCM is effective against various Gram-negative pathogens but is inactive against most Gram-positive species, including *M. tuberculosis*. One notable exception is *M. luteus*, whose growth is inhibited by BCM³. Accordingly, BCM strongly inhibits the *in vitro* enzymatic activity of *M. luteus* Rho³ but hardly affects *M. tuberculosis* Rho⁴. There is currently no rational explanation for this difference since all residues contacting BCM in *Escherichia coli* Rho are conserved in the two actinobacterial Rho factors.

To elucidate the origin of this resistance to BCM, we solved the high-resolution structure (3.3 Å) of *M. tuberculosis* Rho using cryo-EM. We show that the factor can adopt an open, ring-shaped hexamer conformation that mimics that observed for *Escherichia coli* Rho⁵. We identify a mutation in *M. tuberculosis* Rho that creates a steric bulk in the cavity where BCM normally binds. We show that this mutation is a taxa-specific evolutionary feature that alone is sufficient to account for the resistance of *M. tuberculosis* Rho to BCM. We also demonstrate that resistance to BCM has been acquired at the expense of enzymatic proficiency, supporting that the configuration of the cavity is substantially constrained by Rho function and, thus, is an attractive target for future drug development.

REFERENCES

1. D’Heygere et al. *Microbiology* **159**, 1423-36 (2013).
2. Botella et al. *Nat Commun* **8**, 14731 (2017).
3. Nowatzke et al. *J Bacteriol* **179**, 5238-40 (1997).
4. D’Heygere et al. *Nucleic Acids Res* **43**, 6099-111 (2015).
5. Skordalakes & Berger *Cell* **114**, 135-46 (2003).

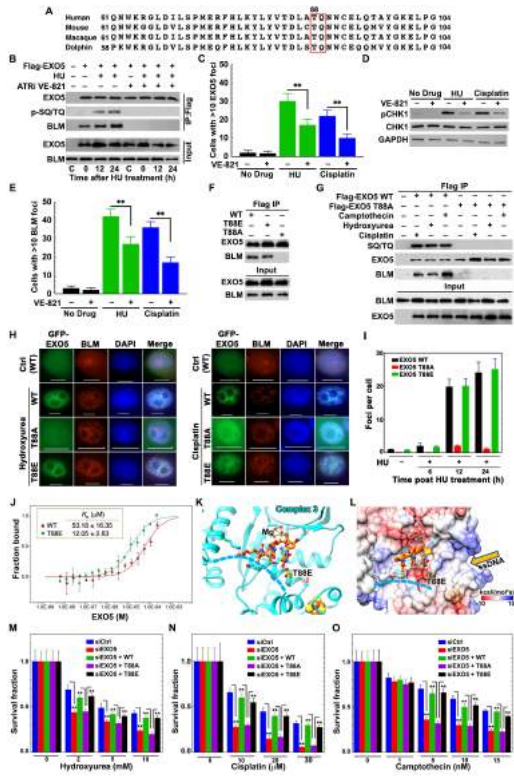


Fig. 3.jpg

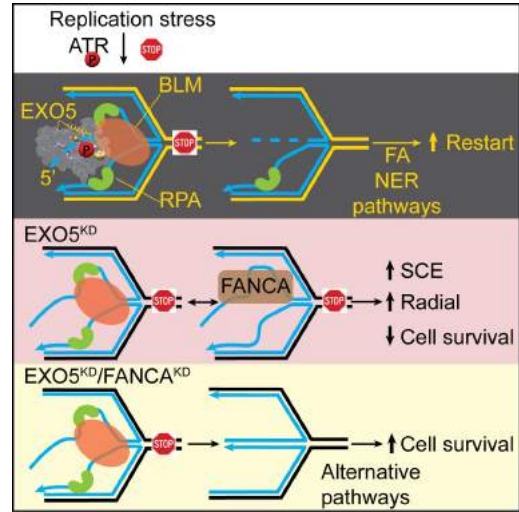


Fig. 4.jpg

Structural Basis of Mitochondria Twinkle Helicase Action and Twinkle Related Mitochondria Diseases

Wednesday, 7th July - 17:00: Oral Session - Oral - Abstract ID: 12

Dr. Yang Gao¹

1. Rice University

Mitochondria contain their own genomes that are uniquely replicated and maintained. Twinkle is the sole helicase responsible for mitochondria DNA replication. Twinkle can self-load onto and unwind mitochondria DNA. Nearly 60 mutations on *twinkle* have been linked to human mitochondria diseases. However, the structural basis of *twinkle* action and *twinkle*-related diseases are unknown. Here we reported the first atomic structure of a vertebrate *twinkle*-DNA complex at 3.5 Å resolution and accompanying biochemical and biophysical studies. In the *twinkle*-DNA complex, the N-terminal primase-like domains are attached to the side of the hexameric lock-washer formed by the C-terminal helicase domains. The N-terminal domains are refrained from interacting with the lagging strand DNA, consistent with the lack of Okazaki fragment synthesis in mitochondria. The new interfaces formed by the N- and C-terminal domains stabilize *twinkle* hexamer during translocation and are hotspots for disease-related mutations. The lock-washer-shaped helicase domains and an intermediate structure of a *twinkle*-DNA complex suggested that the *twinkle* subunit can move as a rigid body during *twinkle* translocation, consistent with the hand-over-hand translocation mechanism. *Twinkle* is with reduced DNA interaction and stochastic ATP hydrolysis, which explains the low efficiency of *twinkle* unwinding and implicates additional regulation of *twinkle* during mitochondria DNA replication. In the absence of DNA, *twinkle* stays as open-ring hexamers or heptamers and the N-terminal domains are disordered. High-speed atomic force microscope analysis suggested that *twinkle* is highly dynamic and can load and unload from DNA by itself. Amazingly, the N-terminal domains of *twinkle* can travel over 100 Å to search for its DNA substrate for loading. Taken together, our data revealed the unique structural and dynamic properties of *twinkle* that fit mitochondria DNA replication.

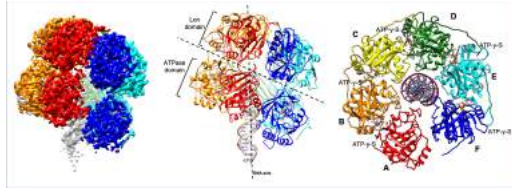
CryoEM structure of RadA, a Superfamily 4 modular helicase involved in natural transformation in *Streptococcus pneumoniae*

Wednesday, 7th July - 17:15: Oral Session - Oral - Abstract ID: 49

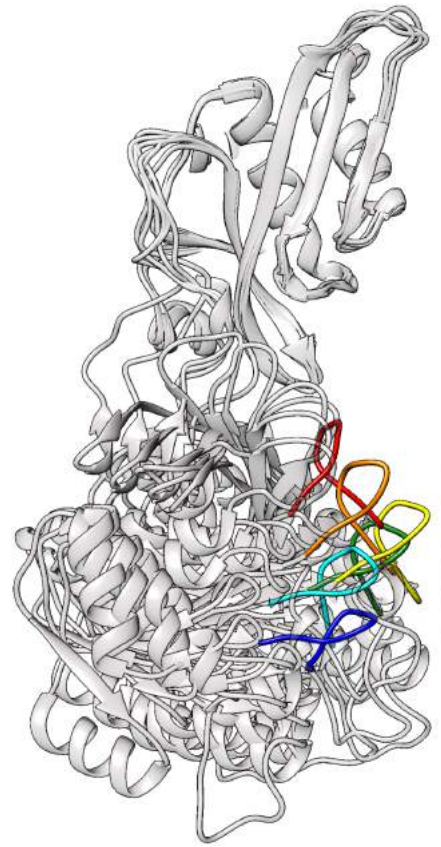
***Dr. Leonardo Talachia Rosa*¹, *Dr. Emeline Vernhes*², *Dr. Patrice Polard*², *Dr. Rémi Fronzes*¹**

1. Institut Européen de Chimie et Biologie, 2. Laboratoire de Microbiologie et Génétique Moléculaires

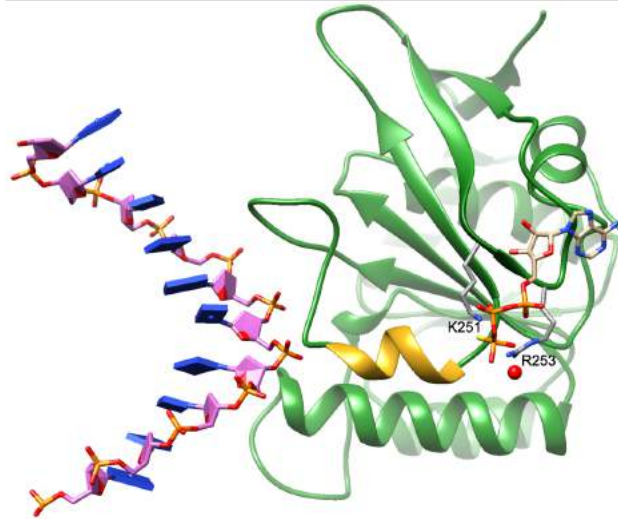
Natural transformation is the Horizontal Gene Transfer process in which bacteria uptake DNA fragments from the environment and incorporate in their own genome through homologous recombination. In *Streptococcus pneumoniae*, RadA is a superfamily 4 helicase responsible for the extension of the Displacement loop during the transformation event. This helicase is composed of an N-terminal C4 zinc domain, a central T7-gp4-like ATPase containing a conserved KNRFG motif, and a C-terminal Lon-protease-like domain. In our previous study, we obtained the crystal structure of RadA, revealing that the Lon domain strongly promotes hexamerisation, even in the absence of ligand. The ATPase domains, however, were retracted in an inactive conformation and their activity mechanism remained elusive. We here report the 3.15 Å cryoEM structure of RadA bound to double stranded DNA and ATP-γ-S (Fig 1). While the C-terminal Lon domain hexamer remained unchanged in relation to the crystal structure, the ATPase domains were orchestrated in a helical rising conformation, much like resembling the T7-gp4 helicase. This helical arrangement is crucial both for DNA and ATP coordination: Each subunit contacts the DNA in the leading strand through a flexible loop, 2 nucleotides above the adjacent subunit, following the DNA-B helix (Fig 2). Coordination of the lagging strand is performed by a second loop, 6 bp below the first contact, when the DNA completes a half-turn. On the ATP binding site, located between adjacent domains, the helical rise is needed for correct positioning of the KNRFG motif arginine finger (R253) and lysine piston (K251) on the gamma-phosphate, which in turn causes proper folding of its N-terminal short helix and positioning of the adjacent DNA binding loop (Fig 3). An incremental relative rotation of the ATPase domains culminates in ATP hydrolysis, DNA release and retraction of the domain in order to coordinate the DNA 12 bp above. Site-directed mutations on the ATPase domains culminated in decreased affinity for DNA. Our results present RadA as a modular helicase, in which the rigid Lon-like domain functions as a loading and hexamerisation platform and the flexible ATPase domain perform classical T7-gp4-like helicase activity.



Picture1.png



Picture2.png



Picture3.png

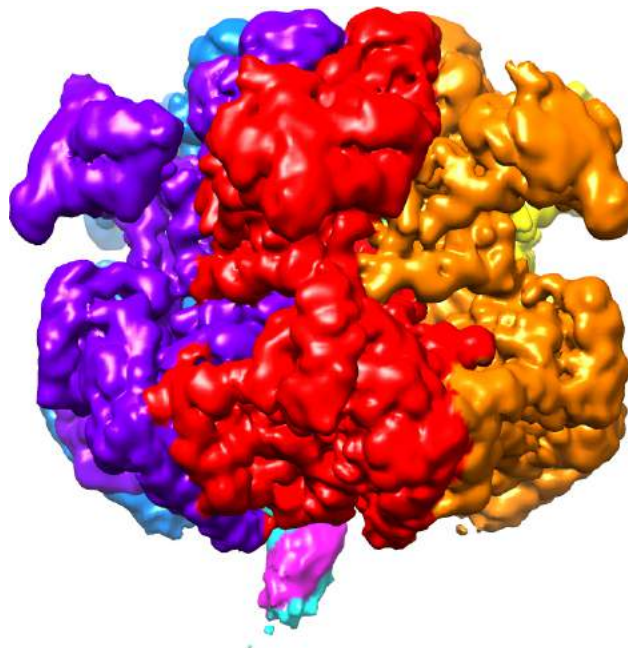
Structure of an MCM ring encircling bona fide melted DNA illustrates a key step of replication initiation

Wednesday, 7th July - 17:30: Oral Session - Oral - Abstract ID: 112

*Dr. Eric Enemark*¹, *Dr. Sanaz Rasouli*², *Dr. Alexander Myasnikov*²

1. University of Arkansas for Medical Sciences, 2. St. Jude Children's Research Hospital

DNA replication is the fundamental process used by all organisms to precisely duplicate the genetic material in preparation for cell division. During DNA replication, a helicase enzyme separates the individual strands of the DNA double-helix so that polymerases can use each strand as a template in the synthesis of new DNA. In eukaryotes and archaea, the replicative helicase enzyme is powered by a 6-membered ring known as the minichromosome maintenance (MCM) complex. The MCM complex initially assembles as an inert double-hexamer that encircles both strands of the DNA. To initiate DNA replication, the complex enigmatically transforms to two single rings that each encircle only one strand of DNA while excluding the other. We feel that we have major and novel insight into the mechanism of MCM:DNA helicase activation based on cryo-EM structures with resolutions ranging from 2.6 Å to 3.7 Å. We identify two fundamentally different classes of structure for the MCM ring in complex with a segment of duplex DNA. In the first class, the DNA is fully base-paired duplex DNA. In the second class, the DNA structure is opened with the loss of some base-pairing interactions. As such, this illustrates the MCM ring encircling **bona-fide melted DNA**— a key intermediate towards the initiation of DNA replication. Further, based on our earlier assignments of ATPase site types (*Nature Communications*, 2019), we can distinguish the ATPase site types of the two classes to show that the melted confirmation correlates with ATP binding. Collectively, the structures illustrate a straightforward mechanism for the MCM ring to melt encircled duplex DNA, a critical step in the transformation from encircling double-stranded DNA to encircling single-stranded DNA.



Dna1conf1a.jpg

Translocation activities of *S. Cerevisiae* Pif1 helicase

Wednesday, 7th July - 19:00: Oral Session - Oral - Abstract ID: 146

***Dr. Kevin Raney*¹, *Dr. Jun Gao*¹, *Dr. John C. Marecki*¹, *Mr. David Proffitt*¹, *Dr. Alicia K. Byrd*¹**

1. University of Arkansas for Medical Sciences

Introduction. Pif1 family helicases are highly versatile with functions in maintenance of nuclear and mitochondrial DNA. *S. cerevisiae* Pif1 is involved in removing difficult-to-replicate regions of DNA such as G-quadruplexes and protein blocks. Besides its DNA helicase activity, Pif1 is also a single-stranded DNA (ssDNA) translocase. Previous studies indicated a looping activity, which implies the existence of an anchor site.

Methods. We examined the structure of scPif1 bound to ssDNA and identified a site that might serve as an anchor site. The anchor site secures the helicase onto the ssDNA. Two variant enzymes were produced, F723A and T464A, and evaluated for binding, ATPase activity, translocation on single-stranded DNA, and DNA unwinding. **Results.** Each of the variants exhibited reduced binding affinity to ssDNA compared to the wtPif1. The ATPase activity was only 30% lower for the variants compared to wtPif1 under conditions in which ssDNA was nearly saturating. Translocation of the enzyme was determined by measuring stopped-flow fluorescence upon dissociation of helicase from ssDNA as a function of increasing lengths of ssDNA. Surprisingly, the variant enzymes appeared to translocate much faster than wtPif1 based on this ensemble assay. However, very little DNA unwinding was observed with variant forms of Pif1.

Discussion. The proposed anchor site provided mixed results in terms of supporting the site containing the amino acid variations as an anchor site. Additional experiments, including single molecule FRET will be required to advance understanding of looping.

WRN helicase stabilizes deprotected replication forks in BRCA2-deficient cancer cells

Wednesday, 7th July - 19:15: Oral Session - Oral - Abstract ID: 101

Dr. Arindam Datta¹, **Dr. Kajal Biswas**², **Mr. Joshua Sommers**¹, **Ms. Haley Thompson**³, **Dr. Sanket Awate**³, **Dr. Claudia Nicolae**⁴, **Dr. George-Lucian Moldovan**⁴, **Dr. Robert Shoemaker**⁵, **Dr. Shyam Sharan**², **Dr. Robert Brosh**¹

1. Translational Gerontology Branch, National Institute on Aging, NIH, **2.** Center for Cancer Research, National Cancer Institute, Frederick, MD 21702, USA, **3.** Translational Gerontology Branch, National Institute on Aging, NIH, NIH Biomedical Research Center, Baltimore, MD 21224, USA, **4.** Department of Biochemistry and Molecular Biology, The Pennsylvania State University College of Medicine, Hershey, PA 17033, USA, **5.** Chemopreventive Agent Development Research Group, Division of Cancer Prevention, National Cancer Institute, NIH, Rockville, MD 20850, USA

Introduction: Stabilization of stalled replication forks is critical for maintaining genome stability under conditions of replication stress. The tumor suppressor BRCA2 protects stalled forks from pathological degradation, thereby ensuring genomic integrity. Here, we investigated the role of RECQ helicase WRN in stabilizing stressed replication forks under condition of BRCA2 deficiency.

Methods: DNA fiber assay, *In vitro* helicase assay, Immunofluorescence, Xenograft animal model

Results: Using single molecule DNA fiber technique we showed that WRN complementation rescues fork restart defects and hyper-degradation of stalled forks in BRCA2-depleted cancer cells. WRN helicase inhibition resulted in severely compromised fork stability and poor replication recovery in BRCA2-deficient cells. Consistent with these results, WRN ATPase activity efficiently catalyzed restoration of a synthetic 'chicken-foot' structure to model replication fork *in vitro*. We showed that WRN helicase inhibitor selectively traps WRN on chromatin leading to rapid fork stalling and MRE11-dependent stalled fork degradation in the absence of BRCA2. Our experimental results further suggest that WRN helicase inhibition results in MUS81-dependent double strand breaks (DSBs) as a consequence of stalled fork hyper-degradation in BRCA2-deficient cells. This leads to aberrant activation of non-homologous end joining (NHEJ) and elevated chromosomal instability in BRCA2-mutated cancer cells. However, inhibition of MRE11 alleviated chromosomal aberrations, suggesting MRE11-mediated fork degradation contributes to WRN inhibitor-induced genomic instability. Targeted inhibition of WRN helicase triggered massive cell death in BRCA2-deficient cancer cells and showed synergistic cytotoxicity with poly (ADP)ribose (PARP) inhibitor olaparib. Furthermore, *in vivo* studies using an athymic nude mouse xenograft model demonstrated marked shrinkage of *BRCA2*^{-/-} tumors upon WRN helicase inhibition.

Discussion: Replication stress is a potential threat to genome stability if not resolved in a timely fashion. We characterized a crucial role of WRN helicase to stabilize stalled replication forks in cancer cells lacking functional BRCA2, a major fork protecting factor. Based on our cell-based and biochemical results, we propose that upon replication stalling, WRN helicase efficiently converts the reversed fork to an active replication fork, thus limiting aberrant nucleolytic processing under conditions of fork deprotection. Collectively, our findings reveal a specialized role of WRN helicase to stabilize replication forks when BRCA2 is deficient.

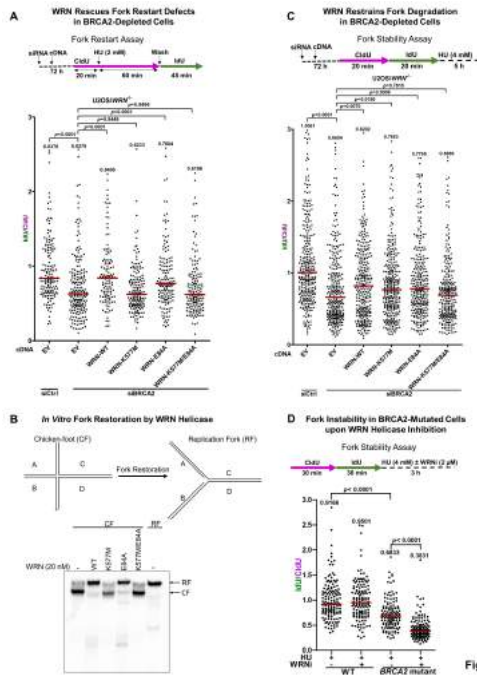


Figure 1.jpg

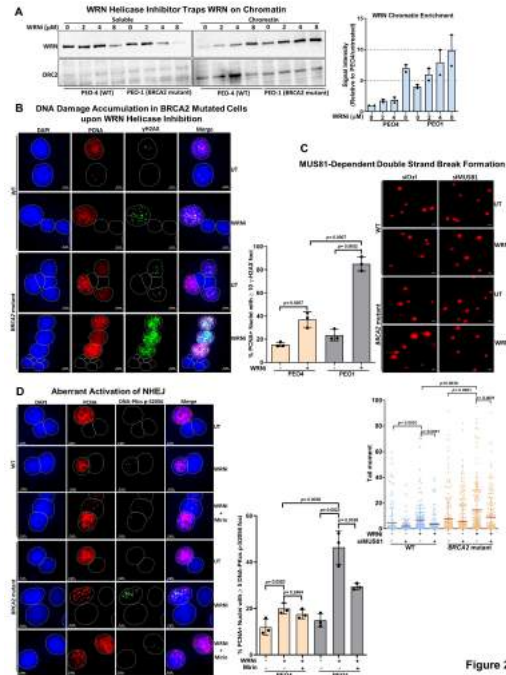


Figure 2

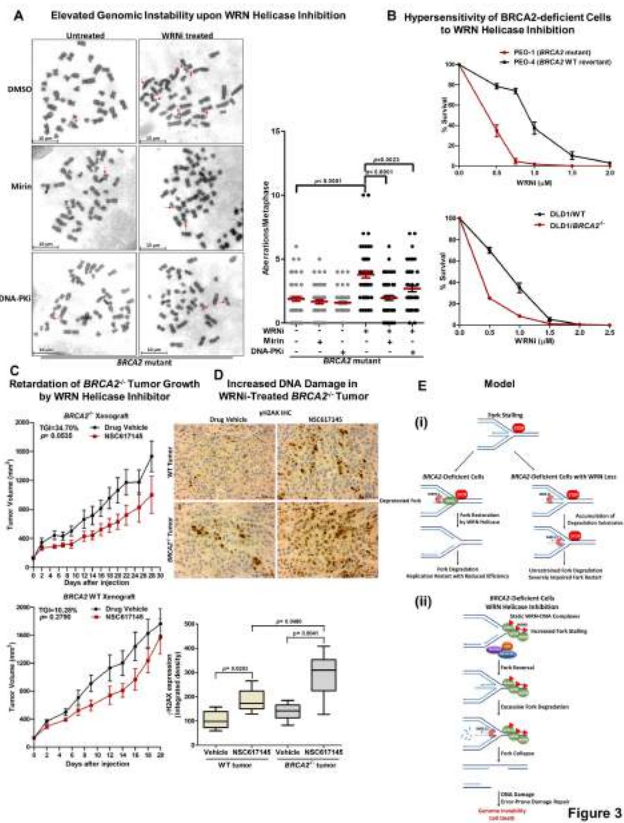


Figure 3

Figure 3.jpg

Nucleosome recognition and DNA distortion by the Chd1 chromatin remodeler

Wednesday, 7th July - 19:30: Oral Session - Oral - Abstract ID: 16

Dr. Ilana Nodelman *¹, **Mr. Sayan Das** *², **Ms. Anneliese Faustino**¹, **Prof. Stephen Fried**¹,
Prof. Greg Bowman¹, **Prof. Jean-Paul Armache**²

1. Johns Hopkins University, 2. Penn State University

Chromatin remodelers are ATP-dependent enzymes that organize nucleosomes within all eukaryotic genomes. We have solved a nucleotide-free state of the Chd1 chromatin remodeler bound to a nucleosome by cryo-electron microscopy to 2.6 Å resolution. The remodeler creates an extended distortion of nucleosomal DNA, delimited by a single nucleotide bulge on each strand – a tracking-strand bulge within the ATPase binding site and a guide-strand bulge one helical turn from the ATPase motor. Remarkably, each DNA bulge displays an A-form geometry. By inducing DNA to visit a conformation characteristic of RNA duplexes, the ATPase stimulates an asymmetric shift of only the tracking strand. Outside the ATPase binding site, the second A-form bulge allows the nucleosome to regain its canonical geometry, where a shift of the guide strand recovers B-form geometry and yields a full 1 bp shift of nucleosomal DNA. The structure also reveals a histone-binding module, called ChEx, which binds the H3 aN helix and the H2A/H2B dimer on the exit-side of the nucleosome. Through its interactions with the acidic patch, the ChEx module may allow Chd1 to block other remodelers and participate in histone reorganization during transcription.

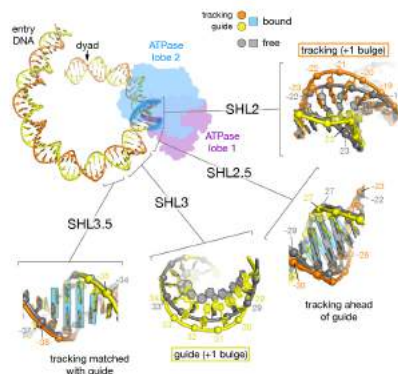
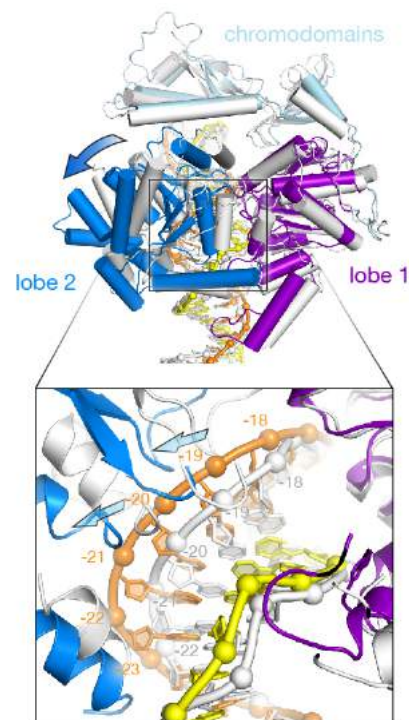


Figure1.jpg



- closed, ADP•BeF₃⁻-bound
- open, nucleotide-free

Figure2.jpg

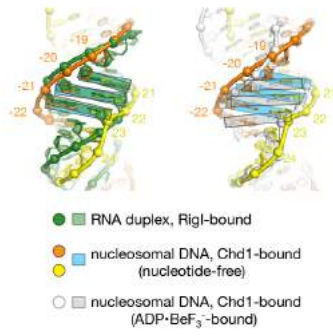


Figure3.jpg

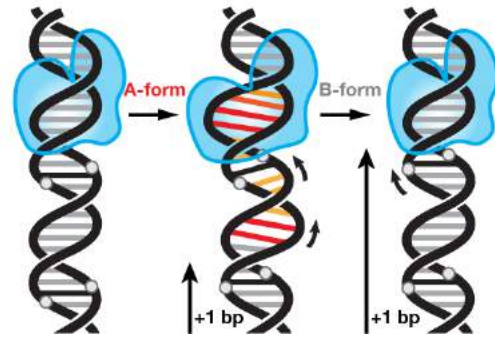


Figure4.jpg

Visualizing the action of SARS-CoV-2 and eukaryotic replicative helicases

Thursday, 8th July - 14:00: Keynote 7 - Oral - Abstract ID: 75

Dr. Shixin Liu¹

1. Rockefeller University

The replicative helicase is a central component of the genome replication machinery across kingdoms, unwinding the downstream nucleic acid duplex to create single-stranded templates for new synthesis by a coupled polymerase. Single-molecule techniques are ideally suited to directly visualize the dynamic behavior of helicases on their substrates in distinctive biochemical and mechanical environments. I will describe our recent efforts to understand the operating principles of viral and eukaryotic replicative helicases. Using an optical-tweezers hairpin unwinding assay, we showed that the SARS-CoV-2 nsp13 is an intrinsically weak helicase whose activity can be dramatically enhanced by a destabilizing force applied to the RNA substrate. Using correlative single-molecule fluorescence detection and force manipulation, we discovered that the yeast CMG harbors a ssDNA gate in its closed ring architecture. CMG uses this gate to vacate the replication fork and diffuse on duplex DNA, as well as to re-enter a fork and restart replication. Finally, we investigated the mechanism for the licensing of eukaryotic origins of replication where MCM helicases are loaded, leading to CMG formation. Our single-molecule assay led to the unexpected finding that the origin recognition complex searches for nucleosomes and actively remodels them to mediate pre-replication complex assembly.

The *E. coli* replisome does not require ATP to replicate DNA.

Thursday, 8th July - 14:30: Oral Session - Oral - Abstract ID: 44

***Dr. Lisanne Spenkelink*¹, *Mr. Richard Spinks*¹, *Dr. Slobodan Jergic*¹, *Dr. Jacob Lewis*¹, *Prof. Nicholas Dixon*¹, *Prof. Antoine van Oijen*¹**

1. University of Wollongong

Introduction

Adenosine triphosphate (ATP) hydrolysis is the main cellular energy source to drive biochemical reactions that are otherwise energetically unfavourable. DNA replication is a process that is thought to rely on ATP hydrolysis to promote the chemical and mechanical activities within the replication system (replisome). In *E. coli*, the DnaB helicase is known to unwind DNA in an ATP-dependent manner. However, ensemble biochemical assays do not separate helicase loading from replisome activity and thus do not separately test the ATP dependence of elongation.

Methods

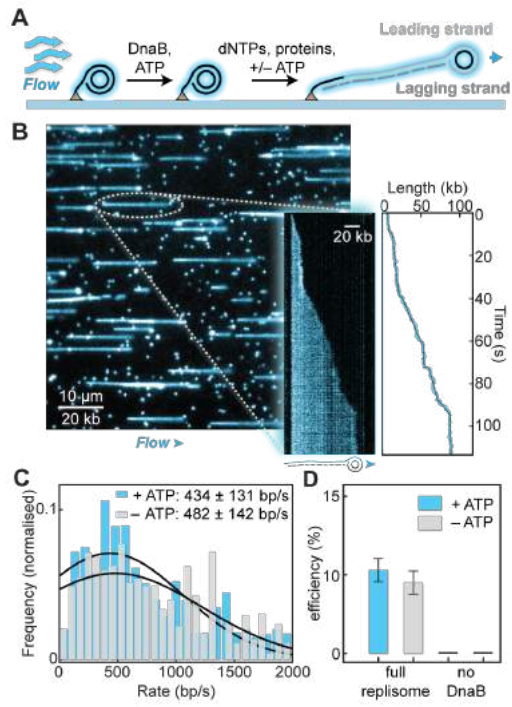
Using a flow-cell based single-molecule rolling-circle replication assay (Figure 1A), we are able to separate helicase loading and replication elongation into discrete steps and test the dependence of replisome-mediated elongation on ATP. In real time, we visualise DNA replication by individual replisomes (Figure 1B). We determine instantaneous replication rates and efficiencies through an automated and unbiased tracking algorithm (Figure 1B, inset).

Results

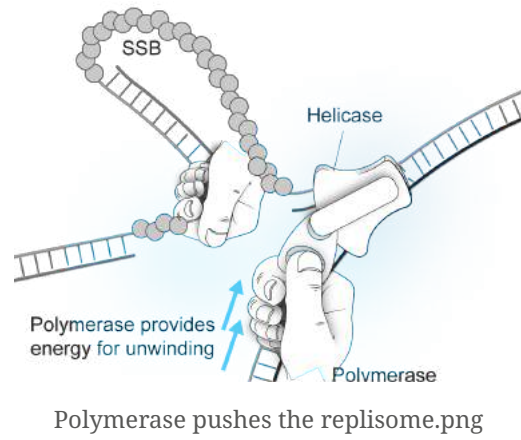
Surprisingly, we see efficient DNA replication in the absence of ATP or any other rNTP (Figure 1 C,D). This result suggests that DnaB does not require ATP hydrolysis for unwinding in the context of the replisome. Next, we interrogated the replisomal mechanisms that allow the DnaB helicase to function without ATP. We establish that nucleotide incorporation by the leading-strand polymerase, not ATP hydrolysis by the helicase, is the main motor driving the replication process.

Discussion

Notably, in the absence of DnaB, polymerase mediated unwinding and synthesis is very inefficient (Figure 1D), indicating the critical role that DnaB still plays during replication. We propose that DnaB provides the platform that dictates the architecture of the *E. coli* replisome to facilitate strand separation (Figure 2). While we show that rNTPs are not required during unimpeded replication, it is tempting to speculate that the helicase could use the energy from ATP hydrolysis to sustain replication through secondary structures or during roadblock bypass.



Single-molecule rolling-circle assay.png



Primase – Helicase pairs from Staphylococcal mobile genetic elements

Thursday, 8th July - 14:45: Oral Session - Oral - Abstract ID: 33

***Dr. Phoebe Rice*¹, *Dr. Heewhan Shin*¹, *Dr. Aleksandra Bebel*², *Dr. Ignacio Mir Sanchis*³**

1. The University of Chicago, 2. (present address) Phage Consultants, 3. Umeå University and Wallenberg Centre for Molecular Medicine

Heewhan Shin, Aleksandra Bebel, Ignacio Mir-Sanchis and Phoebe A. Rice

Some mobile genetic elements such as genomic islands, phages, and plasmids encode at least a subset of their machinery necessary for the own replication. We are studying the primases and helicases encoded by two different families of staphylococcal mobile genetic elements: pathogenicity islands (SaPIs), which are known to replicate after excision from the host chromosome, and SCC elements, which are less well understood but are of concern because they often carry methicillin resistance. Interestingly, in both the SaPIs and the SCCs, the presence of a helicase operon that usually encodes a primase as well is more conserved than the specific type of helicase and primase encoded, implying a mix-n-match approach to evolution.

Both certain SCCs and SaPIs encode a “DUF927” helicase which we have shown has, at its core, an MCM-family ATPase domain. We have determined structures of two of these, one with ssDNA as well as nucleotide cofactors bound. We are also investigating the interactions of one of these, the SaPIBov1 Rep protein, with its cognate AEP-family primase. Other SCC and SaPI Rep proteins belong to the D5 family. We have shown that, while the SaPI ones include an N-terminal AEP-family primase, the SCC one is downstream of an A-family polymerase and a small cofactor protein which confers unexpected primase activity on the polymerase. We will present our recent structural and biochemical work and discuss its implications for the evolution of mobile genetic elements.

Human DNA helicase B protects stalled replication forks from degradation

Thursday, 8th July - 15:00: Oral Session - Oral - Abstract ID: 34

***Dr. Alicia K. Byrd*¹, *Dr. Maroof Khan Zafar*¹, *Ms. Lindsey Hazeslip*¹, *Mr. Matthew Thompson*¹**

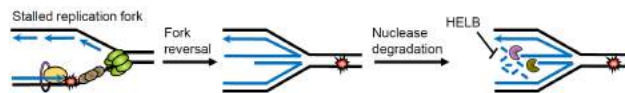
1. University of Arkansas for Medical Sciences

Introduction: Genomic DNA is constantly under assault from environmental factors and intrinsic sources of DNA damage. This can impair progression of the replication fork causing replication stress leading to activation of the replication stress response to protect the integrity of genomic DNA. Deficiencies in this process are associated with cancer and aging. One of the mechanisms of responding to and repairing replication impediments is replication fork reversal which provides an opportunity to repair the damage thereby protecting cellular DNA from genomic instability. Fork reversal creates a four-way junction that resembles a one-ended double-strand break. The regressed arm of the reversed fork must be protected from resection by nucleases to maintain genomic stability. Several proteins such as BRCA1, BRCA2, and RAD51 are involved in protecting reversed forks from degradation. Recently, human DNA Helicase B (HELB) was identified as a negative regulator of homologous recombination by inhibiting EXO1 and BLM-DNA2 mediated end resection. EXO1 and DNA2 can degrade the nascent DNA at stalled replication forks suggesting that HELB may protect stalled replication forks from degradation.

Methods: Single molecule DNA fiber assays were used in wild type and CRISPR-Cas9 generated HELB knockout cells to measure degradation of nascent DNA.

Results: Loss of HELB causes nascent strand degradation in response to replication stress. Knockdown of SMAR-CAL1 or ZRANB3 rescues fork protection in HELB knockout cells indicating that replication fork reversal is required for fork degradation in the absence of HELB. MRE11 and DNA2 nucleases are also required for fork degradation in HELB knockout cells. Interestingly, EXO1 does not appear to degrade reversed forks in the absence of HELB. HELB is epistatic with BRCA2 in fork protection. Consistent with the loss of nascent DNA with replication stalling in the absence of HELB, cells lacking HELB have increased markers of DNA damage and increased double-stranded DNA breaks.

Discussion: HELB protects reversed replication forks from aberrant degradation by MRE11 and DNA2. This increases genomic stability in cells and is consistent with its role in limiting end-resection during homologous recombination.



Model for helb inhibition of fork degradation.png

Analysis of the iron chaperone PCBP1 interactome: intersection of DNA repair and iron trafficking

Thursday, 8th July - 16:00: Poster Session 3-A - Poster - Abstract ID: 99

***Dr. Lorena Novoa-Aponte*¹, *Dr. Sarju Patel*¹, *Dr. Olga Protchenko*¹, *Dr. James Wohlschlegel*², *Dr. Caroline Philpott*¹**

1. Genetics and Metabolism Section, NIDDK, NIH, Bethesda, MD, USA, 2. Department of Biological Chemistry, UCLA, Los Angeles, CA, USA

Iron is used as an essential cofactor by several enzymes involved in DNA replication and repair. However, unchaperoned iron is toxic as it promotes redox stress that may affect DNA stability. Mammals use the iron chaperone PCBP1 to metallate the iron storage protein Ferritin and several iron-dependent enzymes¹. We recently showed that cells and liver tissues from mice lacking PCBP1 have increased DNA damage identified as TUNEL⁺ cells². Additional to its capacity to bind iron, PCBP1 also binds single-stranded nucleic acids. However, the iron chaperone activity of PCBP1 is the one controlling suppression of DNA damage². Our transcriptomic analysis of PCBP1-deleted livers in mice by RNA-seq showed that genes from the Fanconi anemia and homology-directed DNA repair pathways were upregulated in PCBP1 mutant. The CHK1 sensor, required for cell cycle arrest and activation of DNA damage response (DDR), and the histone H2AX, an early responder upon DNA double-strand break (DSB) occurrence, were also upregulated. DSBs trigger phosphorylation of H2AX producing γ H2AX. Confirming the increased rate of DSBs on cells lacking PCBP1, the γ H2AX levels increased when knocking down PCBP1.

Given that DSBs are the most deleterious DNA lesions, we want to elucidate the relationship between DDR and iron metabolism. One possibility is that PCBP1 plays a role in the maintenance of enzymes involved in DDR that need iron for function. Some of those have metal iron centers (DNA-demethylases and -nucleases), and some others Fe-S clusters (DNA-primase, DNA-polymerases, DNA-exonuclease, DNA-glycosylases, and the DNA-helicases FANCI, FANCD1, FANCD2, FANCD3, FANCD4, FANCD5, FANCD6, FANCD7, FANCD8, FANCD9, FANCD10, FANCD11, FANCD12, FANCD13, FANCD14, FANCD15, FANCD16, FANCD17, FANCD18, FANCD19, FANCD20, FANCD21, FANCD22, FANCD23, FANCD24, FANCD25, FANCD26, FANCD27, FANCD28, FANCD29, FANCD30, FANCD31, FANCD32, FANCD33, FANCD34, FANCD35, FANCD36, FANCD37, FANCD38, FANCD39, FANCD40, FANCD41, FANCD42, FANCD43, FANCD44, FANCD45, FANCD46, FANCD47, FANCD48, FANCD49, FANCD50, FANCD51, FANCD52, FANCD53, FANCD54, FANCD55, FANCD56, FANCD57, FANCD58, FANCD59, FANCD60, FANCD61, FANCD62, FANCD63, FANCD64, FANCD65, FANCD66, FANCD67, FANCD68, FANCD69, FANCD70, FANCD71, FANCD72, FANCD73, FANCD74, FANCD75, FANCD76, FANCD77, FANCD78, FANCD79, FANCD80, FANCD81, FANCD82, FANCD83, FANCD84, FANCD85, FANCD86, FANCD87, FANCD88, FANCD89, FANCD90, FANCD91, FANCD92, FANCD93, FANCD94, FANCD95, FANCD96, FANCD97, FANCD98, FANCD99, FANCD100, FANCD101, FANCD102, FANCD103, FANCD104, FANCD105, FANCD106, FANCD107, FANCD108, FANCD109, FANCD110, FANCD111, FANCD112, FANCD113, FANCD114, FANCD115, FANCD116, FANCD117, FANCD118, FANCD119, FANCD120, FANCD121, FANCD122, FANCD123, FANCD124, FANCD125, FANCD126, FANCD127, FANCD128, FANCD129, FANCD130, FANCD131, FANCD132, FANCD133, FANCD134, FANCD135, FANCD136, FANCD137, FANCD138, FANCD139, FANCD140, FANCD141, FANCD142, FANCD143, FANCD144, FANCD145, FANCD146, FANCD147, FANCD148, FANCD149, FANCD150, FANCD151, FANCD152, FANCD153, FANCD154, FANCD155, FANCD156, FANCD157, FANCD158, FANCD159, FANCD160, FANCD161, FANCD162, FANCD163, FANCD164, FANCD165, FANCD166, FANCD167, FANCD168, FANCD169, FANCD170, FANCD171, FANCD172, FANCD173, FANCD174, FANCD175, FANCD176, FANCD177, FANCD178, FANCD179, FANCD180, FANCD181, FANCD182, FANCD183, FANCD184, FANCD185, FANCD186, FANCD187, FANCD188, FANCD189, FANCD190, FANCD191, FANCD192, FANCD193, FANCD194, FANCD195, FANCD196, FANCD197, FANCD198, FANCD199, FANCD200, FANCD201, FANCD202, FANCD203, FANCD204, FANCD205, FANCD206, FANCD207, FANCD208, FANCD209, FANCD210, FANCD211, FANCD212, FANCD213, FANCD214, FANCD215, FANCD216, FANCD217, FANCD218, FANCD219, FANCD220, FANCD221, FANCD222, FANCD223, FANCD224, FANCD225, FANCD226, FANCD227, FANCD228, FANCD229, FANCD230, FANCD231, FANCD232, FANCD233, FANCD234, FANCD235, FANCD236, FANCD237, FANCD238, FANCD239, FANCD240, FANCD241, FANCD242, FANCD243, FANCD244, FANCD245, FANCD246, FANCD247, FANCD248, FANCD249, FANCD250, FANCD251, FANCD252, FANCD253, FANCD254, FANCD255, FANCD256, FANCD257, FANCD258, FANCD259, FANCD260, FANCD261, FANCD262, FANCD263, FANCD264, FANCD265, FANCD266, FANCD267, FANCD268, FANCD269, FANCD270, FANCD271, FANCD272, FANCD273, FANCD274, FANCD275, FANCD276, FANCD277, FANCD278, FANCD279, FANCD280, FANCD281, FANCD282, FANCD283, FANCD284, FANCD285, FANCD286, FANCD287, FANCD288, FANCD289, FANCD290, FANCD291, FANCD292, FANCD293, FANCD294, FANCD295, FANCD296, FANCD297, FANCD298, FANCD299, FANCD300, FANCD301, FANCD302, FANCD303, FANCD304, FANCD305, FANCD306, FANCD307, FANCD308, FANCD309, FANCD310, FANCD311, FANCD312, FANCD313, FANCD314, FANCD315, FANCD316, FANCD317, FANCD318, FANCD319, FANCD320, FANCD321, FANCD322, FANCD323, FANCD324, FANCD325, FANCD326, FANCD327, FANCD328, FANCD329, FANCD330, FANCD331, FANCD332, FANCD333, FANCD334, FANCD335, FANCD336, FANCD337, FANCD338, FANCD339, FANCD340, FANCD341, FANCD342, FANCD343, FANCD344, FANCD345, FANCD346, FANCD347, FANCD348, FANCD349, FANCD350, FANCD351, FANCD352, FANCD353, FANCD354, FANCD355, FANCD356, FANCD357, FANCD358, FANCD359, FANCD360, FANCD361, FANCD362, FANCD363, FANCD364, FANCD365, FANCD366, FANCD367, FANCD368, FANCD369, FANCD370, FANCD371, FANCD372, FANCD373, FANCD374, FANCD375, FANCD376, FANCD377, FANCD378, FANCD379, FANCD380, FANCD381, FANCD382, FANCD383, FANCD384, FANCD385, FANCD386, FANCD387, FANCD388, FANCD389, FANCD390, FANCD391, FANCD392, FANCD393, FANCD394, FANCD395, FANCD396, FANCD397, FANCD398, FANCD399, FANCD400, FANCD401, FANCD402, FANCD403, FANCD404, FANCD405, FANCD406, FANCD407, FANCD408, FANCD409, FANCD410, FANCD411, FANCD412, FANCD413, FANCD414, FANCD415, FANCD416, FANCD417, FANCD418, FANCD419, FANCD420, FANCD421, FANCD422, FANCD423, FANCD424, FANCD425, FANCD426, FANCD427, FANCD428, FANCD429, FANCD430, FANCD431, FANCD432, FANCD433, FANCD434, FANCD435, FANCD436, FANCD437, FANCD438, FANCD439, FANCD440, FANCD441, FANCD442, FANCD443, FANCD444, FANCD445, FANCD446, FANCD447, FANCD448, FANCD449, FANCD450, FANCD451, FANCD452, FANCD453, FANCD454, FANCD455, FANCD456, FANCD457, FANCD458, FANCD459, FANCD460, FANCD461, FANCD462, FANCD463, FANCD464, FANCD465, FANCD466, FANCD467, FANCD468, FANCD469, FANCD470, FANCD471, FANCD472, FANCD473, FANCD474, FANCD475, FANCD476, FANCD477, FANCD478, FANCD479, FANCD480, FANCD481, FANCD482, FANCD483, FANCD484, FANCD485, FANCD486, FANCD487, FANCD488, FANCD489, FANCD490, FANCD491, FANCD492, FANCD493, FANCD494, FANCD495, FANCD496, FANCD497, FANCD498, FANCD499, FANCD500, FANCD501, FANCD502, FANCD503, FANCD504, FANCD505, FANCD506, FANCD507, FANCD508, FANCD509, FANCD510, FANCD511, FANCD512, FANCD513, FANCD514, FANCD515, FANCD516, FANCD517, FANCD518, FANCD519, FANCD520, FANCD521, FANCD522, FANCD523, FANCD524, FANCD525, FANCD526, FANCD527, FANCD528, FANCD529, FANCD530, FANCD531, FANCD532, FANCD533, FANCD534, FANCD535, FANCD536, FANCD537, FANCD538, FANCD539, FANCD540, FANCD541, FANCD542, FANCD543, FANCD544, FANCD545, FANCD546, FANCD547, FANCD548, FANCD549, FANCD550, FANCD551, FANCD552, FANCD553, FANCD554, FANCD555, FANCD556, FANCD557, FANCD558, FANCD559, FANCD560, FANCD561, FANCD562, FANCD563, FANCD564, FANCD565, FANCD566, FANCD567, FANCD568, FANCD569, FANCD570, FANCD571, FANCD572, FANCD573, FANCD574, FANCD575, FANCD576, FANCD577, FANCD578, FANCD579, FANCD580, FANCD581, FANCD582, FANCD583, FANCD584, FANCD585, FANCD586, FANCD587, FANCD588, FANCD589, FANCD590, FANCD591, FANCD592, FANCD593, FANCD594, FANCD595, FANCD596, FANCD597, FANCD598, FANCD599, FANCD600, FANCD601, FANCD602, FANCD603, FANCD604, FANCD605, FANCD606, FANCD607, FANCD608, FANCD609, FANCD610, FANCD611, FANCD612, FANCD613, FANCD614, FANCD615, FANCD616, FANCD617, FANCD618, FANCD619, FANCD620, FANCD621, FANCD622, FANCD623, FANCD624, FANCD625, FANCD626, FANCD627, FANCD628, FANCD629, FANCD630, FANCD631, FANCD632, FANCD633, FANCD634, FANCD635, FANCD636, FANCD637, FANCD638, FANCD639, FANCD640, FANCD641, FANCD642, FANCD643, FANCD644, FANCD645, FANCD646, FANCD647, FANCD648, FANCD649, FANCD650, FANCD651, FANCD652, FANCD653, FANCD654, FANCD655, FANCD656, FANCD657, FANCD658, FANCD659, FANCD660, FANCD661, FANCD662, FANCD663, FANCD664, FANCD665, FANCD666, FANCD667, FANCD668, FANCD669, FANCD670, FANCD671, FANCD672, FANCD673, FANCD674, FANCD675, FANCD676, FANCD677, FANCD678, FANCD679, FANCD680, FANCD681, FANCD682, FANCD683, FANCD684, FANCD685, FANCD686, FANCD687, FANCD688, FANCD689, FANCD690, FANCD691, FANCD692, FANCD693, FANCD694, FANCD695, FANCD696, FANCD697, FANCD698, FANCD699, FANCD700, FANCD701, FANCD702, FANCD703, FANCD704, FANCD705, FANCD706, FANCD707, FANCD708, FANCD709, FANCD710, FANCD711, FANCD712, FANCD713, FANCD714, FANCD715, FANCD716, FANCD717, FANCD718, FANCD719, FANCD720, FANCD721, FANCD722, FANCD723, FANCD724, FANCD725, FANCD726, FANCD727, FANCD728, FANCD729, FANCD730, FANCD731, FANCD732, FANCD733, FANCD734, FANCD735, FANCD736, FANCD737, FANCD738, FANCD739, FANCD740, FANCD741, FANCD742, FANCD743, FANCD744, FANCD745, FANCD746, FANCD747, FANCD748, FANCD749, FANCD750, FANCD751, FANCD752, FANCD753, FANCD754, FANCD755, FANCD756, FANCD757, FANCD758, FANCD759, FANCD760, FANCD761, FANCD762, FANCD763, FANCD764, FANCD765, FANCD766, FANCD767, FANCD768, FANCD769, FANCD770, FANCD771, FANCD772, FANCD773, FANCD774, FANCD775, FANCD776, FANCD777, FANCD778, FANCD779, FANCD780, FANCD781, FANCD782, FANCD783, FANCD784, FANCD785, FANCD786, FANCD787, FANCD788, FANCD789, FANCD790, FANCD791, FANCD792, FANCD793, FANCD794, FANCD795, FANCD796, FANCD797, FANCD798, FANCD799, FANCD800, FANCD801, FANCD802, FANCD803, FANCD804, FANCD805, FANCD806, FANCD807, FANCD808, FANCD809, FANCD810, FANCD811, FANCD812, FANCD813, FANCD814, FANCD815, FANCD816, FANCD817, FANCD818, FANCD819, FANCD820, FANCD821, FANCD822, FANCD823, FANCD824, FANCD825, FANCD826, FANCD827, FANCD828, FANCD829, FANCD830, FANCD831, FANCD832, FANCD833, FANCD834, FANCD835, FANCD836, FANCD837, FANCD838, FANCD839, FANCD840, FANCD841, FANCD842, FANCD843, FANCD844, FANCD845, FANCD846, FANCD847, FANCD848, FANCD849, FANCD850, FANCD851, FANCD852, FANCD853, FANCD854, FANCD855, FANCD856, FANCD857, FANCD858, FANCD859, FANCD860, FANCD861, FANCD862, FANCD863, FANCD864, FANCD865, FANCD866, FANCD867, FANCD868, FANCD869, FANCD870, FANCD871, FANCD872, FANCD873, FANCD874, FANCD875, FANCD876, FANCD877, FANCD878, FANCD879, FANCD880, FANCD881, FANCD882, FANCD883, FANCD884, FANCD885, FANCD886, FANCD887, FANCD888, FANCD889, FANCD890, FANCD891, FANCD892, FANCD893, FANCD894, FANCD895, FANCD896, FANCD897, FANCD898, FANCD899, FANCD900, FANCD901, FANCD902, FANCD903, FANCD904, FANCD905, FANCD906, FANCD907, FANCD908, FANCD909, FANCD910, FANCD911, FANCD912, FANCD913, FANCD914, FANCD915, FANCD916, FANCD917, FANCD918, FANCD919, FANCD920, FANCD921, FANCD922, FANCD923, FANCD924, FANCD925, FANCD926, FANCD927, FANCD928, FANCD929, FANCD930, FANCD931, FANCD932, FANCD933, FANCD934, FANCD935, FANCD936, FANCD937, FANCD938, FANCD939, FANCD940, FANCD941, FANCD942, FANCD943, FANCD944, FANCD945, FANCD946, FANCD947, FANCD948, FANCD949, FANCD950, FANCD951, FANCD952, FANCD953, FANCD954, FANCD955, FANCD956, FANCD957, FANCD958, FANCD959, FANCD960, FANCD961, FANCD962, FANCD963, FANCD964, FANCD965, FANCD966, FANCD967, FANCD968, FANCD969, FANCD970, FANCD971, FANCD972, FANCD973, FANCD974, FANCD975, FANCD976, FANCD977, FANCD978, FANCD979, FANCD980, FANCD981, FANCD982, FANCD983, FANCD984, FANCD985, FANCD986, FANCD987, FANCD988, FANCD989, FANCD990, FANCD991, FANCD992, FANCD993, FANCD994, FANCD995, FANCD996, FANCD997, FANCD998, FANCD999, FANCD1000, FANCD1001, FANCD1002, FANCD1003, FANCD1004, FANCD1005, FANCD1006, FANCD1007, FANCD1008, FANCD1009, FANCD1010, FANCD1011, FANCD1012, FANCD1013, FANCD1014, FANCD1015, FANCD1016, FANCD1017, FANCD1018, FANCD1019, FANCD1020, FANCD1021, FANCD1022, FANCD1023, FANCD1024, FANCD1025, FANCD1026, FANCD1027, FANCD1028, FANCD1029, FANCD1030, FANCD1031, FANCD1032, FANCD1033, FANCD1034, FANCD1035, FANCD1036, FANCD1037, FANCD1038, FANCD1039, FANCD1040, FANCD1041, FANCD1042, FANCD1043, FANCD1044, FANCD1045, FANCD1046, FANCD1047, FANCD1048, FANCD1049, FANCD1050, FANCD1051, FANCD1052, FANCD1053, FANCD1054, FANCD1055, FANCD1056, FANCD1057, FANCD1058, FANCD1059, FANCD1060, FANCD1061, FANCD1062, FANCD1063, FANCD1064, FANCD1065, FANCD1066, FANCD1067, FANCD1068, FANCD1069, FANCD1070, FANCD1071, FANCD1072, FANCD1073, FANCD1074, FANCD1075, FANCD1076, FANCD1077, FANCD1078, FANCD1079, FANCD1080, FANCD1081, FANCD1082, FANCD1083, FANCD1084, FANCD1085, FANCD1086, FANCD1087, FANCD1088, FANCD1089, FANCD1090, FANCD1091, FANCD1092, FANCD1093, FANCD1094, FANCD1095, FANCD1096, FANCD1097, FANCD1098, FANCD1099, FANCD1100, FANCD1101, FANCD1102, FANCD1103, FANCD1104, FANCD1105, FANCD1106, FANCD1107, FANCD1108, FANCD1109, FANCD1110, FANCD1111, FANCD1112, FANCD1113, FANCD1114, FANCD1115, FANCD1116, FANCD1117, FANCD1118, FANCD1119, FANCD1120, FANCD1121, FANCD1122, FANCD1123, FANCD1124, FANCD1125, FANCD1126, FANCD1127, FANCD1128, FANCD1129, FANCD1130, FANCD1131, FANCD1132, FANCD1133, FANCD1134, FANCD1135, FANCD1136, FANCD1137, FANCD1138, FANCD1139, FANCD1140, FANCD1141, FANCD1142, FANCD1143, FANCD1144, FANCD1145, FANCD1146, FANCD1147, FANCD1148, FANCD1149, FANCD1150, FANCD1151, FANCD1152, FANCD1153, FANCD1154, FANCD1155, FANCD1156, FANCD1157, FANCD1158, FANCD1159, FANCD1160, FANCD1161, FANCD1162, FANCD1163, FANCD1164, FANCD1165, FANCD1166, FANCD1167, FANCD1168, FANCD1169, FANCD1170, FANCD1171, FANCD1172, FANCD1173, FANCD1174, FANCD1175, FANCD1176, FANCD1177, FANCD1178, FANCD1179, FANCD1180, FANCD1181, FANCD1182, FANCD1183, FANCD1184, FANCD1185, FANCD1186, FANCD1187, FANCD1188, FANCD1189, FANCD1190, FANCD1191, FANCD1192, FANCD1193, FANCD1194, FANCD1195, FANCD1196, FANCD1197, FANCD1198, FANCD1199, FANCD1200, FANCD1201, FANCD1202, FANCD1203, FANCD1204, FANCD1205, FANCD1206, FANCD1207, FANCD1208, FANCD1209, FANCD1210, FANCD1211, FANCD1212, FANCD1213, FANCD1214, FANCD1215, FANCD1216, FANCD1217, FANCD1218, FANCD1219, FANCD1220, FANCD1221, FANCD1222, FANCD1223, FANCD1224, FANCD1225, FANCD1226, FANCD1227, FANCD1228, FANCD1229, FANCD1230, FANCD1231, FANCD1232, FANCD1233, FANCD1234, FANCD1235, FANCD1236, FANCD1237, FANCD1238, FANCD1239, FANCD1240, FANCD1241, FANCD1242, FANCD1243, FANCD1244, FANCD1245, FANCD1246, FANCD1247, FANCD1248, FANCD1249, FANCD1250, FANCD1251, FANCD1252, FANCD1253, FANCD1254, FANCD1255, FANCD1256, FANCD1257, FANCD1258, FANCD1259, FANCD1260, FANCD1261, FANCD1262, FANCD1263, FANCD1264, FANCD1265, FANCD1266, FANCD1267, FANCD1268, FANCD1269, FANCD1270, FANCD1271, FANCD1272, FANCD1273, FANCD1274, FANCD1275, FANCD1276, FANCD1277, FANCD1278, FANCD1279, FANCD1280, FANCD1281, FANCD1282, FANCD1283, FANCD1284, FANCD1285, FANCD1286, FANCD1287, FANCD1288, FANCD1289, FANCD1290, FANCD1291, FANCD1292, FANCD1293, FANCD1294, FANCD1295, FANCD1296, FANCD1297, FANCD1298, FANCD1299, FANCD1300, FANCD1301, FANCD1302, FANCD1303, FANCD1304, FANCD1305, FANCD1306, FANCD1307, FANCD1308, FANCD1309, FANCD1310, FANCD1311, FANCD1312, FANCD1313, FANCD1314, FANCD1315, FANCD1316, FANCD1317, FANCD1318, FANCD1319, FANCD1320, FANCD1321, FANCD1322, FANCD1323, FANCD1324, FANCD1325, FANCD1326, FANCD1327, FANCD1328, FANCD1329, FANCD1330, FANCD1331, FANCD1332, FANCD1333, FANCD1334, FANCD1335, FANCD1336, FANCD1337, FANCD1338, FANCD1339, FANCD1340, FANCD1341, FANCD1342, FANCD1343, FANCD1344, FANCD1345, FANCD1346, FANCD1347, FANCD1348, FANCD1349, FANCD1350, FANCD1351, FANCD1352, FANCD1353, FANCD1354, FANCD1355, FANCD1356, FANCD1357, FANCD1358, FANCD1359, FANCD1360, FANCD1361, FANCD1362, FANCD1363, FANCD1364, FANCD1365, FANCD1366, FANCD1367, FANCD1368, FANCD1369, FANCD1370, FANCD1371, FANCD1372, FANCD1373, FANCD1374, FANCD1375, FANCD1376, FANCD1377, FANCD1378, FANCD1379, FANCD1380, FANCD1381, FANCD1382, FANCD1383, FANCD1384, FANCD1385, FANCD1386, FANCD1387, FANCD1388, FANCD1389, FANCD1390, FANCD1391, FANCD1392, FANCD1393, FANCD1394, FANCD1395, FANCD1396, FANCD1397, FANCD1398, FANCD1399, FANCD1400, FANCD1401, FANCD1402, FANCD1403, FANCD1404, FANCD1405, FANCD1406, FANCD1407, FANCD1408, FANCD1409, FANCD1410, FANCD1411, FANCD1412, FANCD1413, FANCD1414, FANCD1415, FANCD1416, FANCD1417, FANCD1418, FANCD1419, FANCD1420, FANCD1421, FANCD1422, FANCD1423, FANCD1424, FANCD1425, FANCD1426, FANCD1427, FANCD1428, FANCD1429, FANCD1430, FANCD1431, FANCD1432, FANCD1433, FANCD1434, FANCD1435, FANCD1436, FANCD1437, FANCD1438, FANCD1439, FANCD1440, FANCD1441, FANCD1442, FANCD1443, FANCD1444, FANCD1445, FANCD1446, FANCD1447, FANCD1448, FANCD1449, FANCD1450, FANCD1451, FANCD1452, FANCD1453, FANCD1454, FANCD1455, FANCD1456, FANCD1457, FANCD1458, FANCD1459, FANCD1460, FANCD1461, FANCD1462, FANCD1463, FANCD1464, FANCD1465, FANCD1466, FANCD1467, FANCD1468, FANCD1469, FANCD1470, FANCD1471, FANCD1472, FANCD1473, FANCD1474, FANCD1475, FANCD1476, FANCD1477, FANCD1478, FANCD1479, FANCD1480, FANCD1481, FANCD1482, FANCD1483, FANCD1484, FANCD1485, FANCD1486, FANCD1487, FANCD1488, FANCD1489, FANCD1490, FANCD1491, FANCD1492, FANCD1493, FANCD1494, FANCD1495, FANCD1496, FANCD1497, FANCD1498, FANCD1499, FANCD1500, FANCD1501, FANCD1502, FANCD1503, FANCD1504, FANCD1505, FANCD1506, FANCD1507, FANCD1508, FANCD1509, FANCD1510, FANCD1511, FANCD1512, FANCD1513, FANCD1514, FANCD1515, FANCD1516, FANCD1517, FANCD1518, FANCD1519, FANCD1520, FANCD1521, FANCD1522, FANCD1523, FANCD1524, FANCD1525, FANCD1526, FANCD1527, FANCD1528, FANCD1529, FANCD1530, FANCD1531, FANCD1532, FANCD1533, FANCD1534, FANCD1535, FANCD1536, FANCD1537, FANCD1538, FANCD1539, FANCD1540, FANCD1541, FANCD1542, FANCD1543, FANCD1544, FANCD1545, FANCD1546, FANCD1547, FANCD1548, FANCD1549, FANCD1550, FANCD1551, FANCD1552, FANCD1553, FANCD1554, FANCD1555, FANCD1556, FANCD1557, FANCD1558, FANCD1559, FANCD1560, FANCD1561, FANCD1562, FANCD1563, FANCD1564, FANCD1565, FANCD1566, FANCD1567, FANCD1568, FANCD1569, FANCD1570, FANCD1571, FANCD1572, FANCD1573, FANCD1574, FANCD1575, FANCD1576, FANCD1577, FANCD1578, FANCD1579, FANCD15

How XPD helicase responds to DNA damage and base composition.

Thursday, 8th July - 16:00: Poster Session 3-A - Poster - Abstract ID: 102

***Dr. Remi Fritzen*¹, *Dr. Francesco Colizzi*², *Dr. Giovanni Bussi*³, *Dr. J. Carlos Penedo*¹, *Prof. Malcolm F. White*¹**

1. University of St Andrews, 2. Computational Biology Node, Institute for Research in Biomedicine (IRB Barcelona), The Barcelona Institute of Science and Technology, 08028 Barcelona, 3. Molecular and Statistical Biophysics, Scuola Internazionale Superiore di Studi Avanzati, 34136 Trieste

Many genotoxic agents continuously challenge the integrity of the genome. To restore this integrity many repair processes exist. Nucleotide Excision Repair is one of these processes, it repairs structural DNA lesion, induced, for instance, by UV light. Firstly, the damage is detected, then the DNA is unwound around the lesion which allows access for other factors to excise the damaged DNA strand and finally the gap is filled and the newly synthesised DNA is ligated.

The unwinding step in Nucleotide Excision Repair is undertaken by the XPD helicase. We used two Archaeal model organisms, *Sulfolobus acidocaldarius* (SacXPD) and *Thermoplasma acidophilum* (TacXPD), to characterise their respective activity and address their response to the presence of a damage on either strand of the DNA. We demonstrated that TacXPD activity is impacted by a damage situated on the translocated strand contrary to SacXPD. We then concluded that TacXPD functions as a damage sensor whilst this is not the case for SacXPD and contextualised this result in light of previous comparative structural studies, showing the presence of a cleft capable of accommodating ssDNA in TacXPD.

In the second part of this work, we used TacXPD and two other representative helicases to confirm the impact of the purine/pyrimidine composition of the DNA on the unwinding activity and binding affinities, which was shown only through *in silico* analysis. We demonstrated that a stretch of purine on the displaced strand impacts significantly the helicase activity. This has further biological implication for instance, in gene regulation as some genes present long stretches purine or pyrimidine stretched in their promotor.

DNA damage repair and DEAD Box 1 (DDX1) in embryonic development

Thursday, 8th July - 16:00: Poster Session 3-A - Poster - Abstract ID: 108

*Dr. Lubna Yasmin*¹, *Dr. Yixiong Wang*¹, *Ms. Lazina Hossain*¹, *Dr. Roseline Godbout*¹

1. University of Alberta

INTRODUCTION: Maintaining accurate genome integrity during early embryonic development is essential. In the absence of key DNA repair proteins, embryos will either die or else survive to the blastocyst stage and then undergo apoptosis. DEAD Box1 (DDX1) protein is a member of a family of DEAD box proteins comprising ~40 members in humans. DDX1 has many roles in mammalian cells including RNA transport, RNA processing and the repair of DNA double-strand breaks (DSB). Here, we study the repair of DNA DSBs in developing mouse embryos, with a possible role for DDX1 in this process.

METHODS: DSB repair kinetics were examined after exposing early stage embryos to ionizing radiation. Embryos at three different developmental stages were examined: 1-cell, 2-cell and blastocyst which were immunostained with γ -H2AX (as a surrogate marker for DSBs) and DDX1 antibodies.

RESULTS & DISCUSSION: Previous studies revealed the presence of DDX1 in the cytoplasm of early-stage embryos, with transition to the nucleus in trophoblast cells after hatching. This is in contrast to most mammalian cells tested to date where DDX1 is preferentially located in the nucleus. We carried out a time-dependent analysis of DSB formation and resolution in 2-cell mouse embryos exposed to 2 Gy and 5 Gy radiation (Fig. 1). We found that: (i) DDX1 remained in the cytoplasm of irradiated embryos, suggesting that DDX1 does not play a role in the repair of DSBs at this early stage (Fig. 1), and (ii) γ -H2AX foci returned to baseline levels after 6 hours post-irradiation in 2-cell embryos (Fig. 2). The latter is in contrast to 1-cell and blastocyst stage embryos which had not returned to baseline levels 12 hours post-irradiation. We are currently in the process of examining recruitment of other DNA repair proteins to DSBs, including ATM which has previously been shown to interact with DDX1 at DSBs. Our work indicates that phosphorylated ATM (pATM), normally involved in the repair of DNA DSBs by homologous recombination, is not recruited to DSBs in 2-cell stage embryos. We will focus on homologous recombination and non-homologous end joining proteins to further investigate the repair of DSBs in developing embryos.

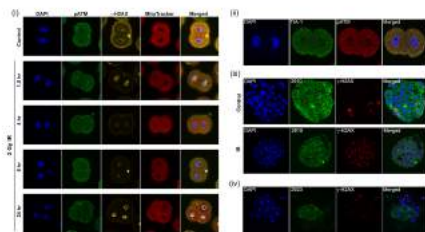


Figure 1. Ionizing radiation (IR)-induced double-strand breaks (DSBs) in 2-cell embryos. (i) Gamma-H2AX is recruited to DSBs in 2-cell embryos 1.5 hr post-IR. pATM is found in both the cytoplasm and nucleus of irradiated embryos. (ii) 116-1 co-localizes with pATM foci, suggesting co-localization with DDX1. (iii) Gamma-H2AX is recruited to DSBs in nucleus embryos 1.5 hr post-IR. (iv) DDX1 is not observed at DSBs in trophoblasts.

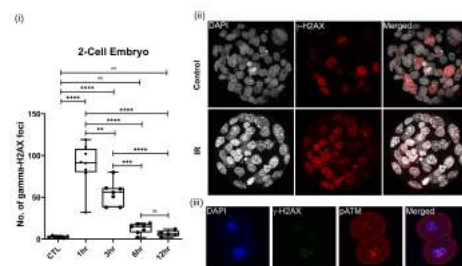


Figure 2. Quantification and localization of gamma-H2AX and pATM in irradiated embryos. (i) Significantly higher numbers of gamma-H2AX foci were observed at 1hr compared to later time points in 2-cell embryos. (ii) 2-cell stage embryos were treated with 2 Gy IR and cultured until late blastocyst stage. Gamma-H2AX foci were still observed in the late blastocyst stage of surviving embryos. (iii) Distinct cytoplasmic and nuclear distribution of pATM in 2-cell embryos treated with 2 Gy IR.

Lubna fig-1 final.jpg

Lubna fig. 2 final.jpg

Directed *E. coli* DnaB exterior surface mutations effect helicase conformation and regulate behavior to preserve genome stability in vivo

Thursday, 8th July - 16:00: Poster Session 3-A - Poster - Abstract ID: 115

***Ms. Megan Behrmann*¹, *Prof. Michael Trakselis*¹**

1. Baylor University

The bacterial replicative helicase, DnaB, is known to switch between two distinct unwinding modes during replication. The function and mechanism of this switch is not yet fully understood, but two primary methods of regulation have been identified: steric exclusion and wrapping (SEW) of the excluded strand, and a shift between dilated and constricted central channel conformational states. To investigate the cellular impact of helicase dysregulation in *E. coli*, we studied four previously identified SEW-deficient mutants through a combination of *in vitro* and *in vivo* techniques. Notably, we determined that these SEW mutants also adopt constricted conformations, suggesting a dynamic model for helicase regulation where both SEW and helicase conformation contribute to the mechanism. Two of the mutants in particular stabilized a fully constricted state, but had distinct effects on genomic stability, highlighting the complex relationship between helicase regulation mechanisms and faithful, efficient DNA replication. Using CRISPR-Cas genomic editing, we determined that these *in vivo dnaB* mutations result in increased DNA damage and chromosome complexity, less stable genomes, and ultimately less viable and fit strains. This work demonstrates the broad and significant impact helicase regulation has on genomic stability and cell survival, supports a combined dynamic regulatory mechanism involving SEW and conformational changes, and relates current mechanistic understanding to functional helicase behavior.

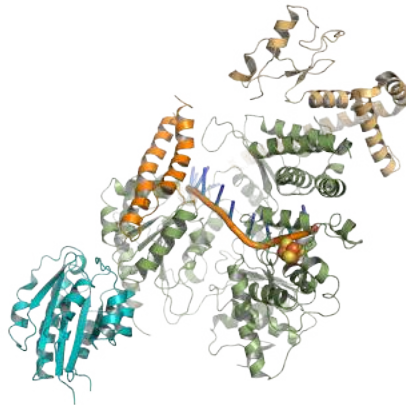
The Arch domain of XPD: A regulatory multitool that is mechanistically essential for transcription and DNA repair

Thursday, 8th July - 16:00: Poster Session 3-A - Poster - Abstract ID: 122

***Dr. Jochen Kuper*¹, *Mr. Stefan Peissert*¹, *Dr. Florian Sauer*¹, *Dr. Arnaud Poterszman*², *Prof. Jean-Marc Egly*², *Prof. Caroline Kisker*¹**

1. Rudolf Virchow Center for Integrative and Translational Bioimaging, 2. IGBMC

The XPD helicase is a central component of the general transcription factor TFIIH which plays major roles in transcription and nucleotide excision repair (NER). During these processes XPD is tightly regulated by different interaction partners. Whereas p44 and p44/p62 activate XPD this stimulation is superseded by the presence of MAT1 belonging to the cyclin activating kinase (CAK) complex. We examined the main interface of the XPD MAT1 interaction constituted by the Arch domain of XPD and the archway domain of MAT1. The analysis of the interface led to the identification of amino acid residues that are crucial for the MAT1-XPD interaction. More importantly, however, functional mutagenesis of the Arch domain revealed that it is not only an interaction hub for other NER factors but also bears functionally essential regions that mediate and control XPD activity towards different DNA substrates. Our results show how MAT1 utilizes these functionally important regions to inhibit XPD helicase function, thus defining the Arch domain as a major mechanistic player within the XPD scaffold.



Xpd.png

Uncovering an allosteric mode of action for a selective inhibitor of human Bloom syndrome protein

Thursday, 8th July - 16:00: Poster Session 3-A - Poster - Abstract ID: 134

*Dr. Xiangrong(Tina) Chen*¹

1. University of Sussex

BLM (Bloom syndrome protein) is a RECQ-family helicase involved in the dissolution of complex DNA structures and repair intermediates. Synthetic lethality analysis implicates BLM as a promising target in a range of cancers with defects in the DNA damage response; however, selective small molecule inhibitors of defined mechanism are currently lacking.

The first part of this project was to obtain sufficient recombinant protein for assay development and for crystallisation studies; resulting in two helicase domain constructs that could be readily expressed and purified. Ten separate assays were then developed to identify small molecular inhibitors of BLM and to determine mode of action. Analysis of 10 series of compounds identified by an NIH high-throughput screen led to two series of compounds being explored further: the first based on ML216, a previously reported inhibitor of BLM; and the second on a separate unrelated series (Series C).

Our data suggest that ML216 is an indirect inhibitor of BLM, inhibiting activity by binding to the DNA rather than protein. In contrast, biophysical data demonstrate that Series C compounds are direct allosteric inhibitors of BLM, binding to the protein only in the presence of a DNA substrate; supported by a series of X-ray crystal structure.

In summary, we identify and characterise Series C inhibitors of BLM's ATPase-coupled DNA helicase activity, by allosteric trapping of a DNA-bound translocation intermediate. Crystallographic structures of BLM-DNA-ADP-inhibitor complexes identify a hitherto unknown interdomain interface, whose opening and closing are integral to translocation of ssDNA, and which provides a highly selective pocket for drug discovery. Comparison with structures of other RECQ helicases provides a model for branch migration of Holliday junctions by BLM.

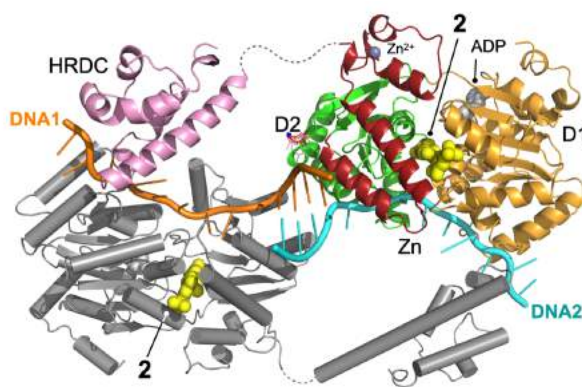


Image1.png

The roles of Hrq1 in ICL repair

Thursday, 8th July - 16:00: Poster Session 3-A - Poster - Abstract ID: 138

***Mr. Robert Simmons*¹, *Ms. Alexandra Hurlock*¹, *Dr. Matthew Bochman*¹**

1. Indiana University - Bloomington

DNA inter-strand crosslinks (**ICLs**) are highly toxic DNA lesions that prevent the opening of double-stranded DNA. These lesions can result in genomic instability or cell death when the DNA is not faithfully repaired. The primarily researched ICL repair pathway in humans is the replication-coupled Fanconi Anemia (**FA**) pathway. However, there are many alternative but poorly understood ICL repair pathways, including one utilizing a nonFA helicase (RECQL4) and nuclease (SNM1A). RECQL4 mutations cause three diseases of genomic instability: Baller-Gerold, Rothmund-Thomson and RAPADILINO syndromes, perhaps due to defects in ICL repair. Unfortunately, RECQL4 is difficult to study *in vivo* and *in vitro* for a variety of reasons, but there is a RECQL4 homologue found in *Saccharomyces cerevisiae* called Hrq1 that can be used as a simple model. Hrq1 functions in ICL repair by synergizing with the Pso2 nuclease (a SNM1A homologue) to digest through ICLs. Hrq1 and Pso2 are currently the only identified participants in this ICL repair pathway, though they are insufficient to complete this entire process on their own. Thus, there are many questions still left unknown: what recruits Hrq1/Pso2 to ICLs, how are these enzymes regulated, and what is the molecular mechanism of repair? We are answering these questions using synthetic genetic array analyses, RNA-seq, and the screening for suppressors of ICL damage sensitivity in *S. cerevisiae*. Currently, this multi-omics approach has revealed the physical and genetic interactomes of Hrq1, suggesting additional roles for the helicase *in vivo*. Further, our genetic approach has surprisingly revealed regions of the Hrq1 protein that are important for substrate recognition and binding, as well as explained why the catalytically inactive *hrq1-K318A* allele is a dominant negative. Decoding and exploring these data sets is a challenging ongoing process but our current results are beginning to fill in our gaps of knowledge of this DNA repair mechanism.

Structural and biochemical characterizations of DHX36 Helicase

Thursday, 8th July - 16:00: Poster Session 3-B - Poster - Abstract ID: 87

Prof. Xuguang Xi¹

1. Laboratoire de Biologie et de Pharmacologie Appliquée (LBPA), UMR 8113 CNRS, Institut D'Alembert, École Normale Supérieure Paris-Saclay, Université Paris-Saclay, 4, Avenue des Sciences, 91190 Gif sur Yvette, France

Four-stranded nucleic acid structures called G-quadruplexes have been associated with important cellular processes, which should require G-quadruplex-protein interaction. Unravelling the structural and mechanistic bases of helicase-catalyzed G-quadruplexes unfolding is fundamental and medical importance to decipher cellular strategies for maintaining chromosome stability. DHX36 helicase (also known as RHAU or G4R1), originally isolated from HeLa cell lysates as a major source of G4-resolving activity and as part of a protein complex that is associated with the AU-rich element of urokinase plasminogen activator mRNA, belongs to the DExH-box family of RNA helicases. Here we report crystal structures of the bovine DHX36 in complex with G-quadruplexes. By combining structural, polymerase extension assay, stop-flow assay and single-molecule fluorescence studies, we show that

- 1) DHX36 is sensitive to the thermal stability of G-quadruplexes structures and ATP is required for DHX36-mediated G-quadruplexes unfolding.
- 2) Although DHX36 cannot unfold G-quadruplexes with high thermal stability such as G4^{Myc}, the DSM of DHX36 alternate binding to the 3'- and 5'-G-tetrad of G4^{Myc} giving an oscillatory curve in single molecular assay.
- 3) The state of DHX36-G4^{Myc} complex can be modulated by different conditions, for example the molar ratio of DHX36/G4^{Myc}, the length of G4^{Myc} 3'-tails and whether the substrate is prefolded.
- 4) DHX36 forms a homodimer which adopts a head-to-tail antiparallel orientation. The two G4s that comprise the dimer stack in a head-to-head orientation via the guanine tetrads formed by the 5'-nucleotides. To rule out the possibility that the determined dimeric structure is a crystal stacking artifact, an integrated biophysical approaches including size exclusion chromatography (SEC), dynamic light scattering (DLS), and SEC coupled small angle X-ray scattering (SEC-SAXS) has been used to confirm the dimeric nature. In accordance with our crystal structure, the data obtained with the above methods demonstrated that DHX36-G4 exists in solution predominantly as a dimer.

Systematically mapping G-quadruplex regulatory elements on *E. coli* transcripts

Thursday, 8th July - 16:00: Poster Session 3-B - Poster - Abstract ID: 109

Ms. Rachel Cueny¹, Dr. Andrew Voter¹, Prof. James Keck¹

1. University of Wisconsin-Madison

G-quadruplexes (G4s) are highly stable four-stranded nucleic acid structures comprised of multiple π -stacked guanine tetrads in DNA or RNA (Figure 1). G4s can act as barriers to DNA replication, transcription, and translation, making it essential for cells to have mechanisms to process stable G4s. Despite their potential impediment to core activities in cells, many G4 forming sequences are found in organisms ranging from *E. coli* to humans, indicating that G4s may have important regulatory roles. *In vivo* studies of G4s have primarily focused on eukaryotic model systems, while G4 formation and regulation in prokaryotes has been less well characterized. Our lab recently carried out a transposon-sequencing screen in *E. coli* to identify genes that are involved in G4 processing. An *E. coli* library of ~500,000 transposon insertion mutants was grown in the presence or absence of the G4 stabilizing compound N-methyl mesoporphyrin IX (NMM) and insertion sites that were depleted or enriched in the presence of NMM were mapped by sequencing. We found that insertions in *tufA* and *tufB*, both of which encode for elongation factor Tu (EF-Tu), were beneficial for growth in the presence of NMM (Figure 2). EF-Tu brings charged tRNAs to the ribosome to facilitate translation elongation. We confirmed that deletion of *tufA* or *tufB* allows *E. coli* to overcome the G4 stabilizing effects of NMM and Braco-19, a structurally distinct G4 stabilizing compound (Figure 3). This, along with other translation hits identified by our screen, lead to a model in which stabilized mRNA G4s could cause ribosome stalling, with *tufA* or *tufB* deletions allowing cells to overcome the toxic effects of stabilized RNA G4s. To test this model, we plan to carry out ribosome profiling in the presence and absence of NMM in both normal and *tufA::kan* cells, which will allow us to determine whether and where ribosomes are being stalled as predicted, to identify potential G4s structures that are forming in mRNA, and to determine if disrupting *tufA* alleviates ribosome stalling at folded mRNA G4s.

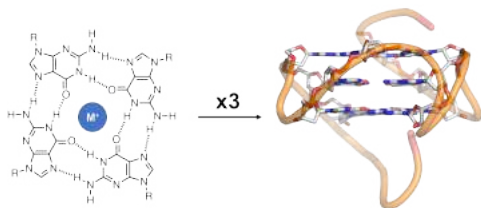


Figure 1 g4 structure.png

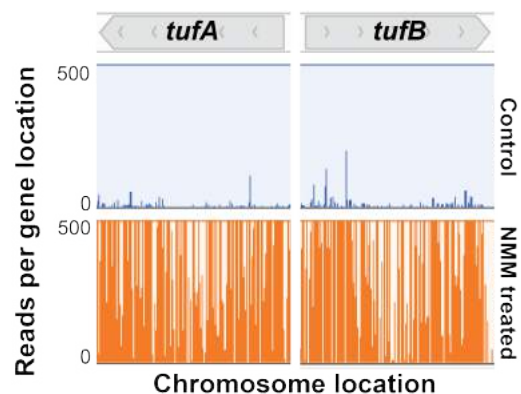


Figure 2 tufa tufb insertions.png

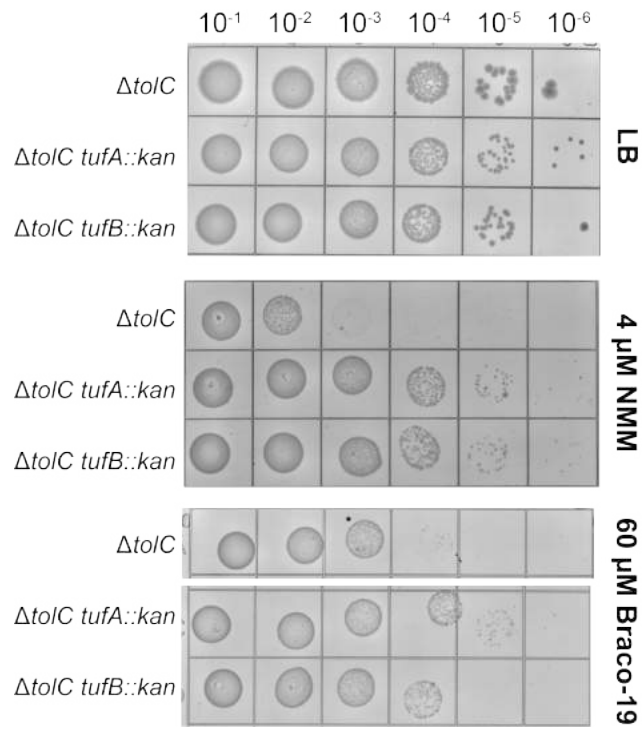


Figure 3 tufa tufb spot plates.png

G-quadruplex processing in *Bacillus subtilis*

Thursday, 8th July - 16:00: Poster Session 3-B - Poster - Abstract ID: 144

***Ms. Sarah McMillan*¹, *Prof. James Keck*¹, *Ms. Rachel Cueny*²**

1. University of Wisconsin-Madison, 2. University of Wisconsin

G-quadruplexes (G4s) are noncanonical DNA or RNA secondary structures that have the potential to act as blockages to essential cellular processes and that have been implicated in regulating processes such as transcription and translation in prokaryotic organisms. Recent work from our lab has provided evidence that G4s regulate translation in *E. coli*. Several genetic screens determined that translation factors are important for *E. coli* to grow in the presence of the G4-stabilizing compound N-methyl Mesoporphyrin (NMM). To expand our understanding of G4-mediated regulation in prokaryotic organisms, I am determining what processes are regulated by G4s and how G4s are processed in the gram-positive bacteria *Bacillus subtilis*. Preliminary evidence suggests that the translation-related hits from our *E. coli* genetic screens are not important for growth in NMM in *B. subtilis*. This suggests that translation may not be regulated by G4s in *B. subtilis* in the same ways that it is in *E. coli* and that G4s are used to regulate distinct processes in these bacteria. To further explore this possibility, a CRISPR interference screen has been used to knockdown essential *B. subtilis* genes and determine whether the knockdowns are highly sensitive to G4-stabilizing compounds. Additionally, a transposon sequencing screen is being conducted to determine what genes are conditionally essential in the presence of NMM and another G4-stabilizer, Braco-19, in *B. subtilis*.

The structure of self-loading MCM-like helicases encoded by staphylococcal virus satellites reveals unique and conserved motions

Thursday, 8th July - 16:00: Poster Session 3-B - Poster - Abstract ID: 20

***Dr. Cuncun Qiaou*¹, *Dr. Ignacio Mir Sanchis*¹**

1. Umeå University and Wallenberg Centre for Molecular Medicine

A group of self-loading helicases encoded by staphylococcal mobile elements were identified recently, but the mechanism through which they recognize their cognate origin of replication remains elusive. Here we studied all three unexplored self-loading helicases called Rep, that are found in SaPIs, a family of pathogenicity islands present in *Staphylococcus aureus*. These genomic islands encode the Toxic Shock Syndrome Toxin and other virulent factors, making this work relevant from a biomedical perspective. We demonstrate that all three Reps are functional homologs of MCM replicative helicases in terms of polarity. Our cryoEM structures of the Rep from SaPI5 at 3.3 Å and the Rep from SaPI1 at 4Å resolution show that in both cases the DNA binding domain moves with respect the ATPase domain through rotation and tilting, which exposes the DNA recognition motif that otherwise is occluded by the adjacent subunit. Such movements are ATP independent, which explains why Reps do not need ATP for origin recognition and duplex melting. Additionally, our biochemical characterization demonstrates different evolutionary strategies of these helicases in terms of nucleotide usage.

A Mechanical Mechanism for Translocation of Hexameric and Nonstructured Helicases

Thursday, 8th July - 16:00: Poster Session 3-B - Poster - Abstract ID: 38

Prof. Ya-chang Chou¹

1. National Tsing-Hua University

Introduction: A mechanical mechanism for translocation of ring-shaped helicases and nonstructured helicases on DNA was proposed recently. The asymmetry in the helicase structures and the random thermal motions of the helicases and the DNA molecule were considered as the bases for the generation of the force required for translocation of the helicases on DNA. The ring-shaped helicase comprises a channel at its center with two unequal ends, through which strands of DNA can pass. The random collisions between the portion of the DNA strand in the central channel and the wall of the channel generate an impulsive force on DNA toward the small end of the channel regardless the small end is the C- or N- terminal domain. Same occurs for the DNA molecule weakly attached to the asymmetric cleft between the two subdomains of the nonstructured helicases. When the helicase arrives at the junction of ssDNA and dsDNA (a fork), the collision between the helicase and the closest base pair may produce sufficient impulsive force to break the weak hydrogen bond of the base pair. Thus, the helicase may advance and repeat the process of unwinding the dsDNA strand.

Method: This mechanism was tested in a macroscopic simulation system where the helicase was simulated using a truncated-cone structure and DNA was simulated with bead chains.

Results: Many features of translocation and unwinding such as translocation on ssDNA and dsDNA, unwinding of dsDNA, rewinding, strand switching, and Holliday junction resolution were reproduced. Two recent observations showed that (a) the translocation speed (v_t) helicases decreased in the small region of the applied tension, and (b) the v_t of the NS helicase translocating on RNA was higher than that on DNA. The dependence of v_t on the physical parameters are consistent the mechanical mechanism.

Discussion: The fact, that the small ends of the central channels of the actual ring-shaped helicases lead the translocation of the helicases on DNA (and the same are true for the small ends of the cleft of the nonstructured helicases), is a support for the mechanical mechanism.

	Helicase	Domain ahead	Small end ahead?
Eukaryotic	E1	NTD	Yes
	CMG	NTD	Yes
Bacterial	DnaB	CTD	Yes
	T7	CTD	Yes
	Rho	CTD	Yes

Table.png

The *E. coli* RecBCD nuclease domain regulates DNA binding and helicase activity, but not ssDNA translocation

Thursday, 8th July - 16:00: Poster Session 3-B - Poster - Abstract ID: 51

***Ms. Nicole Fazio*¹, *Dr. Linxuan Hao*¹, *Dr. Rui Zhang*¹, *Dr. Timothy Lohman*¹**

1. Department of Biochemistry and Molecular Biophysics, Washington University School of Medicine, 660 S. Euclid Ave., St. Louis, MO 63110

While helicases have been studied for decades, much is still unknown about the mechanism of helicase-catalyzed double stranded (ds)DNA unwinding. Previous hypotheses, based on structural models, have described DNA unwinding as a simple mechanical consequence of pulling the DNA duplex across a wedge domain in the protein by the single stranded (ss)DNA translocase activity. However, many ssDNA translocases cannot unwind dsDNA without some form of activation, such as oligomerization, binding to an accessory protein, deletion of an auto-inhibitory domain, or the application of assisting force. Here, we present evidence that dsDNA unwinding by *E. coli* RecBCD helicase occurs by a fundamentally different mechanism than ssDNA translocation. Using stopped-flow fluorescence, we compared the kinetics of ssDNA translocation and dsDNA unwinding of RecBCD and a nuclease domain deletion variant (RecB^{Δnuc}CD). Our results show that deletion of the nuclease domain has no effect on ssDNA translocation rates, whereas the DNA unwinding rate of RecB^{Δnuc}CD is significantly slower compared to RecBCD. In addition, direct DNA binding studies indicate that RecB^{Δnuc}CD binds with significantly higher affinity to DNA ends compared to RecBCD. These results are surprising as currently available RecBCD structures show the nuclease domain positioned away from the duplex DNA interaction site. To gain further insight into the role of the nuclease domain, we solved cryo-EM structures of RecBCD and RecB^{Δnuc}CD both alone and bound to blunt-ended DNA. In both RecBCD alone and RecBCD bound to DNA, we found multiple structural classes that differ in the positioning of the RecB nuclease domain as well as in the flexibility of the RecD motor subunit, indicating conformational heterogeneity. Combined, our results indicate that the nuclease domain is dynamic and has a role in regulating dsDNA unwinding, but not ssDNA translocation, emphasizing that DNA unwinding is not a simple consequence of ssDNA translocation. (Supported by NIH R35 GM136632 to TML).

DHX36 function at G-quadruplexes and its connection to stress response

Thursday, 8th July - 16:30: Keynote 8 - Oral - Abstract ID: 86

Mr. Daniel Hilbig¹, Dr. Stefan Juranek¹, Prof. Katrin Paeschke¹

1. University Hospital Bonn

DHX36 is a highly conserved DEAH-box helicase. It is a multifunctional RNA helicase that has been described to support telomere maintenance, translation and mRNA stability by unwinding G-quadruplex (G4) structures. Previously we globally mapped DHX36 occupancy in human cell lines where we could correlate its binding to regions that can fold G4 structures. In detailed system wide analysis, we demonstrated that DHX36 decreased target mRNA stability which led to an increase in target mRNA abundance in the cell. This accumulation of mRNA stimulated the formation of stress granules and a robust stress response (PKR/EIF2AK2 phosphorylation). Indicating that DHX36 function is tightly connected to stress response. In current analysis we further characterized DHX36 function and relevance during viral stress response.

Revealing the dynamics of Pif1 helicase when it collides with the G4 quadruplex using single-molecule assays

Thursday, 8th July - 17:00: Oral Session - Oral - Abstract ID: 97

***Dr. Jessica Valle Orero*¹, *Dr. Martin Rieu*¹, *Prof. Vincent Croquette*¹, *Prof. Jean-Baptiste Boule*², *Dr. Phong-Lan-Thao TRAN*²**

1. ECOLE NORMALE SUPERIEURE, 2. national museum of natural history

G-quadruplexes (G4) are secondary structures formed by guanine-rich DNA/RNA sequences. G4 motifs are found in different regions of the genome, such as at telomeres, promoters, or replication origins. These structures can be very stable and may act as a roadblock for replication fork or for transcription bubble. Cell has developed specialized proteins that can either stabilize or remove these structures, among those the helicase Pif1 (*S. cerevisiae*) is involved in inducing G4-linked genomic instabilities, and capable of removing these G4 structures. To date, our knowledge of the G4 biology is largely inferred from *in vitro* biophysical studies of G4s in single-stranded DNA context. The interaction between Pif1 and G4 structures have already been studied using a single-molecule approach, however they fail to capture the helicase dynamics during translocation and interaction with the G4 in a double stranded context. We have developed dsDNA assays where we induced very stable G4 structures (c-Myc G4, lifetime > 1hour), and observe in real time Pif1 opening the duplex and resolving the G4. Our results show that the helicase can reduce the lifetime of G4 from hours to seconds, but moreover once G4 is resolved it can resume translocation without changing state from a monomer to dimer, as previously reported. We have observed that the presence of other roadblocks, besides the G4, within our dsDNA assays, induces strand switching. Our quantitative analysis allows us to build a model that characterizes the helicase pif1 dynamics under a dsDNA-G4 context. Our model will be particularly pertinent to study the role of protein motors to remove stable structures during replication.

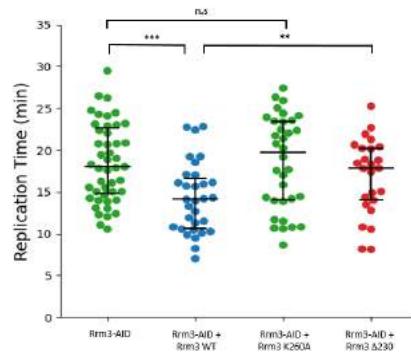


Figure 3. Rrm3 catalytic activity is essential for replisome progression through leading strand G4s. Replication rate of strains lacking Rrm3-ΔID (after induced degradation with Auxin) with G4s in the leading strand template, with WT Rrm3, the catalytically dead K260A mutant Rrm3, and Rrm3 with N-terminal deletion, complemented in the URA3 locus. Cells with catalytically dead Rrm3 show similar rates to cells lacking Rrm3. Replication time was measured in strains where the mid-array distance was approximately 30.6kb. ***p<0.001, **p<0.05 ns = not significant

Figure 3. rrm3 catalytic activity is essential for replisome progression through leading strand g4s.png

Anyone for a PiNT? The function of the Pif1 N-Terminus

Thursday, 8th July - 17:30: Oral Session - Oral - Abstract ID: 147

***Dr. Matthew Bochman*¹, *Dr. David Nickens*¹, *Dr. Lata Balakrishnan*²**

1. Indiana University - Bloomington, 2. IUPUI

PIF1 family helicases are evolutionarily conserved and play multiple roles in cells that underpin genome integrity. Among eukaryotes, PIF1 helicases share a conserved core helicase domain that is defined by a PIF1 family signature sequence, but most also contain N- and C-terminal domains that vary in size and are not conserved at the primary sequence level. What does appear to be conserved, though, is that these domains are predicted to be natively disordered, and experiments with bacterial and yeast PIF1 helicases demonstrate that they are important domains for function. We have been investigating the roles of the *Saccharomyces cerevisiae* Pif1 N-terminus (PiNT) in an effort to determine how such disordered domains impact PIF1 activity. Using a PiNT truncation mutant (Pif1 Δ N), we found that the PiNT regulates the biochemistry of Pif1 *in vivo* and *in vitro*, relieving the toxicity of Pif1 over-expression, affecting the regulation of telomerase, and impacting DNA binding and unwinding. Further, the PiNT contains two lysine residues that are acetylated *in vivo*. Using recombinant proteins and limited proteolysis, we found that the acetylation appears to induce a conformational change in Pif1 but not Pif1 Δ N. Finally, our most recent work indicates that the PiNT is necessary for Pif1 to undergo liquid-liquid phase separation (which can be relieved by incubation with DNA), as well as to drive the phase separation of other proteins onto which the PiNT is fused. Our ongoing work with the disease-linked human PIF1 (hPIF1) suggests that its N-terminal domain behaves similarly to that of the *S. cerevisiae* PiNT, and we speculate that misregulation of hPIF1 activity via aberrant post-translational modifications and/or phase separation are associated with cancer.

Modulation of DnaB helicase conformation and contacts interrupts replisome coupling, creating genome instability

Thursday, 8th July - 19:00: Oral Session - Oral - Abstract ID: 10

***Prof. Michael Trakselis*¹, *Ms. Megan Behrmann*¹, *Ms. Himasha Perera*¹, *Ms. Malisha Welikala*¹**

1. Baylor University

Helicase regulation is vital for replisome progression, where the hexameric helicase unwinds duplex DNA and coordinates replication fork activities to ensure the immediate synthesis of daughter strands. Mechanisms for helicase regulation involve interactions with both DNA strands and global hexameric conformational shifts between dilated and constricted states. We have created several mutations in the *Escherichia coli dnaB* gene that shift the equilibrium towards a constricted state and disrupt interactions with the excluded strand, allowing for faster unwinding. These *dnaB:mut* strains present with increased DNA damage and chromosome complexity, less stable genomes, and ultimately less viable and fit strains. Interestingly, individual *dnaB* strains have distinct effects on genomic stability, suggesting a complex relationship between helicase regulation mechanisms and faithful, efficient DNA replication. This work explores the genomic impacts of helicase dysregulation *in vivo*, supporting a combined dynamic regulatory mechanism involving DNA contacts and protein conformational changes and relates current mechanistic understanding to functional helicase behaviors.

Nanopore Tweezers reveal detailed dynamics of SF1 and SF2 helicases

Thursday, 8th July - 19:15: Oral Session - Oral - Abstract ID: 32

Dr. Jon Craig¹, **Dr. Andrew Laszlo**¹, **Prof. Maria Mills**², **Dr. Momcilo Gavrilov**³, **Mr. Dmitriy Bobrovnikov**³, **Prof. Taekjip Ha**³, **Dr. Keir Neuman**⁴, **Prof. Jens Gundlach**¹

1. University of Washington, 2. University of Missouri, 3. Johns Hopkins University, 4. NIH National heart lung and blood institute

We developed single-molecule picometer resolution nanopore tweezers (SPRNT), a nanopore-based single-molecule technique for studying enzymes that move on nucleic acids. SPRNT measures enzyme position on a NA template with sub-Ångstrom spatial resolution on millisecond timescales, while simultaneously providing the DNA sequence passing through the enzyme. With helicases, this resolution reveals the individual steps, and in some cases sub-steps, of the ATP hydrolysis cycle at physiological conditions providing a wealth of information on the mechanochemistry of helicase motion. We have used these features of SPRNT to characterize several helicases including SF1 helicase PcrA and SF2 helicase Hel308. I will show how SPRNT can be used to probe the energy landscape of translocation and unwinding revealing never-before-seen detail about the inchworm mechanism. SPRNT's ability to determine an enzyme's sequence-specific location reveals new ways in which the underlying DNA sequence affects helicase motion. We find that the single-stranded DNA sequence on which the helicase walks strongly affects both translocation and surprisingly has a strong influence on unwinding. Rather than being a specific feature of any individual helicase, the presence of ssDNA sequence-dependence appears to be universal and has been observed with 8 different SF1 and SF2 helicases, including SARS-Cov2-nsp13. This is a strong effect and has important implications for how helicases act *in vivo* and for interpretation of single-molecule data in which the individual steps cannot be resolved. SPRNT is an ideal tool for detecting sequence-dependent behavior and determining the structural basis for how it arises.

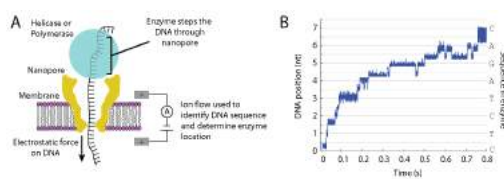


Figure1-06.png

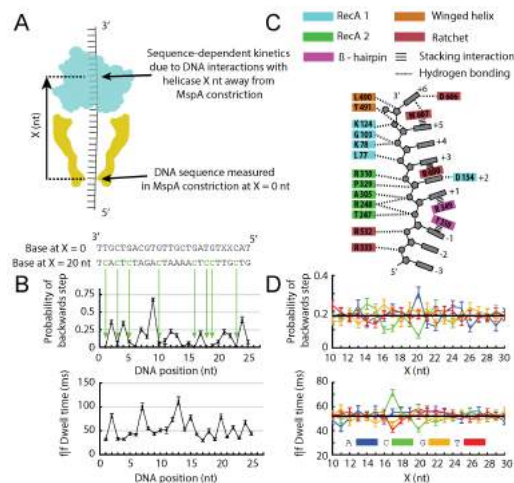


Figure6.png

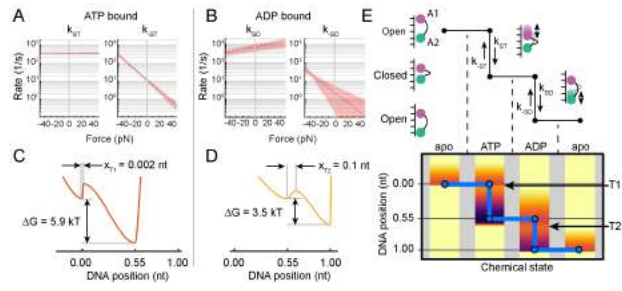


Figure4-06.png

The dynamic human Origin Recognition Complex

Thursday, 8th July - 19:30: Oral Session - Oral - Abstract ID: 105

Dr. Matt Jaremko*¹, *Dr. Ken On*¹, *Dr. Dennis Thomas*¹, *Prof. Bruce Stillman*¹, *Prof. Leemor Joshua-Tor

¹

1. Cold Spring Harbor Laboratory

Genome replication is essential in all forms of life for transmitting genetic materials from one generation to the next. In eukaryotic cells, this genetic material is densely packed into chromatin within the nucleus. Essential factors are required to reorganize the chromatin and provide access to DNA for the replication machinery. One such essential factor is the origin recognition complex (ORC), a six-subunit AAA+ ATPase that binds to specific replication initiation sites called origins of replication across the genome. Once bound to DNA, ORC recruits CDC6 and the replicative helicase MCM complex to origins and assemble the MCM complexes into a double-hexameric, inactive confirmation on the DNA. The MCM complexes are activated upon S-phase entry and begin to unwind the DNA duplex, allowing the replication machinery to access and replicate the DNA. To date, much of our knowledge on how ORC contributes to MCM helicase recruitment has been illustrated in budding yeast. However, little is known about how the very first step of replication initiation: DNA-binding of ORC, is achieved. Here, we used a structural approach to investigate human ORC and its role in DNA replication initiation. We uncovered dynamic regions in the complex that are regulated by the different nucleotide states of ORC. Our results provide important insights into ORC-dependent recruitment of key factors in DNA replication initiation.

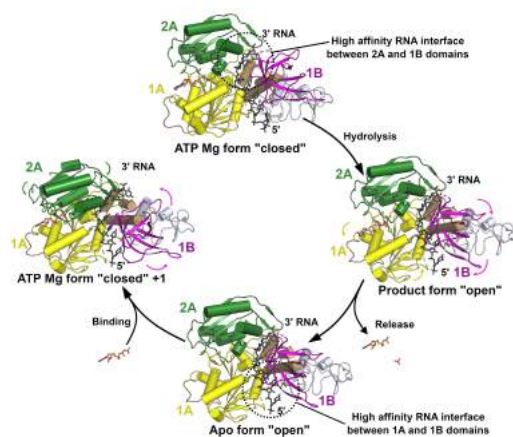
Structure, Mechanism and Crystallographic fragment screening of the SARS-CoV-2 NSP13 helicase

Friday, 9th July - 14:30: Oral Session - Oral - Abstract ID: 1

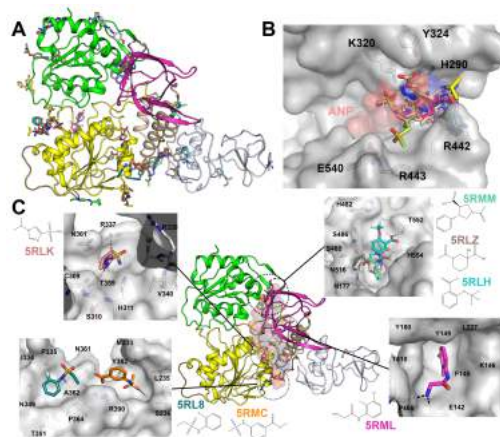
*Dr. Joseph Newman*¹

1. University of Oxford

The global COVID-19 pandemic is caused by the SARS-CoV-2 virus and has infected over 100 million and caused over 2 million fatalities worldwide at the point of writing. There is currently a lack of effective drugs to treat people infected with SARS-CoV-2. The SARS-CoV-2 Non-structural protein 13 (NSP13) is a superfamily1B helicase that has been identified as a possible target for anti-viral drugs due to its high sequence conservation and essential role in viral replication. We present high resolution crystal structures of SARS-CoV-2 NSP13 solved in the APO form and in the presence of both phosphate and the non-hydrolysable ATP analogue (AMP-PNP). Comparisons of these structures reveal details of global and local conformational changes that are induced by nucleotide binding and hydrolysis and provide insights into the helicase mechanism and possible modes of inhibition. Structural analysis reveals two pockets on NSP13 that are classified as “druggable” and include one of the most conserved sites in the entire SARS-CoV-2 proteome. To identify possible starting points for anti-viral drug development we have performed a crystallographic fragment screen against SARS-CoV-2 NSP13 helicase. The fragment screen reveals 65 fragment hits across 52 datasets, with hot spots in pockets predicted to be of functional importance, including the druggable nucleotide and nucleic acid binding sites, opening the way to structure guided development of novel antiviral agents.



Nsp13-mechanism.jpg



Nsp13-fragments.jpg

RIG-I's helicase domain is regulated by the intrinsically disordered CARD2-helicase linker

Friday, 9th July - 14:45: Oral Session - Oral - Abstract ID: 142

***Mr. Brandon Schweibenz*¹, *Dr. Swapnil Devarkar*¹, *Dr. Jie Zheng*², *Dr. Bruce Pascal*², *Dr. Patrick Griffin*², *Dr. Smita Patel*¹**

1. Rutgers University, 2. Department of Integrative Structural and Computational Biology, The Scripps Research Institute, Jupiter, Florida 33458

The helicase RIG-I (Retinoic Acid Inducible Gene-I) is a cytosolic sensor that recognizes pathogenic RNA, and acts as the first line of defense against viral infection. RIG-I's C-terminal domain (CTD) is the domain that initially binds and discriminates between self- and nonself-RNAs through recognizing 5' end identity. For signaling to occur, however, the helicase domain needs to bind to this RNA, which releases the signaling tandem caspase associated recruitment domains (CARD1 and CARD2) from their autoinhibitory interface with RIG-I's helicase insertion subdomain (Hel2i). The helicase domain itself binds RNAs nonspecifically. Our study reveals a previously unknown role of the CARD2-helicase linker (CHL) in regulating helicase-RNA binding activity. Using *in vitro* cell signaling assays in conjunction with hydrogen-deuterium exchange mass-spectroscopy and RNA binding assays in both pre-steady state and steady state conditions, we demonstrate here that the previously poorly characterized CHL has two important regulatory functions. Firstly, it maintains the autoinhibitory CARD2:Hel2i interface. Secondly, the CHL dynamically gates the helicase domain from nonspecific RNA-binding events. Nonself-RNAs that make long-lived interactions with CTD remain in proximity to the helicase domain and can eventually bind, while RNAs attempting to bind the helicase domain from solution, independently of the CTD, are blocked. These functions are dependent on the CHL's exceptional electronegativity. As a newly discovered regulatory region, CHL represents a novel target for RIG-I-based therapeutics.

Successfully completing the final stretch – helicases involved in termination of DNA replication

Friday, 9th July - 15:00: Oral Session - Oral - Abstract ID: 128

**Dr. Sarah Midgley-Smith¹, Dr. Juachi Dimude¹, Dr. Katie Jameson², Dr. Michelle Hawkins²,
Dr. Christian Rudolph¹**

1. Division of Biosciences, Brunel University London, UK, 2. Department of Biology, University of York, UK

Replication termination, the final stage of genome duplication, is a highly complex process, and failures in bringing DNA synthesis to an accurate conclusion can have catastrophic consequences for cell viability and genome stability. While initiation and elongation of DNA replication are well understood, termination has received little attention. It was simply assumed that two converging replication fork complexes would fuse, followed by the disassembly of the replisomes and ligation of the nascent strands. But recent data have revealed that fork fusions have to be extensively choreographed, both in prokaryotic and eukaryotic cells.

Our research in *Escherichia coli* has shown that a variety of proteins are involved in the processing of fork fusion intermediates, such as RecG helicase. In cells lacking RecG, over-replication occurs in the chromosomal termination area, but can also be observed in other chromosomal areas if forks are forced to fuse in ectopic locations. Thus, termination has the potential to trigger chromosomal over-replication and recombination, and our data suggest that more than 50% of fusions can generate such problematic intermediates that will interfere with the final stages of the replication process.

In *E. coli*, forks normally fuse in a specialised termination area opposite the origin, which forms a ‘replication fork trap’ via the binding of Tus protein to genomic terminator sites. And while this fork trap can efficiently contain fork fusion intermediates, which allows their rapid processing, it also can be problematic: our *in vitro* reconstitution experiments of a fork fusion event that takes place directly at a *ter*-Tus complex showed that a stretch of the chromosome remains under-replicated, which will require additional helicases for completion. Thus, our data highlight that the final stage of DNA replication is highly complex and requires a variety of helicases and other proteins for successful completion. Indeed, in eukaryotic cells replication is initiated at hundreds if not thousands of replication origins, resulting in thousands of termination events, and recent work has shown that, as in *E. coli*, a number of proteins, including the helicases Rrm3 and Pif1, are important for the successful completion of DNA synthesis.

Engineering photo-controlled Rep helicase

Friday, 9th July - 16:00: Poster Session 4-A - Poster - Abstract ID: 24

Dr. Sonisilpa Mohapatra¹, Dr. Tunc Kayikcioglu¹, Dr. Chang-Ting Lin¹, Prof. Taekjip Ha¹

1. Johns Hopkins University

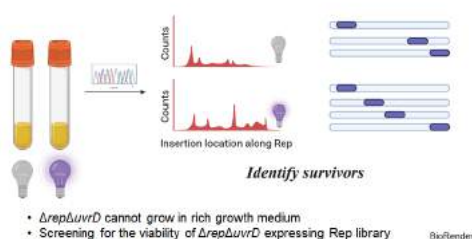
One way to decipher the role of a protein in cellular processes is by controlling its activity on demand. Light can be used to control proteins in a spatiotemporal manner with minimal invasion. We are interested in designing light-controlled helicases to understand the mechanistic details of their functioning as well as to modulate their functionalities.

A photosensitive protein, LOV can be inserted the helicase to allow light controlled structural and functional modulation. As our first prototype helicase, we are working on engineering a photo-controlled Rep, an *E. coli* DNA helicase. We designed three different LOV inserted Rep variants and measured their unwinding rates in presence/absence of light. Our measurements identified a photo-deactivated and a photo-enhanced Rep.

To improve upon the contrast of these photo-controlled Rep, we decided to scan the effects of LOV insertion in different regions of Rep. Using *in silico* DNA library design and a high-throughput assembly approach, we have generated a 700-membered library of LOV inserted Rep (Rep-LOV). The members of the library are Rep with LOV domain inserted at different locations, scanning one amino acid position of Rep at a time. We developed functional assays for high-throughput *in vivo* screening of Rep-LOV in a light dependent manner. The viability of $\Delta rep\Delta uvrD$ cells while exogenously expressing Rep-LOV library is studied with and without light. The variants that complement cell viability in rich medium in light on/off conditions are identified through next generation sequencing. We tested our assay on a small-scale prototype library and successfully identified light sensitive mutants. We will be expanding on this work to isolate photoswitchable Rep from the 700 membered library. The mutants that display stronger contrast in survival efficiency in a light dependent manner will be expressed and purified. The *in vitro* unwinding activity of these light modulated Rep mutants will be characterized and put into use for various biotechnological applications.

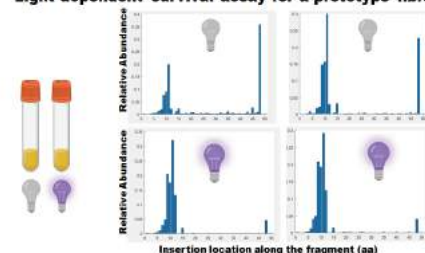
The platform that we have developed for tuning activity of Rep by light can potentially be applied to a diverse range of helicases in humans, many of which have uncharacterized structure and functions, but are frequently dysregulated in cancers.

Light based high-throughput screening assay



Screening assay.png

Light dependent survival assay for a prototype library



Prototype screening.png

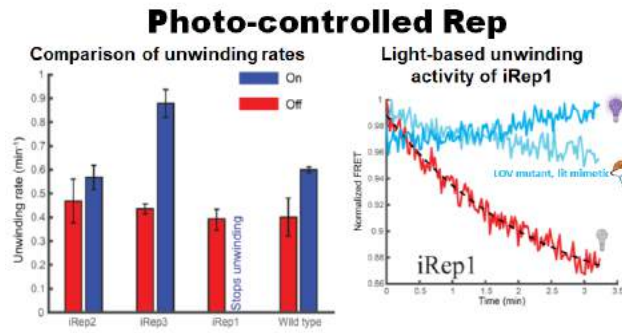


Photo controlled rep.png

DNA replication initiation and restart: single molecule approach for the study of helicase loading.

Friday, 9th July - 16:00: Poster Session 4-A - Poster - Abstract ID: 62

***Dr. Simone Pellicciari*¹, *Ms. Meijing Dong*², *Prof. Feng Gao*², *Prof. Heath Murray*¹**

1. Newcastle university, 2. Tianjin University

Genome replication is a fundamental requirement for the proliferation of all cells. Despite many years of extensive studies of these processes, the mechanism that leads to helicase recruitment on to the single strand DNA (ssDNA) remains unclear. In the model organism *B. subtilis* this event is mediated by several loading protein such as DnaD, DnaB and DnaI, which make contact with the helicase (DnaC) and promote its recruitment. Studying the early stage of this process, we were able to show that DnaA require a conserved set of nucleotide elements called BUS system (Basal Unwinding System) to initiate the helicase loading process, using DNA probe juxtaposing fluorescent dyes and their relative quenchers, and that this elements are functionally conserved throughout the bacterial kingdom(1). To understand the spatio-temporal interactions of the mediator proteins in the helicase loading process, we had to adopt a more sensitive technique such as total internal fluorescent microscopy, which allow us to visualize each component at single molecule level (TIRF-SM). Due to the inability of DnaA to be labelled *in vitro* and complexity of the initiation machinery assembly, which involves the simultaneous loading of two DnaC hexamer, we decided to use the primosomal protein PriA as a tool to reconstitute the helicase recruitment process. PriA coordinates the fork repair pathway, a nucleotide sequence independent mechanism that recruit a single helicase on the lagging strand via the same DnaD-B-I complex involved in the replication initiation. We believe that this approach will allow us to understand the complex relations among the protein involved in the helicase loading process, and that this information can be useful to expand the knowledge on this fundamental process that can be exploited as an unexplored drug target (2,3).

Transcription engine and factor protein stepping along DNA revealed from computational microscope

Friday, 9th July - 16:00: Poster Session 4-A - Poster - Abstract ID: 76

Dr. Liqiang Dai¹, **Dr. Lin-Tai Da**², **Mr. Chao E**³, **Dr. Chunhong Long**⁴, **Dr. Jin Yu**⁵

1. Shenzhen JL Computational Science and Applied Research Institute, 2. Shanghai JiaoTong University, 3. Beijing Computational Science Research Center, 4. Chongqing University of Posts and Telecommunications, 5. University of California, Irvine

Transcription machinery consists of core enzymes and factor proteins, which can translocate and move along DNA at different stages of gene transcription regulation. We have studied mechanochemistry of a transcription engine, a viral RNA polymerase (RNAP) from bacteriophage T7, by simulating its translocation during elongation [1]. More recently, we have demonstrated transcription factor (TF) protein (monomeric WRKY domain protein and heterodimeric Myc-Max protein) stepping along DNA during diffusional search [2,3]. For the RNAP enzyme that makes a transcription bubble along DNA for template-based polymerization, 1-bp stepping or RNAP translocation appears Brownian but rectified by cognate nucleotide incorporation. We examined the RNAP translocation along with nucleotide incorporation and selection using all-atom molecular dynamics (MD) simulation and chemical master equation approaches, showing structural dynamics, energetics, and kinetic mechanisms of the RNAP selective ratcheting. Employing the structure-based simulations, we have also studied 1D diffusion of TFs along DNA. A complete 1-bp stepping cycle during diffusion of a small plant TF, the WRKY domain protein, has been identified from our unbiased atomic equilibrium simulations. The simulations reveal non-synchronized hydrogen bonding breaking and reformation at the protein-DNA interface, along with stochastic behaviors of protein slipping, directional reversal, and strand crossing. Preferential binding onto one strand of DNA becomes prominent when the protein domain binds onto specific DNA. We additionally implemented coarse-grained (CG) simulations to sample processive protein diffusion on the DNA and sequence-dependent step size distributions. For a heterodimeric oncogenic protein Myc-Max, interestingly, we have identified inchworm stepping of the protein (similar to PcrA helicase we studied previously [4]) in the CG simulation as it diffuses along DNA, with two DNA binding basic regions (BR) alternating stepping upon open and close transitions, and with occasional left-right BR swapping. These studies show great potential to computationally examine protein-DNA structural dynamics across scales to reveal physical and functional mechanisms in genetic and epigenetic regulations.

[1] L-T Da, et al, & J Yu. *NAR* 2017, 45:7909-7921

[2] L Dai, et al., & J Yu. *PNAS* 2021, 118:e2102621118

[3] L Dai & J Yu. *BBRC2020*, 533:97-103

[4] J Yu, T Ha, & K Schulten. *Biophys J* 2006, 91:2097-2114

Human DNA Helicase B aids replication of G-quadruplexes

Friday, 9th July - 16:00: Poster Session 4-A - Poster - Abstract ID: 107

Mr. Matthew Thompson¹, **Dr. Maroof Khan Zafar**¹, **Ms. Lindsey Hazeslip**¹, **Dr. Alicia K. Byrd**¹

1. University of Arkansas for Medical Sciences

Introduction:

DNA helicase enzymes have varied roles in maintaining genome stability beyond the unwinding of dsDNA. A variety of helicases are recruited to chromatin during the replication stress response to aid replication progression past DNA secondary structures, but the specific roles of individual helicases in these processes have not been fully delineated. G-quadruplexes (G4 DNA) are an abundantly-occurring DNA secondary structure formed by tandem runs of guanines that interact via Hoogsteen hydrogen bonding, and certain helicases (e.g. PIF1, FANCI, BLM, WRN) are recruited to unwind G-quadruplexes at the replication fork. Human DNA Helicase B (HELB or HDHB) is an SF1B helicase that is a candidate for G-quadruplex unwinding. HELB is recruited to chromatin by RPA-coated ssDNA during the replication stress response, and its helicase activity may be utilized to aid replication progression through G-quadruplexes and other DNA secondary structures.

Methods:

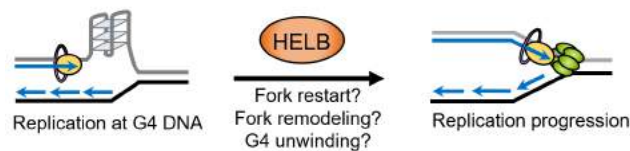
Single molecule DNA fiber spreading assays were used to assess overall replication progression in wild-type and CRISPR-Cas9-generated HELB-knockout U2OS cell lines. Prior to thymidine analogue labeling, cells were treated with or without pyridostatin (PDS) for 24 hours to stabilize genomic G-quadruplexes.

Results:

A significant reduction in replication track length was observed when HELB-knockout cells were treated with PDS compared to untreated HELB-knockout cells. Wild-type cells displayed no reduction in track length upon treatment, and untreated HELB-knockout cells did not display significantly reduced track lengths when compared to untreated wild-type cells.

Discussion:

The reduction in replication track length was only observed when G-quadruplexes were stabilized in HELB-knockout cells, and this suggests that HELB is involved in replication of G-quadruplex-forming DNA. This suggests that HELB may utilize its RPA-binding and helicase activities to aid replication progression via processes such as replication fork remodeling, replication fork restart, or the direct unfolding of G-quadruplexes.



Graphicalabstract.png

Rapid single-molecule characterisation of nucleic-acid enzymes

Friday, 9th July - 16:00: Poster Session 4-A - Poster - Abstract ID: 118

***Mr. Stefan Mueller*¹, *Dr. Lisanne Spenkelink*¹, *Prof. Antoine van Oijen*¹**

1. University of Wollongong

Introduction

Maintenance of DNA, involving replication, repair, and recombination, requires different enzymes with a range of different activities. Development of information-rich biochemical assays that report on these activities is an important step towards our understanding of the molecular mechanisms of disease pathways such as anti-microbial resistance and cancer. Traditionally, the activity of DNA-modifying enzymes is characterised through ensemble-biochemical methods, such as gel electrophoresis and fluorimetry. These methods have the drawback of averaging over large ensembles of molecules and, therefore, provide no access to information on subpopulations, molecular mechanisms and intermediate states. However, knowledge of these properties is often crucial to understanding of the molecular processes underlying DNA metabolism. Here we present a novel single-molecule assay to rapidly characterise proteins involved in DNA metabolism. Our method is simple to implement relative to existing single-molecule experiments. We observe hundreds of individual molecules at a time and implemented a highly automated data analysis pipeline to rapidly analyse large datasets.

As proof of principle we characterised strand-displacement DNA synthesis by the bacteriophage phi29 DNA polymerase using the *S.cerevisiae* single-stranded binding protein RPA as a probe for single-stranded DNA. Demonstrating the richness of information accessible through this assay, we report rate constants for DNA synthesis by the phi29 DNA polymerase and binding by RPA.

Methods

We use wide-field total-internal reflection fluorescence microscopy, coupled with microfluidic flow cells, to observe Phi29 DNA polymerase dependent strand-displacement synthesis on the single-molecule level (Figure 1A). The fluorescence intensities of hundreds of individual DNA molecules are simultaneously detected and synchronised (Figure 1B) to create a post-synchronised average trajectory containing kinetic information (Figure 1C).

Results and Discussion

We obtained kinetic properties of phi29 DNAP strand-displacement synthesis and the binding of RPA to ssDNA. More importantly, we describe a simple assay, which provides quantitative information about the molecular mechanisms of nucleic-acid metabolism. In contrast to many other single-molecule methods kinetic reaction parameters of hundreds of molecules can be extracted from image data in a matter of minutes.

Furthermore, our method is highly customisable. Theoretical possibilities include but are not limited to rapid characterisation of helicases, polymerases, complete replisomes, as well as nucleases.

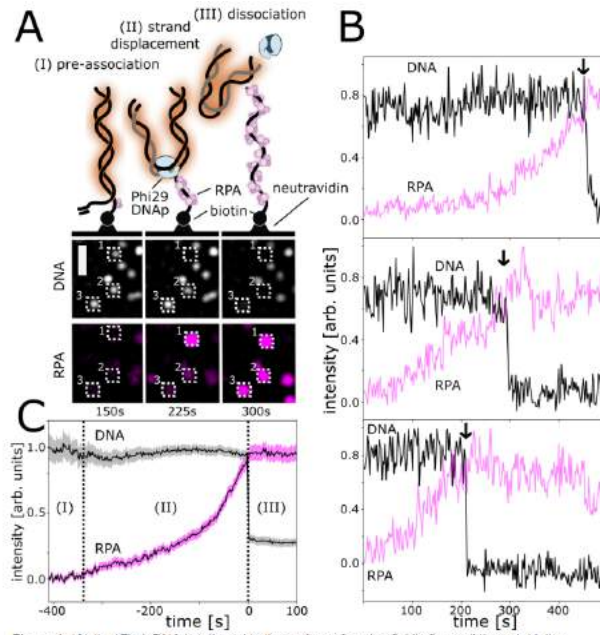


Figure 1. (A) (top) First, DNA is tethered to the surface of a microfluidic flow cell through biotin-neutravidin interaction (I). Second, strand-displacement synthesis is initiated by introducing $\Phi 29$ DNAP and all four dNTPs in the presence of RPA (II). Upon completion of the synthesis of the full template, the daughter strand dissociates, leaving behind RPA-bound ssDNA (III). (bottom) Montage of a TIRF microscopy movie. Scale bar = 2 μm . (B) Representative single-molecule trajectories. (C) Average of 101 synchronized trajectories. The shaded area depicts the standard error of the mean.

Figure1.png

Tradeoff between dissipation and uncertainty in helicases

Friday, 9th July - 16:00: Poster Session 4-A - Poster - Abstract ID: 148

Dr. Maria Mañosas¹, Dr. Felix Ritort¹, Dr. Xavier Viader¹, Dr. Vegard Sordal², Mr. Victor Rodriguez³

1. Small Biosystems Lab, Departament de Física de la Materia Condensada, Facultat de Física, Universitat de Barcelona, Carrer de Martí i Franquès, 1, 08028 Barcelona, 2. University of Oslo, 3. Facultat de Física, Universitat de Barcelona, Carrer de Martí i Franquès, 1, 08028 Barcelona

Helicases are molecular machines that convert chemical energy into mechanical work to unwind nucleic acids. They work out of equilibrium in strong Brownian agitation while being fuelled only by the ATP hydrolysis delivering an amount of energy just a few times higher than the thermal energy ($k_B T$). Working in this noisy environment they incur thermodynamic costs. The recently derived thermodynamic uncertainty product Q [1] is used to characterize the tradeoff between the thermodynamic costs (dissipation) and the uncertainty (fluctuations) of non-equilibrium dynamical processes, such as the activity of molecular machines. An uncertainty relation has been derived showing that the Q product has a lower bound of $2k_B$ [1]. For molecular machines the latter reads as: $Q = \sigma_T 2D/V \geq 2k_B$, where V and D are respectively the molecular machine mean rate and diffusivity, and σ_T is the entropy production rate.

Here, we use optical and magnetic tweezers to manipulate a DNA hairpin and study the unwinding activity of two DNA helicases: T4 gp41 and E. Coli RecQ. Using the measured DNA extension as a reaction coordinate, the activity of individual helicases can be followed in real time (Fig. 1). From the experimental traces we can measure the mean unwinding rate V and the helicase diffusion constant D along the DNA. The Q product is estimated assuming a tight chemomechanical coupling of one base-pair unwound per ATP. By varying the applied force and the ATP concentration we investigate how the dissipation/uncertainty tradeoff depends on the working conditions (Fig. 2). We find that both the ATP concentration and the applied force affect the value of the Q product. Interestingly, despite the differences in structure and function between the two helicases studied, both helicases present similar dependencies for the dissipation/uncertainty tradeoffs. However, the Q product is systematically larger for the gp41 helicase, which might be related to its passive character [2]. The experimental results are compared with simulations of a biased random walk moving on a DNA chain.

[1] Barato, A. C & Seifert, U, *Phys. Rev. Lett.* 114, 158101 (2015).

[2] Manosas, M., Xi, X. G., Bensimon, D., & Croquette, V. *NAR* 38(16), 5518-5526 (2010).

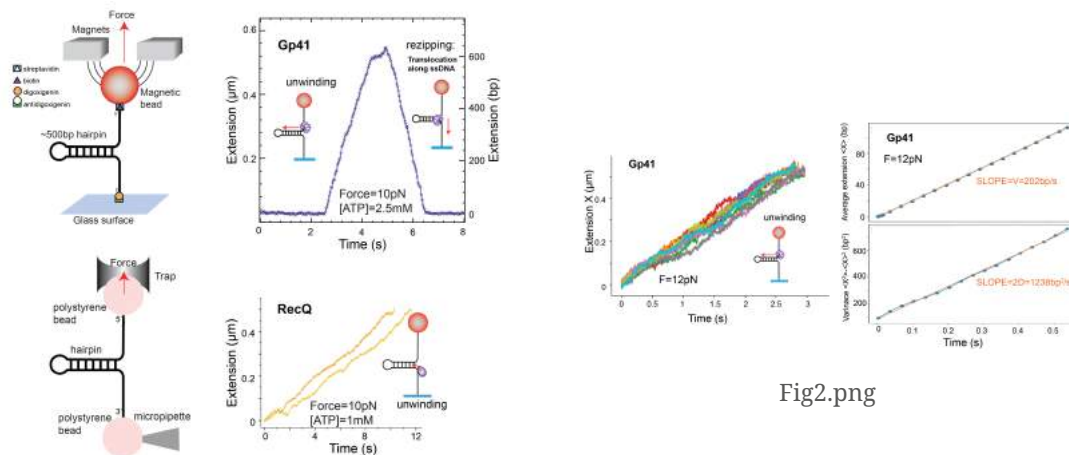


Fig2.png

Fig1.png

Rapid helicase-SSB assisted isothermal amplification of long DNA fragments

Friday, 9th July - 16:00: Poster Session 4-A - Poster - Abstract ID: 155

***Dr. Momcilo Gavrilov*¹, *Dr. Chun-Ying Lee*¹, *Prof. Sua Myong*¹, *Prof. Taekjip Ha*¹**

1. Johns Hopkins University

DNA and RNA amplification is an essential method involved in the rapid molecular diagnostics, gene manipulations, and genetic analyses including the detection of bacteria, viruses, and diagnosis of genetic disorders. The most widely used method for DNA/RNA amplification is the polymerase chain reaction (PCR), implemented through thermal cycling. A promising next generation method is the enzymatic isothermal amplification; however, existing isothermal methods are limited to producing only short amplicons, complex heterogeneous mixed and branched products, and often involve using multiple sets of complicated pairs of primers. Here we present a helicase and SSB (Single-Stranded Binding protein) assisted rapid isothermal amplification method named SHARP (SSB-Helicase Assisted Rapid Polymerase chain reaction). SHARP completely eliminates thermal cycling from DNA amplification and keep all desired PCR features in place such as up to 6 kilo base pairs amplicons, 5 to 30 min amplification time, primers design principles and convenience, detection limit, and product downstream application. We will explain how unique properties of PcrA helicase play a crucial role in the SHARP reaction and we will show several applications of our new biotechnology tool.

The human DEAD-box helicase 3 interacts with ER-alpha and regulates its activity

Friday, 9th July - 16:00: Poster Session 4-B - Poster - Abstract ID: 47

***Dr. Martina Schroeder*¹, *Mrs. Jyotsna Pardeshi*¹, *Dr. Lili Gu*², *Dr. Niamh McCormack*¹, *Dr. Yvette Hoehn*¹**

1. Maynooth University, 2. Maynooth University (now Trinity College Dublin)

DDX3 is an RNA helicase that potentially regulates gene expression at various levels, such as transcription, splicing, mRNA export, and translation initiation. It has also been implicated in regulation of cell cycle progression and apoptosis. Our lab has previously investigated the role of DDX3 in innate immune signalling, where it enhances autophosphorylation and activation of the kinase IKK ϵ , and links the activated kinase to its substrate, the transcription factor IRF3. This process facilitates IRF3 activation and expression of anti-viral mediators.

Interestingly, both DDX3 and IKK ϵ have independently been shown to act as breast cancer oncogenes. In breast cancer, DDX3 has been shown to be upregulated and linked with various differentiation, cell proliferation and migration pathways. IKK ϵ was suggested to phosphorylate Estrogen receptor alpha (ER α) at Serine 167 and thereby drive expression of ER α -responsive genes in an estrogen-independent manner, leading to cell proliferation and resistance to anti-estrogen treatment.

Our work suggests that DDX3 and IKK ϵ collaborate to mediate ER α phosphorylation and activation, akin to the mechanism we elucidated for IRF3 activation in innate immune signalling. shRNA-mediated knockdown of DDX3 in breast cancer cell lines (MCF7s and T47Ds) resulted in reduced ER α phosphorylation, reduced ERE-controlled reporter gene expression, decreased expression of ER α target genes, and decreased cell proliferation. Vice versa, overexpression of DDX3 resulted in enhanced ER α phosphorylation and activity. Furthermore, we have evidence that DDX3 directly binds to ER α from co-immunoprecipitation and pulldown experiments.

In conclusion, our research provides a novel molecular mechanism that might contribute to the oncogenic effect of DDX3 in breast cancer, potentially linking it to the development of resistance against endocrine therapy.

Proteomics Reveal Rocaglate Inhibitors of the eIF4A1 DEAD-box RNA Helicase Remodel the Translation Machinery and Translatome

Friday, 9th July - 16:00: Poster Session 4-B - Poster - Abstract ID: 79

Dr. Jonathan Schatz¹, **Dr. David Ho**¹, **Mr. Tyler Cunningham**¹, **Ms. Paola Manara**¹, **Dr. Stephen Lee**¹

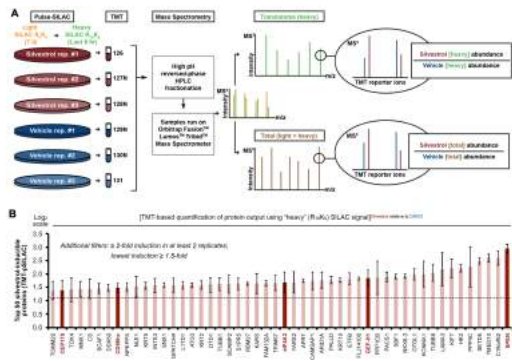
1. Sylvester Comprehensive Cancer Center at the University of Miami Miller School of Medicine

Introduction: DEAD-box RNA helicase enzymes are emerging targets in cancer therapy. Inhibition of eukaryotic initiation factor 4A1 (eIF4A1), the critical mRNA helicase that mediates cap-dependent translation initiation, is well validated preclinically. Rocaglates, natural and synthetic compounds whose unique mechanism of action includes sequence-specific clamping of eIF4A1 to RNA, show high potency against multiple cancer types in vitro and in vivo. Zotatifin is the first-in-class clinical rocaglate, under phase I evaluation in solid tumor malignancies and as an antiviral against SARS-COV2. Critically, the full cellular impact and mechanisms of these potent molecules are undefined at a proteomic level.

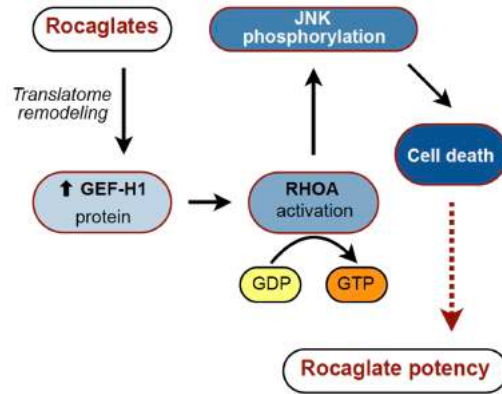
Methods: We conducted original mass-spectrometry analyses of translational reprogramming by rocaglates. TMT-SILAC assessed acute changes in protein production, while MATRIX, which captures high-resolution profiles of the translation machinery, revealed translation factors that drive reprogramming in response to rocaglate exposure. We validated results biochemically, in cellulo, and in vivo using patient-derived xenograft (PDX) tumors in mice.

Results: We found rocaglates, including zotatifin, had effects far more complex than simple “translational inhibition” as currently defined. Indeed, translatome analysis by TMT-pulse-SILAC (**Fig. 1A**) revealed myriad up-regulated proteins that drive hitherto unrecognized cytotoxic mechanisms (**Fig. 1B**). The GEF-H1 guanine exchange factor for examples drives anti-survival RHOA/JNK activation (**Fig. 2**), revealing novel candidate biomarkers of rocaglate clinical outcomes. Surprisingly, these responses are eIF4A-independent, indicating a broader translational adaptation than currently understood and suggesting roles for additional RNA helicase enzymes, which are the subject of active unbiased proteomic analyses. PDX tumors showed these new mechanisms of rocaglates are observed at pharmacologic concentrations in vivo, with effects substantially stronger on tumors compared to non-malignant tissues. Translation machinery analysis by MATRIX (**Fig. 3A**) revealed rocaglate-induced dependence on specific translation factors including eEF1e1 that drive remodeling (**Fig. 3B**).

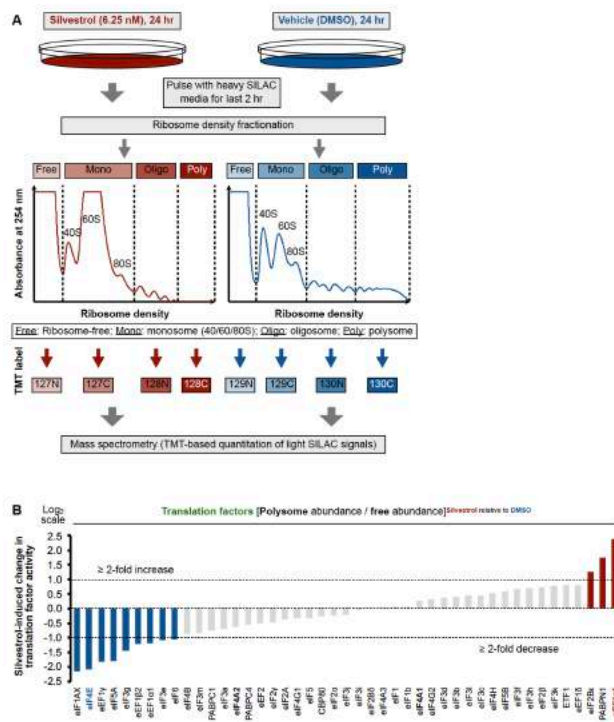
Discussion: Our original proteome-level interrogation revealed that the complete cellular response to these historical “translation inhibitors” is mediated by comprehensive translational landscape remodeling. Effects on a broader suite of RNA helicase enzymes than eIF4A1 alone we suggest mediate the potent antitumor activities of these unique compounds, elucidation of which permits development of novel precision approaches to targeted translational deregulation in cancer.



Helicases-schatz-fig1.png



Helicases-schatz-fig2.png



Helicases-schatz-fig3.png

Translation of the eIF4B mRNA drives cell division dynamics in sea urchin embryos.

Friday, 9th July - 16:00: Poster Session 4-B - Poster - Abstract ID: 89

Mr. Florian Pontheaux¹, Dr. Julia Morales¹, Prof. Patrick Cormier¹

1. Station Biologique de Roscoff, Sorbonne Université, CNRS

mRNAs translation into proteins is a fine-tuned process. In sea urchins, at the egg-to-embryo transition, translation stimulation is required as soon as the first cell cycle progression. Interestingly, the egg-to-embryo transcriptome analysis revealed that the translation factor eIF4B is the only factor among the initiation complex to be neo-translated (Chassé et al., 2019). On the one hand, mammalian eIF4B is known to potentiate the RNA helicase eIF4A activity. On the other hand, eIF4B overexpression is a poor prognostic marker in cancer. Therefore, we tested if eIF4B mRNA translation induced by fertilization is essential for the embryonic cell division dynamics in sea urchins.

Firstly, we characterized the sea urchin eIF4B and its function following fertilization. We produced an antibody directed against the sea urchin eIF4B. This eIF4B antibody reveals an endogenous 78kDa protein in sea urchin eggs and embryos. By cap-column purification, we showed that eIF4B copurifies with the cap-binding protein eIF4E after fertilization. We further showed that exogenous eIF4B mRNA translation stimulates the translation of a Luciferase reporter mRNA both *in vitro* in reticulocyte lysate and *in vivo* after microinjection in sea urchin eggs (Fig1). Secondly, we addressed the relationship between the eIF4B neo-translation and the embryonic cell cycle. The inhibition of eIF4B translation with microinjected morpholinos reveals a delay in the first mitotic divisions of the embryos (Fig2A). On the contrary, eIF4B overexpression with microinjected exogenous mRNA accelerates the embryonic cell cycle (Fig2B). Taking together, our results demonstrate that the sea urchin eIF4B controls translational activity and that the efficiency of eIF4B mRNA translation is involved in the control of the embryonic cell-cycle dynamics.

This study opens new insights about embryonic cell proliferation regulated by mRNA translation. The neo-translation of the eIF4B mRNA can be viewed as a positive feedback loop enhancing the stimulated translation and will help to exhibit a first translational network at the egg-to-embryo transition in sea urchin.

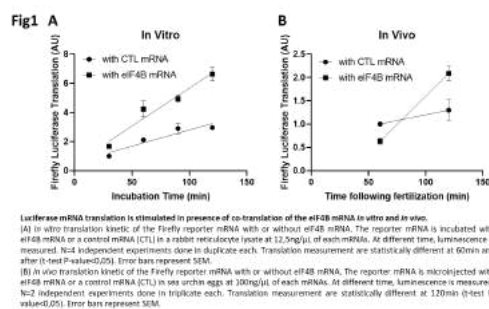


Figure1.png

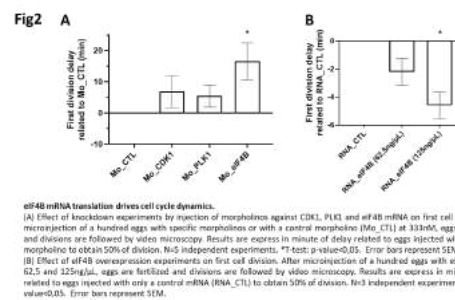


Figure2.png

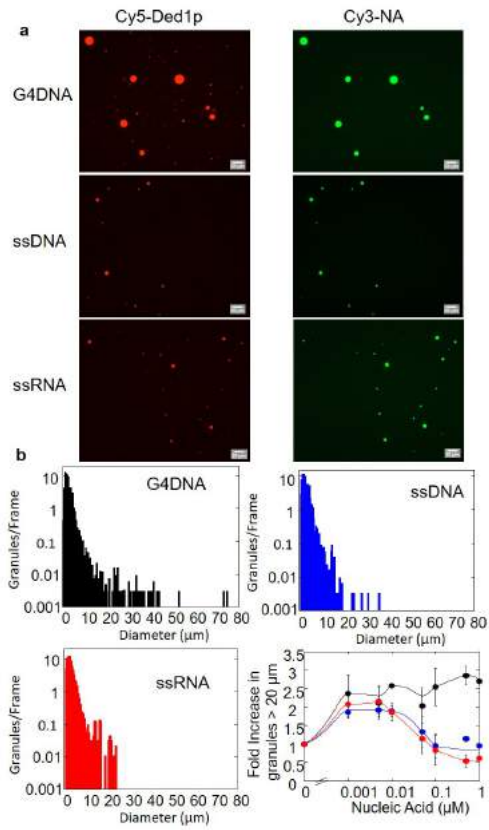
G-quadruplex DNA inhibits unwinding activity but promotes liquid-liquid phase separation by the DEAD-box helicase Ded1p

Friday, 9th July - 16:00: Poster Session 4-B - Poster - Abstract ID: 104

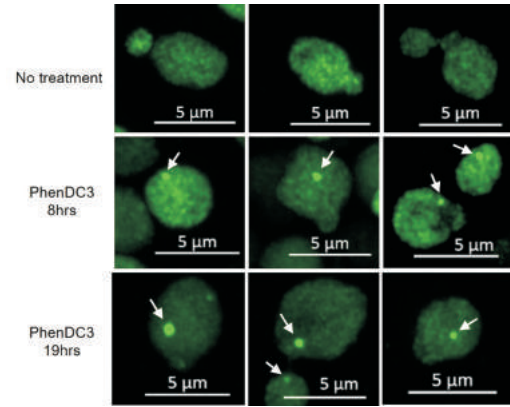
Dr. Jun Gao¹, **Mr. Zhaofeng Gao**², **Ms. Andrea A. Putnam**², **Dr. Alicia K. Byrd**¹, **Ms. Sarah Venus**², **Dr. John C. Marecki**¹, **Dr. Andrea D. Edwards**¹, **Ms. Haley M. Lowe**¹, **Dr. Eckhard Jankowsky**², **Dr. Kevin Raney**¹

1. University of Arkansas for Medical Sciences, 2. Case Western Reserve University

G-quadruplexes (G4) are four-stranded nucleic acid structures of stacked planar guanine tetrads. The guanines in each plane interact through Hoogsteen hydrogen bonding. G4 structures play important roles in gene expression, DNA replication, and telomere maintenance. In addition, G4 structures have been linked to genomic instability and human diseases, including cancer and neurodegenerative disorders. DEAD-box RNA helicases, characterized by a highly conserved “Asp-Glu-Ala-Asp” (DEAD) motif, are found in all eukaryotes, as well as in many bacteria and archaea. These enzymes are involved in most aspects of cellular RNA metabolism and in the formation of stress granules and P-bodies, cellular RNA-protein condensates that form by liquid-liquid phase separation (LLPS). Many DEAD-box helicases have been linked to diseases, including cancer, neurodegeneration and viral infections. The DEAD-box RNA helicase Ded1p, an ortholog of human DDX3X, is involved in translation initiation and localizes to stress granules and P-bodies. By the *in vitro* unwinding experiments, we found that G4DNA inhibits RNA unwinding activity of Ded1p. Cy5-labelled Ded1p incubated with Cy3-labelled G4DNA (or ssDNA, ssRNA), granule size was measured by microscopy, and we observed G4DNA promotes liquid-liquid phase separation (LLPS) of Ded1p *in vitro*. *Saccharomyces cerevisiae* cells expressing Ded1-GFP from its endogenous chromosomal locus were grown to early-log phase at 28°C, then treated with 10 μM Phen-DC3 (a well-characterized G4 stabilizer) for 19 hours, showed that Ded1-GFP forms a non-membrane organelle-like structure at the outside of the nucleus in the cell. This observation indicate that Phen-DC3 promotes LLPS of Ded1-GFP in cells. In summary, we demonstrated that G4DNA inhibits RNA unwinding activity of DEAD-box helicase Ded1p, and promotes LLPS of Ded1p. Our findings suggest possible new roles for G4 structures and DEAD-box RNA helicases.



G4dna-ded1-llps-in-vitro.jpg



Phendc3-ded1gfp-in-cells.jpg

Correlating the conformational dynamics of the DEAD-box helicase eIF4A with translation efficiencies

Friday, 9th July - 16:00: Poster Session 4-B - Poster - Abstract ID: 129

***Dr. Anirban Chakraborty*¹, *Dr. Linda Krause*¹, *Dr. Alexandra-Zoi Andreou*¹, *Dr. Dagmar Klostermeier*¹**

1. Institute for Physical Chemistry, University of Muenster

The eukaryotic translation initiation is a tightly regulated process requiring the interplay of several translation initiation factors (eIFs). The role of eIF4A, an ATP-dependent RNA helicase, is the resolution of secondary structure elements within the 5'-untranslated regions (5'-UTR) of mRNA to enable ribosome recruitment and scanning. Previous studies from our lab have shown that the factors eIF4B and eIF4G jointly stimulate eIF4A ATPase and unwinding activity by accelerating the switching of eIF4A between closed and open states (3,4). The activity of eIF4A is additionally modulated by single-stranded regions in RNA substrates (1). Recent genome-wide studies have identified eIF4A-dependent mRNAs in yeast (2). In this study, we investigate the connection between eIF4A conformational dynamics and the efficiency of mRNA translation. Yeast extracts depleted of eIFs were used in *in vitro* translation assays where we monitored the translation efficiency of mRNAs in which the 5'-UTRs of eIF4A-dependent mRNAs are fused to a reporter gene. To validate the effects of these 5'-UTRs on translational efficiencies, luciferase reporter assays were performed in wildtype yeast cells. The eIF4A conformation in the presence of these UTRs was monitored in single-molecule FRET experiments. We found that with different 5' UTRs, both, the eIF4A conformational equilibrium and mRNA translation efficiency showed differences. To understand the kinetics of conformational changes of eIF4A in the presence of these 5'-UTRs, smFRET experiments will be performed using TIRF microscopy under translating conditions.

References:

- [1] A.Z. Andreou, U. Harms, D. Klostermeier, Single-stranded regions modulate conformational dynamics and ATPase activity of eIF4A to optimize 5'-UTR unwinding, *Nucleic Acids Res.* 47 (2019) 5260–5275.
- [2] N.D. Sen, F. Zhou, N.T. Ingolia, A.G. Hinnebusch, Genome-wide analysis of translational efficiency reveals distinct but overlapping functions of yeast DEAD-box RNA helicases Ded1 and eIF4A, *Genome Res.* 25 (2015) 1196–1205.
- [3] U. Harms, A.Z. Andreou, A. Gubaev, D. Klostermeier, eIF4B, eIF4G and RNA regulate eIF4A activity in translation initiation by modulating the eIF4A conformational cycle, *Nucleic Acids Res.* 42 (2014) 7911–7922.
- [4] A.Z. Andreou, D. Klostermeier, eIF4B and eIF4G Jointly Stimulate eIF4A ATPase and Unwinding Activities by Modulation of the eIF4A Conformational Cycle, *Journal of Molecular Biology.* 426 (2014) 51–61

Dissecting the role of the eIF4E/5'-cap interaction for eIF4A activity with a model RNA

Friday, 9th July - 16:00: Poster Session 4-B - Poster - Abstract ID: 137

***Dr. Linda Krause*¹, *Dr. Alexandra Zoi Andreou*¹, *Dr. Dagmar Klostermeier*¹**

1. Institute for Physical Chemistry, University of Muenster

eIF4A is a minimal DEAD box helicase involved in eukaryotic translation initiation. In complex with the scaffolding protein eIF4G and the cap-binding protein eIF4E (together eIF4F) it resolves secondary structure elements in the 5'-UTR of mRNAs to allow for ribosomal scanning. eIF4A has a coupled helicase- and ATPase activity; both activities are stimulated by eIF4G [1]. While the cap-binding function of eIF4E is well-established, its effect on eIF4A activity is not fully understood. The eIF4A/eIF4G complex binds and unwinds RNA in the absence of eIF4E and/or the 5'-cap. Using a series of eIF4G deletion variants and eIF4E, we observe that the stimulation of the eIF4A helicase activity is largely dependent on individual domains of eIF4G, but not on the eIF4E/5'-cap interaction. Especially the RNA binding domain 2 of eIF4G is important for tighter RNA binding and faster unwinding (of the RNA) by eIF4A. The presence of eIF4E and the 5'-cap, on the other hand, is not connected to a general increase in eIF4A activity as observed with eIF4G. Instead, eIF4E and the 5'-cap have more complex effects on eIF4A RNA unwinding- and ATPase activity: eIF4E inhibits the unwinding activity of eIF4A independent of the 5'-cap, while the 5'-cap has an inhibitory effect on eIF4A ATPase activity independent of eIF4E. Furthermore, eIF4E also influences the eIF4A activity independent of the eIF4E/4G interaction. This points towards a regulatory role of the eIF4E/5'-cap interaction and possibly additional functions of eIF4E and the 5'-cap besides the direction of eIF4F to the 5'-end of the mRNA. Taken together, these studies shed further light on the complex interplay of eIF4G, eIF4E and the 5'-cap in eIF4A stimulation.

[1] Andreou AZ, Klostermeier D (2014) eIF4B and eIF4G Jointly Stimulate eIF4A ATPase and Unwinding Activities by Modulation of the eIF4A Conformational Cycle. *J Mol Biol* 426:51–61. <https://doi.org/10.1016/j.jmb.2013.09.027>

DEAD-box ATPases are regulators of RNA-containing biomolecular condensates

Friday, 9th July - 16:30: Keynote 11 - Oral - Abstract ID: 130

Prof. Karsten Weis¹

1. ETH Zürich

The ability of proteins and nucleic acids to undergo liquid-liquid phase separation (LLPS) has emerged as an important molecular principle of how cells rapidly and reversibly compartmentalise their components into membraneless organelles such as the nucleolus, processing bodies or stress granules. How the assembly and turnover of these organelles is regulated, and how these biological condensates selectively recruit or release components remains poorly understood.

We have recently demonstrated that members of the large and highly abundant family of RNA-dependent DEAD-box ATPases (DDXs) regulate RNA-containing phase-separated organelles in pro- and eukaryotes. Using *in vitro* reconstitution and *in vivo* experiments we showed that DDXs promote phase separation in their ATP-bound form, and ATP hydrolysis induces compartment turnover and RNA release. This mechanism of membraneless organelle regulation reveals a novel principle of cellular organisation that is conserved from bacteria to man. We further found that DDXs can control RNA flux between phase-separated organelles, suggesting that a cellular network of dynamic, DDX-controlled compartments establishes biochemical reaction centres that affords cells spatial and temporal control of various RNA processing steps regulating the composition and fate of ribonucleoprotein particles.

DDX6 mutations responsible for intellectual disability and dysmorphic features associated with RNA misregulation and P-body defects

Friday, 9th July - 17:00: Oral Session - Oral - Abstract ID: 131

*Mrs. Marianne Benard*¹, *Mrs. Michele Ernoult-Lange*¹, *Mrs. Ada Allam*¹, *Mr. Christopher Balak*²,
*Mrs. Amelie Piton*³, *Mrs. Dominique Weil*¹

1. Institut de Biologie Paris Seine, CNRS-Sorbonne university, Paris, 2. Translational Genomics Research Institute (TGen), Phoenix, 3. IGBMC, Strasbourg

Introduction: Intellectual disability (ID) resulting from abnormal neurodevelopment affects about 1% of the population. Hundreds of genes with pathogenic variants have been implicated, which encode proteins involved in various neurospecific (eg synaptic function) or ubiquitous (eg post-transcriptional regulation) processes. Recently, we evidenced five unrelated ID patients carrying rare de novo missense heterozygous mutations in the DDX6 gene (Weil Bioch Soc Trans 2020). The DDX6 helicase is involved in mRNA decay, translation repression and P-body assembly. P-bodies are RNP condensates that coordinate the storage of poorly translated mRNAs, which encode proteins with regulatory functions (Hubstenberger Mol Cell 2017). In human cells, P-body condensation requires catalytically active DDX6 and its partners LSM14A and 4E-T (Ayache MBoC 2015).

Methods: To investigate the causative role of DDX6 mutations in ID, we combined transcriptomic analysis, fluorescence microscopy, complementation assays and co-immunoprecipitations. To further decipher the dysfunctions resulting from DDX6 mutations, we set up an acellular assay to reconstitute DDX6-dependent P-body-like RNP condensates (Figure 1) (Courel eLife 2019) and used CRISPR/Cas9 to introduce patient mutations in a model cell line.

Results: All patient DDX6 variants result in a single amino acid change in either motif QxxR or V of the helicase (Figure 2). Our transcriptomic analysis of patient-derived cells revealed defects in mRNA regulation, which overlap the defects observed after DDX6 silencing in cell lines. Moreover, patient cells contain less P-bodies than controls and, indeed, the patient DDX6 variants are defective for P-body assembly in cell lines (Figure 3), probably related to their defective interaction with LSM14A and/or 4E-T. Like the patient cells, the heterozygous DDX6 mutant clones have a reduced P-body number. While the RNP condensate reconstitution assay recapitulates the requirement for DDX6 ATPase activity, experiments with DDX6 harboring patient mutations are underway.

Discussion: Altogether, our data demonstrated the causative role of heterozygous missense DDX6 variants in a neurodevelopmental syndrome associated with RNA misregulation and P-body defects (Balak AJHG 2019). The acellular reconstitution assay and the mutant cell models will allow for deciphering the cellular pathways most affected by the expression of mutant DDX6, and therefore most likely to lead to the neurodevelopmental disease.

Figure 2 : Localization of DDX6 patient mutations

(PMID:31422817)

Figure 1: In vitro reconstitution assay of DDX6-dependent P-body-like condensates

(PMID:31856182)

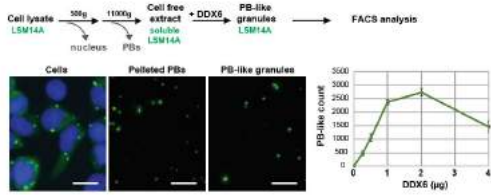


Fig 1.jpg

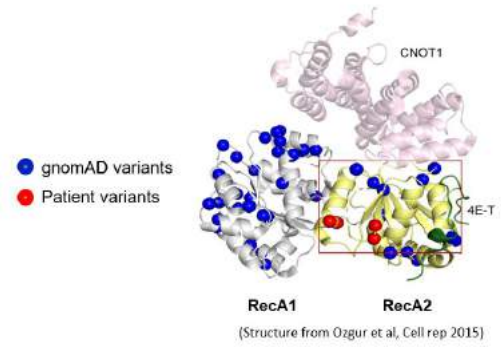


Fig 2.jpg

Figure 3 : P-body defect resulting from DDX6 patient mutations

(PMID:31422817)

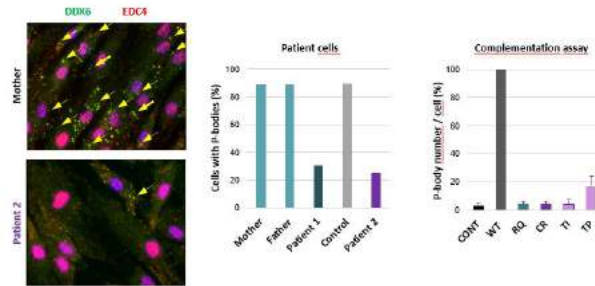


Fig 3.jpg

Translation regulation by the RNA helicase Ded1 during cell stress

Friday, 9th July - 17:15: Oral Session - Oral - Abstract ID: 143

*Dr. Peyman Aryanpur*¹, *Dr. Telsa Mittelmeier*¹, *Dr. Timothy Bolger*¹

1. University of Arizona

Cellular identity, function, and physiology are all determined by the proper regulation of gene expression, and various pathologies can be the result of defects in this process. Changes in gene expression are a primary response to changing conditions, and in many cases, coordinated pathways affect gene expression at multiple levels. The Bolger lab focuses on the critical roles that DEAD-box RNA helicases play in these processes through their ability to modulate RNA-RNA and RNA-protein interactions. We have recently identified the DEAD-box protein Ded1 as a novel mediator of the translational response to TOR inactivation, which occurs during various cellular stress conditions. Interestingly, Ded1 is normally required to promote translation initiation; however, during cellular stress, we have found that Ded1 acts to promote down-regulation of bulk translation instead. Specifically, our evidence suggests that when TOR is inhibited, Ded1 remodels pre-initiation complexes to remove the translation factor eIF4G and release it for degradation. Further, Ded1 has been previously shown to play a role in the dynamics of stress granules (SGs), cytoplasmic accumulations of mRNAs and RNA-binding proteins. Our most recent work has attempted to broaden our understanding of Ded1 function during cellular stress by examining the interplay between these different roles. Interestingly, although Ded1 is required for survival during multiple stress conditions, the direct effects on translation appear to be separate from those on SG dynamics, with distinct functional requirements for each. We propose a biphasic model of Ded1 function in cellular stress where it has an early role in repressing normal translation and then a later role in promoting survival through SGs and translation adaptation (Figure 1). These studies thus further elucidate the role of translation regulation in cellular stress responses and will have implications for pathologies where stress pathways are misregulated, including cancer and aging.

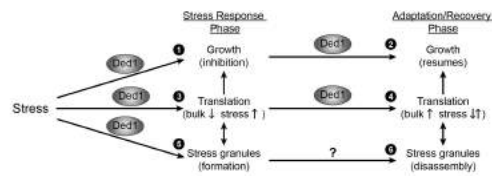


Figure 1: Ded1 has multiple effects during cellular stress responses. A model for Ded1 function during both the initial stress response and during adaptation/recovery. Ded1 plays roles in both translation regulation and formation of SGs during the stress response, leading to growth inhibition (1, 3, & 5). Likewise, Ded1 function is important for translation upregulation in the recovery phase, leading to resumption of growth (2,4). A role in SG disassembly has not been identified to date (6).

Fig1-model-legend.jpg

Roles of Local DNA Conformation and Conformational Dynamics on DNA Polymerase Holoenzyme Formation in the Bacteriophage T4 DNA Replication System

Friday, 9th July - 17:30: Oral Session - Oral - Abstract ID: 84

***Dr. Patrick Herbert*¹, *Mr. Dylan Heussman*¹, *Mr. Jack Maurer*¹, *Ms. Maya Pande*¹, *Mr. Steve Weitzel*¹,
*Prof. Peter von Hippel*¹, *Prof. Andrew Marcus*¹**

1. University of Oregon

DNA replication elongation requires the coordinated function of a number of DNA-protein sub-assemblies. These subassembly complexes function primarily at single-stranded (ss) - double-stranded (ds) DNA junctions within the overall replication complex (Figure 1). As a consequence conformational changes and 'breathing' fluctuations at these junctions play an important role in the multiple steps of the elongation process. Here we focus on the formation of the DNA polymerase/sliding clamp holoenzyme at primer/template (p/t) ss-dsDNA junctions within the replication complex (Figures 1 and 2). To study these local interactions we have developed a novel molecular probing method that relies on the use of excitonically-coupled Cy3 dimers covalently (and rigidly) inserted into the sugar-phosphate backbones of duplex DNA at opposing positions within complementary strands (Figure 3). Linear absorption and circular dichroism (CD) spectra report on the local orientation of these (Cy3)₂ dimer probes, and hence on the local conformation of the DNA sugar-phosphate backbones. In addition, we have developed a microsecond polarization-sweep (MPS) single-molecule microscopy technique to study site-specific DNA breathing dynamics (Figure 4). Taken together, these methods are utilized to define the changes in local ss-dsDNA conformation and conformational dynamics that facilitate the sequential steps of DNA polymerase holoenzyme assembly (Figure 2). Our initial CD/Abs studies of p/t DNA constructs with (Cy3)₂ dimer probes positioned near the ss-dsDNA junction exhibit unique conformations and conformational disorder in comparison to equivalent measurements deeper within duplex DNA segments. Notably, MPS single-molecule studies can be used to monitor the breathing dynamics of the (Cy3)₂ dimer probes at the p/t DNA junction that accompany the binding of the activated clamp/clamp loader and DNA polymerase (Figure 2). Using these probes we have observed the local conformations of the sugar-phosphate backbones that we previously characterized by CD/Abs spectroscopy, and find that DNA breathing at the p/t DNA junction slows significantly on binding DNA polymerase and other proteins involved in the regulation of replication. In this report we will discuss the potential biological roles of these local conformational changes in the overall clamp loading and DNA polymerase holoenzyme assembly processes that are central to the control of DNA elongation.

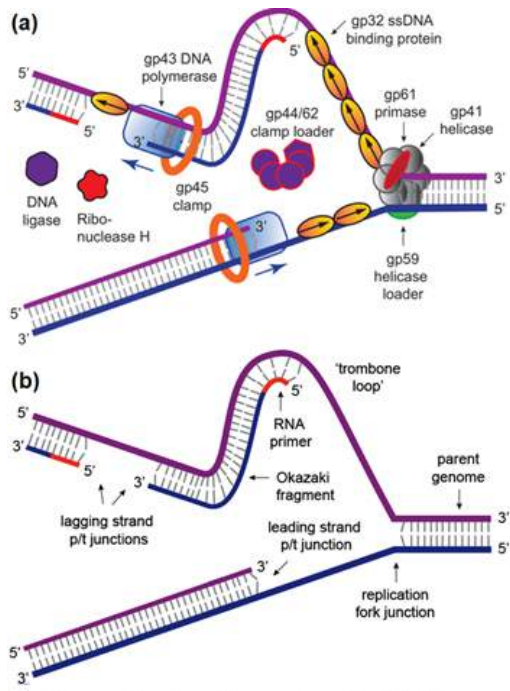


Figure 1. The elongation complex of the T4 DNA replication system showing protein components (a) and the underlying ss-dsDNA junctions (b).

Fig1.png

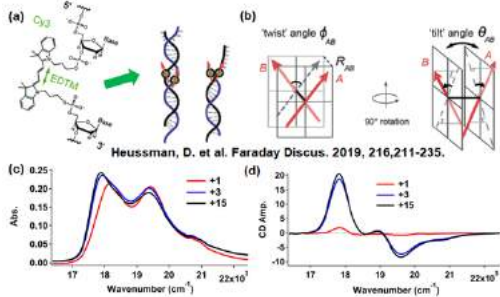


Figure 3. Use of Cy3-dimer probes to investigate local DNA conformations.

Fig3.png

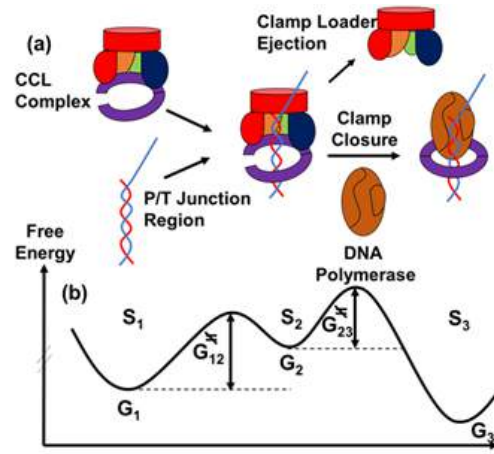
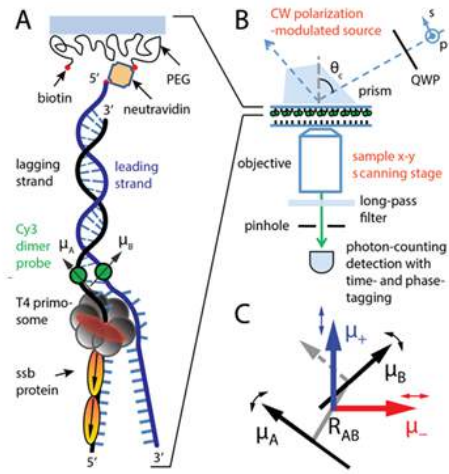


Figure 2. T4 DNA holoenzyme assembly process

Fig2.png



Maurer, J. et al. In Prep.

Figure 4. MPS technique for using Cy3-dimers as a probe of local DNA 'breathing' within DNA-protein complexes.

Fig4.png

SARS CoV-2 NSP13 Helicase Displaces Proteins and Rapidly Unwinds RNA and DNA

Friday, 9th July - 19:00: Oral Session - Oral - Abstract ID: 31

***Dr. John Marecki*¹, *Mr. Harrison Russell*¹, *Mr. David Proffitt*¹, *Dr. Kevin Raney*¹**

1. University of Arkansas for Medical Sciences

Introduction: The SARS CoV-2 (SARS2) pandemic has placed a spotlight on the study of coronaviruses, and a reemergence of interest in the study of the SARS2 encoded SF1B helicase, non-structural protein 13 (NSP13). A single amino acid mutation differentiates the SARS2 NSP13 from SARS1 suggesting the helicase is well-conserved and participates in critical stages during the viral life cycle. Its role may involve the resolution of extensive secondary structures in the positive-stranded SARS2 RNA genome (~30 kB). Recent studies suggest that two NSP13 monomers participate in the genome replication complex, though the roles for the helicase activities are still unclear. In addition, previous SARS1 NSP13 work has been hampered by the presence of *N*-terminal affinity tags that appear to interfere with the zinc binding domain (ZBD) and some activities of the enzyme.

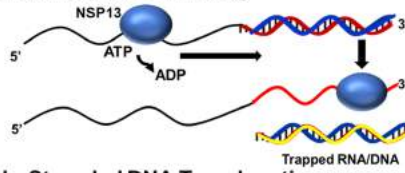
Methods: We purified the native SARS2 NSP13 to define the nucleic acid binding, ATP-mediated translocation, duplex unwinding and protein displacement helicase activities in detail.

Results: Anisotropy measurements demonstrate low nM affinities of NSP13 for both RNA and DNA, and multiple-turnover helicase assays confirm its rapid 5' to 3' duplex RNA and DNA unwinding activity. At saturating nucleic acid concentrations, we observed an ATPase rate of over 700 sec⁻¹ for RNA-dependent, and over 800 sec⁻¹ for DNA-dependent activities. These rates greatly exceed the reported ATP hydrolysis rates for the SARS1 NSP13. Using intrinsic tryptophan fluorescence and stopped-flow ensemble assays, we measured a rapid DNA translocation rate of 660 nucleotides/sec, suggesting that NSP13 moves 1.2 nucleotides per ATP hydrolyzed. To model the removal of RNA-binding proteins, we examined the ability of saturating amounts of NSP13 (250 nM) to displace streptavidin bound to biotin at the 3' end of DNA and RNA oligonucleotides. NSP13 efficiently displaced bound streptavidin both from T30 and U30 oligomers.

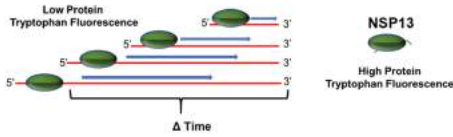
Conclusions: NSP13 has a robust ATPase activity that rapidly translocates to unwinds duplex RNA and is capable of producing force during ATP hydrolysis. The data support a robust ATPase activity that is matched by almost equally fast translocation on ssDNA. The ability to displace streptavidin indicates that NSP13 is likely able to remove proteins from nucleic acid.

Functional Studies of the SARS CoV-2 Non-Structural Protein 13 (NSP13) Helicase

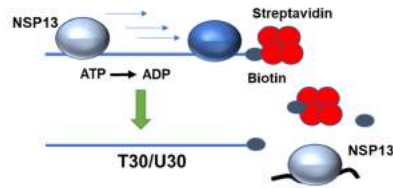
RNA/DNA Duplex Unwinding



Single-Stranded DNA Translocation



Protein Displacement



Marecki et al functions of nsp13.png

Force-dependent stimulation of RNA unwinding by SARS-CoV-2 nsp13 helicase

Friday, 9th July - 19:15: Oral Session - Oral - Abstract ID: 3

*Dr. Keith Mickolajczyk*¹, *Dr. Patrick Shelton*¹, *Dr. Michael Grasso*¹, *Ms. Xiacong Cao*², *Ms. Sara Warrington*¹, *Dr. Amol Aher*¹, *Dr. Shixin Liu*¹, *Dr. Tarun Kapoor*¹

1. *The Rockefeller University*, 2. *University of Science and Technology of China*

The superfamily-1 helicase non-structural protein 13 (nsp13) is required for SARS-CoV-2 replication. The mechanism and regulation of nsp13 has not been explored at the single-molecule level. Specifically, force-dependent unwinding experiments have yet to be performed for any coronavirus helicase. Here, using optical tweezers, we find that nsp13 unwinding frequency, processivity, and velocity increase substantially when a destabilizing force is applied to the RNA substrate. These results, along with bulk assays, depict nsp13 as an intrinsically weak helicase that can be potently activated by piconewton forces. Such force-dependent behavior contrasts the known behavior of other viral monomeric helicases such as Hepatitis C NS3, instead drawing stronger parallels to ring-shaped helicases. Our findings suggest that mechanoregulation, which may be provided by a directly bound RNA-dependent RNA polymerase, enables on-demand helicase activity on the relevant polynucleotide substrate during viral replication.

Authors Index

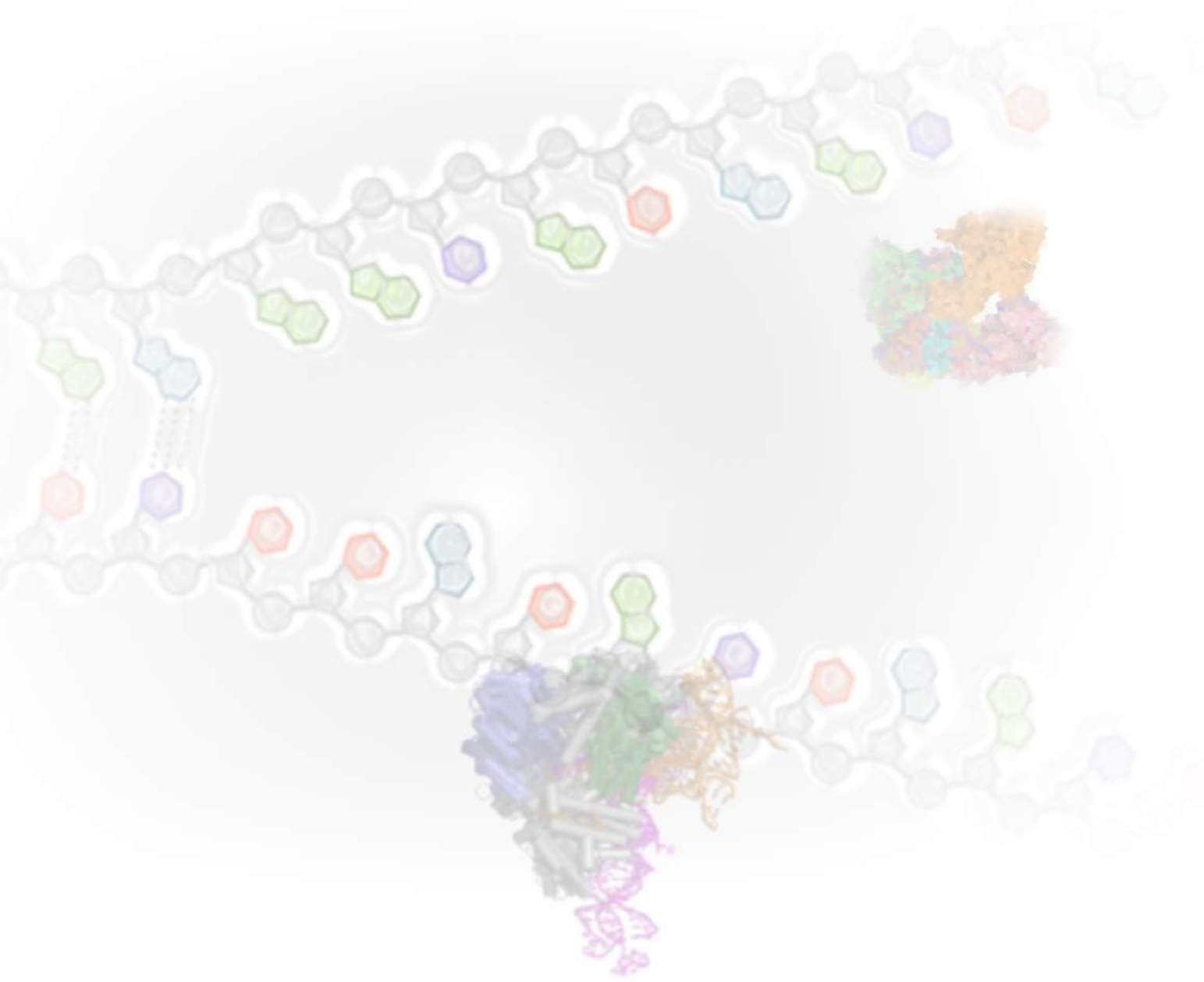
Aharoni, A.	98	Bukovska, G.	22
Aher, A.	133	Burge, C.	18
Aicart-Ramos, C.	41	Bussi, G.	83
Alghoul, E.	44	Byrd, A.	72, 81, 112, 121
Ali, Y.	4		
Allam, A.	126	C. S. Kuhn, G.	52
Andreou, A.	123, 124	Campbell, E.	60
Anindita, P.	54, 59	Campos-Doerfler, L.	50
Antelmann, H.	39	Cao, X.	133
Antony, E.	41	Chadda, A.	7
Aquino, G.	2	Chakraborty, A.	123
Armache, J.	75	Chen, W.	16
Aryanpur, P.	128	Chen, X.	87
Awate, S.	73	Chou, Y.	94
		Cohen-Gonsaud, M.	65
Bacolla, A.	66	Colizzi, F.	83
Balak, C.	126	Constantinou, A.	44
Balakrishnan, L.	100	Conti, E.	33
Balci, H.	12	Cormier, P.	120
Barthel, T.	39	COSTE, F.	65
Basbous, J.	44	Cox, M.	5
Bebel, A.	80	Craig, J.	102
Behrmann, M.	85, 101	Croquette, V.	97
Benard, M.	126	Cueny, R.	90, 92
Biswas, K.	73	Cunningham, T.	118
Bloom, L.	4, 6		
Bobrovnikov, D.	102	Da, L.	111
Bochman, M. (India)	100	Dai, L.	111
Bochman, M. (Indiana University - Bloomington)	88	Darst, S.	60
Bohnsack, K.	2	Das *, S.	75
Bohnsack, M.	2	Das, T.	26
Bolger, T.	128	Datta, A.	57, 73
Bonde, N.	5	De Falco, M.	11
Bonneau, F.	33	De Felice, M.	11
Boudvillain, M.	65	Deaconescu, A.	28
Boule, J.	97	Devarkar, S.	106
Bourgeois, C.	3	Dillingham, M.	41
Bowman, G.	75	Dimude, J.	107
Bron, P.	65	Dixon, N.	78
Brosh, R.	57, 73	Dong, M.	110
Brown, J.	16	Duckworth, A.	49
Brugger, C.	28	Dudenhausen, E.	4

<p>E, C. 111</p> <p>Eastlund, A. 21</p> <p>Edwards, A. 121</p> <p>Egly, J. 86</p> <p>Enemark, E. 71</p> <p>Ernoul-Lange, M. 126</p> <p>Faustino, A. 75</p> <p>Fazio, N. 95</p> <p>Feng, Q. 18</p> <p>Fenyk, S. 46</p> <p>Fischer, C. 21</p> <p>Franta, Z. 54, 59</p> <p>Fried, S. 75</p> <p>Fritzen, R. 83</p> <p>Fronzes, R. 69</p> <p>Galburt, E. 7</p> <p>Galej, W. 35</p> <p>Ganguly, A. 26</p> <p>Gao, F. 110</p> <p>Gao, J. 72, 121</p> <p>Gao, Y. 68</p> <p>Gao, Z. 121</p> <p>Garg, M. 14</p> <p>Gavrilov, M. 102, 116</p> <p>Geiser, J. 63</p> <p>Gerlach, P. 33</p> <p>Godbout, R. 14, 84</p> <p>Gonzalez, D. 63</p> <p>Grant, T. 49</p> <p>Grass, L. 39</p> <p>Grasso, M. 133</p> <p>Griffin, P. 106</p> <p>Grinkevich, P. 54</p> <p>Grünweller, A. 64</p> <p>Gu, L. 117</p> <p>Gundlach, J. 102</p> <p>Gupta, S. 50</p> <p>Ha, T. 29, 31, 43, 102, 108, 116</p> <p>Hackert, P. 2</p> <p>Halbeisen, M. 59</p> <p>Halgasova, N. 22</p> <p>Hamadeh, Z. 20</p> <p>Hambarde, S. 66</p> <p>Hao, L. 95</p> <p>Hartmann, R. 64</p> <p>Hausmann, S. 63</p>	<p>Hawkins, M. 107</p> <p>Hazeslip, L. 81, 112</p> <p>Herbert, P. 129</p> <p>Heringer, P. 52</p> <p>Heussman, D. 129</p> <p>Hilbig, D. 96</p> <p>Ho, D. 118</p> <p>Hoehn, Y. 117</p> <p>Hormeno, S. 41</p> <p>Hossain, L. 84</p> <p>Hurlock, A. 88</p> <p>Jameson, K. 107</p> <p>Jankowsky, E. 121</p> <p>Jardine, P. 21</p> <p>Jaremko, M. 104</p> <p>Jensen, D. 7</p> <p>Jergic, S. 78</p> <p>Johnson, S. 34</p> <p>Joshua-Tor, L. 104</p> <p>Juranek, S. 96</p> <p>Kapoor, T. 133</p> <p>Kappenberger, J. 23</p> <p>Kayarat, S. 25</p> <p>Kayikcioglu, T. 108</p> <p>Ke, A. 30</p> <p>Keck, J. 5, 49, 90, 92</p> <p>Kim, D. (Brown University) 28</p> <p>Kim, D. (Konkuk University) 61</p> <p>Kisker, C. 23, 86</p> <p>Klauck, E. 39</p> <p>Klostermeier, D. 123, 124</p> <p>Koegel, A. 33</p> <p>Krause, L. 123, 124</p> <p>Krick, K. 18</p> <p>Krogh, N. 2</p> <p>Kuper, J. 23, 86</p> <p>Kuppa, S. 41</p> <p>Kölmel, W. 23</p> <p>Lansdorp, P. 20</p> <p>Laszlo, A. 102</p> <p>Lee, C. 116</p> <p>Lee, H. 16</p> <p>Lee, R. 57</p> <p>Lee, S. 118</p> <p>Lewis, J. 78</p> <p>Li, L. 14</p>
--	--

Lin, C.	108	Novoa-Aponte, L.	82
Liu, S. (Rockefeller University)	77	Obermann, W.	64
Liu, S. (The Rockefeller University)	133	Okoniewski, S.	32
Lohman, T.	7, 38, 95	On, K.	104
Loll, B.	39	Onwubiko, N.	55
Long, C.	111	Paeschke, K.	96
Lowe, H.	121	Pan, K.	2
Lyumkis, D.	28	Pande, M.	129
Malone, B.	60	Pandita, T.	66
Manara, P.	118	Pardeshi, J.	117
Marcus, A.	129	Parfentev, I.	39
Marecki, J.	72, 121, 131	Pascal, B.	106
Margeat, E.	65	Patel, S. (Genetics and Metabolism Section, NIDDK, NIH, Bethesda, MD, USA)	82
Martin, K.	65	Patel, S. (Rutgers University)	106
Maurer, J.	129	Paul, T.	31
Mañosas, M.	115	Peissert, S.	86
McCormack, N.	117	Pellicciari, S.	46, 110
McKenzie, A.	5	Penedo, J.	83
McMillan, S.	92	Perera, H.	101
Mickolajczyk, K.	133	Perkins, T.	32
Midgley-Smith, S.	107	Pfleiderer, M.	35
Mills, M.	102	Philpott, C.	82
Mir Sanchis, I.	80, 93	Piton, A.	126
Mittelmeier, T.	128	Polard, P.	69
Mohapatra, S. (Johns Ho)	108	Pommier, Y.	48
Mohapatra, S. (Johns Hopkins University)	43	Pontheaux, F.	120
Moldovan, G.	73	Poterszman, A.	86
Morales, J.	120	Proffitt, D.	72, 131
MORENO-HERRERO, F.	41	Protchenko, O.	82
Morgan, A.	21	Putnam, A.	121
Mueller, S.	113	Qiaou, C.	93
Mukhopadhyay, S.	26	Raney, K.	72, 121, 131
Murray, H.	46, 110	Rasouli, S.	71
Mustafa, G.	12	Reha, D.	59
Myasnikov, A.	71	Rice, P.	80
Myong, S.	31, 116	Rieu, M.	97
Müller, C.	64	Ritort, F.	115
Nasheuer, H.	55	Rodriguez, V.	115
Neuman, K.	102	Romero, Z.	5
Newcomb, E.	6	Rudolph, C.	107
Newman, J.	105	Ruiz Manzano, A.	7
Nguyen, B.	7	Russell, H.	131
Nickens, D.	100	Saha, S.	48
Nicolae, C.	73		
Nielsen, H.	2		
Nodelman *, I.	75		

Sandmeir, F.	33	Tu, S.	16
Saridakis, E.	65	Tuma, R.	54, 59
Satyshur, K.	49	Urlaub, H.	2, 39
Sauer, F.	86	Uyetake, L.	32
Schaefer, I.	33	Valentini, M.	63
Schatz, J.	118	Valle Orero, J.	97
Scheuer, T.	23	van Oijen, A.	78, 113
Schmidt, K.	9, 50	Varon, M.	98
Schroeder, M.	117	Vaulin, N.	45
Schweibenz, B.	106	Venus, S.	121
Schönwetter, E.	23	Vernhes, E.	69
Semenova, E.	45	Viader, X.	115
Severinov, K.	45	Vishwakarma, R.	65
Sharan, S.	73	von Hippel, P.	129
Shastri, V.	9	Voter, A.	90
Shelton, P.	133	Wahl, M.	39
Shiekh, S.	12	Wang, W.	14
Shin, H.	80	Wang, Y.	14, 84
Shiriaeva, A.	45	Warrington, S.	133
Shoemaker, R.	73	Weeks, S.	4
Simmons, R.	88	Weil, D.	126
Simon, I.	65	Weis, K.	125
Sinclair, A.	28	Weitzel, S.	129
Sommers, J.	57, 73	Welikala, M.	101
Soong, B.	43	Weng, Z.	16
Sordal, V.	115	White, M.	83
Spenkelink, L.	78, 113	Wilkinson, O.	41
Spinks, R.	78	Winterhalter, C.	46
sprangers, r.	36	Wohlschlegel, J.	82
Stevens, D.	46	Wollenhaupt, J.	39
Stillman, B.	104	Wurm, J.	36
Subramanian, V.	9	Wörner, J.	23
Suhanovsky, M.	28		
Tainer, J.	66	Xi, X.	89
Talachia Rosa, L.	69	Yang, O.	43
Taylor, A.	32	Yasmin, L.	84
Tessmer, I.	55	Yu, J.	111
Thomas, D.	104	Zafar, M.	81, 112
Thompson, H.	73	Zhang, C.	28
Thompson, M.	81, 112	Zhang, D.	16
Tomko, E.	7	Zhang, R.	95
Trakselis, M.	85, 101	Zheng, J.	106
Tran, E.	1	Ziebuhr, J.	64
TRAN, P.	97		
Tsai, C.	66		

THANK YOU



**Helicases and Nucleic Acid-Based Machines:
Structure, Mechanism and Regulation and
Roles in Human Disease**